Design and Analysis of a Climbing Robot for Window Cleaning

A thesis submitted in partial fulfilment of the requirements

for the Degree of Master of Engineering in Mechanical Engineering

in the University of Canterbury

by ZhiHong Yu

University of Canterbury

2019

Acknowledgements

Engaging in a study of Masters Research has benefited me greatly. I have learnt a lot and have improved my academic skills in mechanical engineering. The wonderful bond with my family has been strengthened and I have received the wonderful supervision from my main supervisor and co-supervisor, and have developed lovely friendships with my working mates and friends.

On the journey of this study, building a robotic structure that is quite different from my previous profession was a challenge. However, I enjoyed it so much as this opportunity expanded my knowledge in mechanical field. I have gained a lot of knowledge of mechanical structure design.

I would like to thank my main supervisor Chris Pretty and co-supervisor XiaoQi Chen, who changed their statuses during my study. Their guidance on my project and thesis considerably helped me finish them in different aspects. Before my ex-supervisor XiaoQi Chen transferred university, he supported me to build the frame of the conceptual robotic design. My current supervisor Chris Pretty, then provided clear instruction to improve the detailed design.

Special thanks go to my working mates. Talking with them about my project really helped to solve numerous of problems and generate new ideas. Especially, Angus McGregor, whose sincere suggestions and encouragements really helped me improve my thesis.

Most importantly, many many thanks to my family. My husband and my gorgeous daughter have provided the wonderful and continuous motivation and support. Also, my husband's and my direct family members have supported me spiritually during the whole period of my study.

Abstract

With the spread of skyscrapers with large areas of glass windows, robotic cleaners, which can replace and so protect people from the risk of falling, have been seen as a viable option as robotic technology becomes more and more advanced. Various kinds of adhesion, actuation and locomotion systems exist for the different needs of climbing robots enabling them to work in different circumstances with different abilities, both on ferrous-magnetic and non-ferrous-magnetic surfaces, ground and walls and with slow or fast motion. Today there are many types of adhesion: magnetic, vacuum and dry, etc. Likewise, different sorts of locomotion are popular: legged locomotion, tracked locomotion and wheeled locomotion. However, there are increasing problems using climbing robots, such as complex structures, stepping over obstacles and high price. Some of these limitations are gradually being solved.

This thesis develops a robotic structure, named Hubbot. It will achieve a combined set of motions, consisting of linear motion, rotational motion, leg extension/retraction motion and interference avoidance motion. It has a simple and light weight structure. From the perspective of a simple design, a hub will be presented as well as some symmetrical legs instead of a multi-joint legged moving structure. From the perspective of reducing the weight, a rack and pinion gear is driven by a hung, reversible motor. From the perspective of operating savings, Electric Linear Actuators (ELA) are suggested to replace pneumatic cylinders.

A literature review described drawbacks of common locomotion mechanism, such as more complicated structure in legged locomotion mechanism than other mechanisms, especially translation locomotion mechanism. With respect to actuation mechanisms, ELA has the obvious advantages of light weight and high force and a simple structure among all actuators, even alternative to pneumatic actuator. Likewise, with comparison to other adhesion mechanisms, vacuum suction mechanisms present the simpler structure as well as flexible working terrains, but they could not work on rough or cracked surface. (A table makes the comparisons clearer and much more.)

Requirements for a window cleaning robot, such as light weight and working conditions, are presented. To address the problems mentioned before, the potential design using a hub is described. The rack and pinion gears mentioned above that are separately mounted to the two modules drive them to linearly move successively using one servo motor. However, the rack

must totally separate from the pinion before each module is driven to rotate respect to each other by another servo motor. These reduce the number of motors needed. Those symmetrical pillars may avoid a complicated Degree of Freedom (DOF) as well as help the robot move and overcome barriers flexibly via 4 ELAs and 4 fixed legs. Further, the four position arrangements of these legs are proposed and compared as well as the assembly of these legs and solenoid valves. (A table makes the comparisons clearer.) Most importantly, based on the working situations of this robot, the kinematic and dynamic analysis regarding its velocity and acceleration, adhesion force and motor force, are performed.

Furthermore, a structural optimization of the rotational mechanism is shown by three different bearing arrangements. The aim is to choose the best one to ensure the rigidity of the shaft and reduce the cost of the robot. Also, the method of attaching these kinds of bearings is indicated and compared by 3D CAD models. (A table makes the comparisons clearer.)

Finally, a functional embodiment design is presented as well as its whole structure's exploded view, consisting of three mechanisms: locomotion, adhesion and actuation. The four motions are highlighted showing in detail through their sequence formulations.

Table of contents

1 Introduction 1

1.1 Motivation 1

1.2 Thesis scope and structure 2

2 Literature review 3

2.1 Locomotion system 3

2.1.1 Wheeled locomotion 3

2.1.2 Legged locomotion 4

2.1.3 Tracked locomotion 5

2.1.4 Transition locomotion 5

2.1.5 Combined locomotion 7

2.2 Adhesion system 9

2.2.1 Vacuum adhesion 9

2.2.2 Magnetic adhesion 12

2.2.3 Dry adhesion 13

2.3 Actuation system 14

2.3.1 Electric motor 15

2.3.2 Pneumatic Cylinder 18

2.3.3 ELA 19

2.4 Existing Window Cleaning Robots 22

2.5 Summary 23

3 Mechanical Design of the Window Cleaning Robot 24

3.1 Introduction 24

3.2 Design Requirements 26

3.3 Conceptual Ideas of Mechanical Design 27
3.3.1 Assumptions and Assumption 27
3.3.2 Preferred Robotic System 28
3.3.3 Development of Translation Locomotion System 34
3.4 Conclusions 46
4 Analysis of Robotic Structure 47
4.1 Kinematic and Dynamic Analysis for Adhesion Forces 47
4.2 Kinematic Analysis in the Leg Extension/retraction Motion 51
4.2.1 Leg Extension/Retraction Motions of Suction Pads 51
4.2.2 Leg Extension/Retraction Motions of Pinion 55
4.3 Forces Analysis in the Linear and Rotational Motions 55
4.3.1 Rotational Motions 58
4.3.2 Linear Motions 64
4.4 Payload Capacity 73
4.5 Final Robotic Structure 75
4.6 Estimated Costs of Hubbot 80
4.7 Summary 81
5 Comparisons of Existing Window Cleaning Robots and Hubbot 82
5.1 Introduction 82
5.2 Discussion of Success Criteria 88
5.2.1 Safety Comparisons 88
5.2.2 Comparisons of Parameters 88
5.2.3 Comparisons of Motion Mechanisms 89
5.2.4 Comparison of Actuation System 90
5.2.5 Economic Comparisons 91

5.2.6 Comparisons of Cleaning Capacity 92
5.3 Summary 93
6 Conclusions and Recommendations 94
6.1 Performance achieved by Hubbot 94
6.1.1 Performance Measured against Design Requirements 94
6.1.2 Performance of Motion Mechanisms 95
6.1.3 Performance Regarding Adhesion Mechanisms 95
6.1.4 Performance Regarding Spanning Obstacles 96
6.2 Merits of Hubbot 97
6.3 Recommendations for Future Work 98

List of Figures

Fig. 1.1. Applications of climbing robots 1
Fig. 2.1. Wheeled climbing robot 4
Fig. 2.2. Wheeled climbing robot 4
Fig. 2.3. Tracked climbing robot 5
Fig. 2.4. Translation climbing robot 6
Fig. 2.5. Process of transferring climbing of the translation robots 7
Fig. 2.6. A wheel-leg wall climbing robot [14] 8
Fig. 2.7. A leg-wheel wall climbing robot [31] 8
Fig. 2.8. A Wheel-Track hybrid robot [12] 8
Fig. 2.9. Active vacuum adhesion 10
Fig. 2.10. The mechanism of vacuum-based wet adhesion Experiment 11
Fig. 2.11. Passive suction adhesion 12
Fig. 2.12. Magnetic adhesion 13
Fig. 2.13. Dry adhesion 14
Fig. 2.14. Categories of electric motors 16
Fig. 2.15. Applications of stepper and servo motors 16
Fig. 2.16. Examples of common applications of electric motors 17
Fig. 2.17. Examples of using a single motor to reduce the weights of robots 17
Fig. 2.18 Structure and applications of pneumatic actuators 19
Fig. 2.19. Structure and applications of ELA 20
Fig. 2.20. Structure and applications of LinMot 21
Fig. 3.1. Proposed working area and trajectory on a rectangular window 28
Fig. 3.2. Concept sketch for a translation locomotor consisting of two frames, each with an independent set of suction pad 29
Fig. 3.3. Diagram of the assembly of the suction pad, valve and actuator 31
Fig. 3.4. Linear translation and rotation of proposed robot 32
Fig. 3.5. Diagram of the linear motion mechanism 35
Fig. 3.6. Working process of the linear motion mechanism 35
Fig. 3.7. Separate the pinion from the rack 36
Fig. 3.8. Elements of affecting the displacement 36
Fig. 3.9. Comparisons of unchanged and changed modules 37
Fig. 3.10. Diagram and section view of the 3D hub 38

Fig. 3.11. Rotational mechanism having a special hub.....38
Fig.3.12. Rotational shaft and bearing arrangements 38
Fig.3.13. Three potential bearing-shaft arrangements 40
Fig. 3.14. Curved rack and pinion.....41
Fig. 3.15. Elements of the interference avoidance motion mechanism 42
Fig. 3.16. Options of Leg Extension Arrangement.....43
Fig. 3.17. Two way, two position, normally closed solenoid valve 44
Fig. 3.18. Options of leg extension arrangement.....45
Fig. 4.1. Analysis of kinds of forces for preventing the robot falling down.....47
Fig. 4.2. Four states of the suction pads.....50
Fig. 4.3. The status of the suction pads during extension/retraction motion 51
Fig. 4.4. 100mm L12 actuator size of Actuonix's L series.....51
Fig. 4.5. Status of the suction pads 52
Fig. 4.6. Diagram of designed suction pads.....54
Fig. 4.7. Diagrams and dimensions of the SMC (SX10 Series) solenoid valve 54
Fig. 4.8. Assembly of the ELA, solenoid valve and suction pads 55
Fig. 4.9. Linear with parabolic blend displacement profile 56
Fig. 4.10. Plot of the velocity of linear with parabolic blend displacement 56
Fig. 4.11. Plot of the acceleration 58
Fig. 4.12. Diagram of the rotating components of module 2.....59
Fig. 4.13. Rotational motion of module 2 with module 1 attached to the glass 59
Fig. 4.14. Diagram of the rotating components of module 1.....59
Fig. 4.15 Rotational motion of module 1 with module 2 attached to the glass 60
Fig. 4.16. Displacement plot of each module rotates 90° over 1s 60
Fig. 4.17. Angular velocity plot of each module rotates 90° over 1s 62
Fig. 4.18 Angular acceleration plot as each module rotates 90° over 1s.....62
Fig. 4.19. The structure of 298:1 micro metal gearmotor HPCB 12V with extended motor shaft for encoder 63
Fig. 4.20. Diagram of the moving components of module 2 65
Fig. 4.21. Diagram of translational motion for module 2 65
Fig. 4.22. Diagram of the moving components of module 1 65
Fig. 4.23. Diagram of translational motion for module 1 66
Fig. 4.24. Displacement (20mm) plot of the linear motions of the robot 66

Fig. 4.25. Linear velocity plot of the linear motions of the robot for 20mm 67
Fig. 4.26. Linear acceleration plot of the linear motions of the robot 68
Fig. 4.27. Diagram showing forces on robot when climbing 69
Fig. 4.28. Assembly and position of the pinion and rack 73
Fig. 4.29. Whole robotic structure of this project 75
Fig. 4.30. Exploded view of the whole robotic structure 76
Fig. 4.31. Timeline of the whole working process of Hubbot 80

Lists of Tables

Table 2.1 Comparison of main locomotion systems....9
Table 2.2 comparison of main adhesion systems....14
Table 2.3 Compares main common actuation mechanisms....21
Table 2.4 Compares main common actuation mechanisms....22
Table 3.1 Morphological matrix for sub-systems....24
Table 3.2 Comparisons of the three arrangements of bearings....41
Table 4.1 Four outcomes of the adhesion force....50
Table 4.2 Electric linear actuators mounted on module 1....52
Table 4.3 Values of the moments of inertia and torques of each rotating module....63
Table 4.4 Specification of 298:1 Micro Metal Gearmotor HPCB 12V with Extended Motor Shaft....64
Table 4.5 Values of the masses and torques of each moving module....70
Table 4.6 Electric linear actuators mounted on the module 2 plate for pinion interference avoidance....73
Table 4.7 Sequence for linear motions....77
Table 4.8 Sequence for rotational motions....78
Table 4.9 Estimated Costs of Hubbot....80
Table 5.1 Success Criteria of Window Cleaning Robots....82
Table 5.2 Robot Statistics of These Existing Robots and Hubbot....82
Table 5.3 Evaluation Matrix of These Existing Robots and Hubbot....86
Table 5.4 Results of the Evaluation Matrix in Success Criteria....87

1 Introduction

1.1 Motivation

The purpose of this project is to design a capable of a simple and light weight robotic structure, named Hubbot. It combines a set of motions composed of parallel linear motion, rotational motion, leg extension/retraction motion and interference avoidance motion.

In modern society, there is an increasing need for climbing robots to clean, weld or inspect different kinds of surfaces of high buildings, large oil tanks and rough concrete facilities (shown in Figure 1.1) [1, 2], replacing workers in these hazardous environments. Consequently, robotic technologies have been developed and applied according to the needs in different fields.

(1)Cleaning window glass [1]

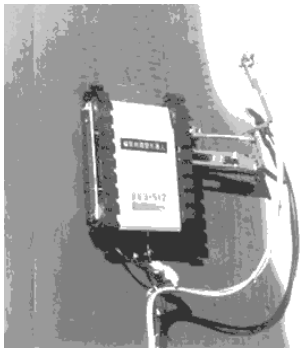

(2) Inspecting oil tanks [2]

(3) Inspecting Concrete Structures [2]

Fig. 1.1. Applications of climbing robots

However, some problems, such as difficulty in overcoming barriers and complex structures, also emerge. So, the robotic structure developed in this thesis will be designed to clean window glass. Therefore, this thesis will focus on solving the two issues that are:

- To step over higher barriers flexibly. (through actuations offering flexible strokes instead of multi-joint legs)

- To simplify the robotic mechanical structure. (with increasing the payloads and ensuring the robot to adhere firmly to the climbing surface)

1.2 Thesis scope and structure

Chapter 1 presents the purpose and motivation for this research of designing a simpke, light-weight window-cleaning robot. That is because the existing climbing robots have problems that arise from their complicated structure and weight. Also, the main contents of each chapter are introduced.

Chapter 2 presents the background of the three main systems for wall climbing robots: the locomotion system, adhesion system and actuation system. They are introduced in detail through a view of the literature, specifically indicating their individual advantages and disadvantages.

Chapter 3 presents the general considerations (common requirements) for wall climbing robots and then focuses on window glass cleaning robots. To address the problems above, the conceptual mechanical designs are proposed. In detail, the three systems are discussed as well as the four motions. Moreover, relevant design options of the corresponding sub-systems are introduced and contrasted to optimize this robot's final structure. They are indicated in tables to make the comparisons clear.

Chapter 4 discusses the kinematic analysis of velocity and acceleration, and the dynamic analysis of adhesion and motor forces in different working conditions to ensure this robot can work safely. All the related standard and non-standard elements are selected and designed before they are assembled together to show the functional embodiment design.

Chapter 5 compares the existing window cleaning robots to Hubbot. Based on their success criteria, they are introduced and compared in these aspects, such as safety, motion mechanism and capacity for cleaning glass. They are indicated in a table to make the comparison clear as well as their evaluation results.

Chapter 6 concludes the completed work with comparisons to the existing window cleaning robots. Also, the future work is discussed, such as spanning wider obstacles fast, manufacturing physical prototype and adding the cleaning system.

2 Literature review

There are three common subsystems that make up wall-climbing robots: the actuation mechanism, the adhesion mechanism and the locomotion mechanism. The last two systems are key components [3-5] that usually decide the category of a robot [6], such as vacuum adhesion mechanism and legged locomotion mechanism. However, they will only work with the help of the actuation mechanism. In the context of climbing robots, various sorts of actuation, adhesion and locomotion systems, have different merits and drawbacks [4, 7].

2.1 Locomotion system

The abilities of these robots, including working precision and speed as well as cost, are directly affected by the chosen locomotion systems. Various kinds of locomotion have been studied and tested as prototypes and products and are popular in modern society, such as legged locomotion, tracked locomotion and wheeled locomotion. The characteristics of these main locomotion mechanisms are as follows.

2.1.1 Wheeled locomotion

Wheeled locomotion mechanisms can move quickly as well as flexibly. Also, there are no considerations of multiple DOF and gaits, which simplifies the structure of wheeled robots [8-11]. However, they are less able to span barriers or overcome uneven surfaces [12], although they can step over some barriers [9, 13]. For example, the Alicia 1 and 2 robots can step over barriers of about 10 mm at normal speed [9] . Also, wall climbing wheeled robots have difficulty adhering firmly to surfaces because they have a very small contact area between their surfaces. Therefore, vacuum suction pads [9, 14] or permanent magnets [9-11, 15, 16], must be incorporated into wheeled robots, often the latter when working on a rough or cracked surface [8, 9]. As shown in Figure 2.1, the two climbing robots that have two wheels and four wheels respectively are all attached with magnetic adhesion. Moreover, the limited contact area reduces the payload capacity due to the reduced holding force available.

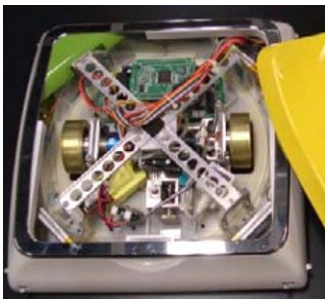

(1) Wallwalker (two wheels & a vacuum cup) [9] (2) A climbing robot (four wheels & permanent magnets) [15]

Fig. 2.1. Wheeled climbing robot

2.1.2 Legged locomotion

Legged locomotion mechanisms have clear advantages, such as the ability to step over obstacles, walking over rough surfaces and high mobility. However, legged locomotion is slow and energy inefficient [12] due to current shortcomings in the mechanical structure and control. For example the multiple degrees of freedom, gait planning and control are very complex [4, 8, 17]. Nevertheless, legged locomotion can be implemented with reliable adhesion mechanisms, such as vacuum suction pads, magnetic devices and dry components, as seen in many robotic applications. For instance, RAMR 1 that includes two-leg with two suction pads is presented [4, 9]. Furthermore, four-leg [8, 9, 18] (shown in Figure 2.2 (1)), six-leg [9, 19-22] (shown in Figure 2.2 (2)) and eight-leg [8, 17, 23, 24] (shown in Figure 2.2 (3)) climbing robots were gradually developed to provide more security and greater payloads in various hazardous working fields [9].

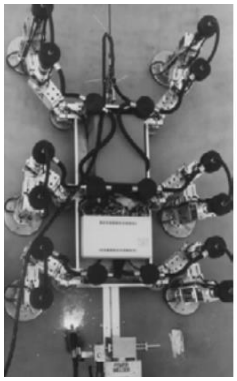

(1) NINJ-I(having four legs) [9] (2) REST 1 (having six legs) [9] (3) Research on bionic crab-liked robot prototype(having eight legs) [24]

Fig. 2.2. Wheeled climbing robot

2.1.3 Tracked locomotion

Tracked locomotion and wheeled locomotion have similar motion systems and abilities. Multiple degrees of freedom and gait planning are also not involved in the mechanical design or operation of tracked locomotion systems. The motion of tracked systems is generally slower and its structure is more complex than wheeled systems, with performance being close to legged locomotion [12]. However, tracked locomotion has greater ability to span obstacles as well as reliable adhesion because of larger contact areas [8, 9, 25]. Cleanbot II has 52 suction pads and one chain track. It is designed to both move continuously and overcome the barriers less than 6mm in height [9, 26] (indicated in Figure 2.3 (1)). Apart from that, a two-tracked in-pipe inspection mobile robot has been developed to work on different pipe and duct surfaces, such as pipe 210mm in diameter and rectangular duct 230mm wide [25] (shown in Figure 2.3 (2)).

(1) Cleanbot II (having a chain-track) [9]

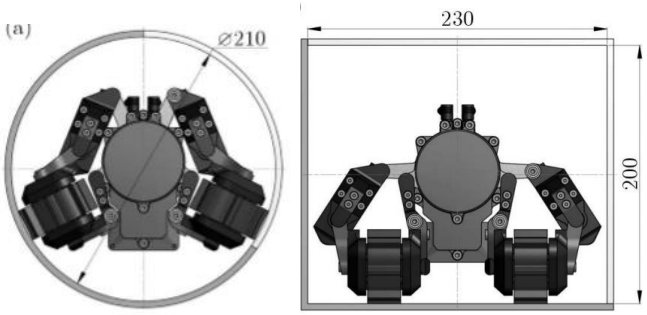

(a) Pipe Ø210mm (b) Rectangular duct 230 mm

(2) A two-tracked in-pipe inspection mobile robot [25]

Fig. 2.3. Tracked climbing robot

2.1.4 Transition locomotion

Transition locomotion are like a simple form of legged robot, in which there are two legs. One is attached to the surface, while the other moves to a new position, before attaching to the surface and allowing the first to move to a new position. Robots implementing transition locomotion have a simple mechanical structure but are larger size and slower than other systems. They are usually applied to high work, such as indoor inspection [27] (indicated in Figure 2.4 (1)) and cleaning windows of high-rise buildings [4, 9, 19, 28-30] (shown in Figure 2.4 (2) (3), Figure 2.5), because they ensure that the robot always has a positive connection to the surface. In Sky Cleaner 3, the vacuum suckers are attached to two perpendicular cylinders

(the X and Y cylinders) individually, contributing to the two cylinders' alternating linear motions. The robot moves parallel to window glass via these suckers in the X cylinder extending and retracting to allow and cancel the adhesion forces when those suckers with the Y cylinder are retracting and extending. The motions are sequence movements [29]. In [19], shown in Figure 2.5 (2), the sliding robot has a four-bar mechanism consisting of the main body and the side bodies. Each unit (cylinder) can slide to a new position against each other via two motors and their separate adhesive suckers working like those suckers of Sky Cleaner 3.

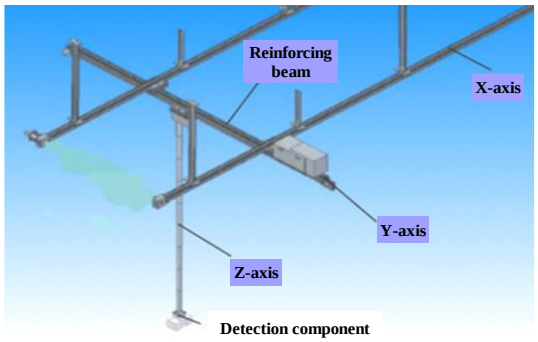

(1) Installation diagram of indoor inspection robot [27]

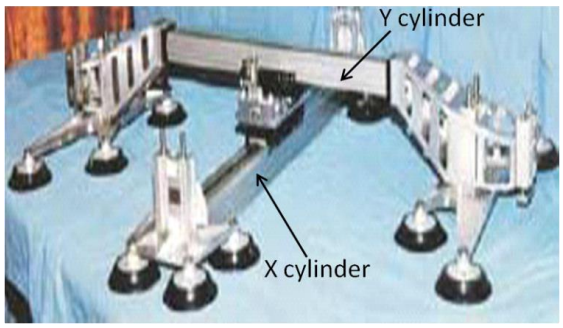

(2) Translation mechanism of Sky Cleaner 1,2 and 3 [9]

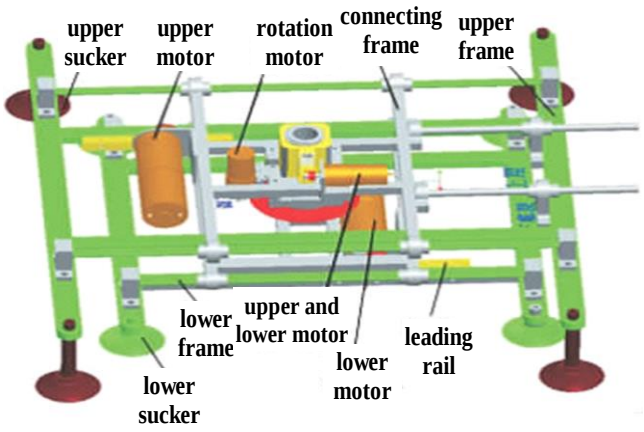

(3) Structure of glass-wall cleaning robot [30]

Fig. 2.4. Translation climbing robot

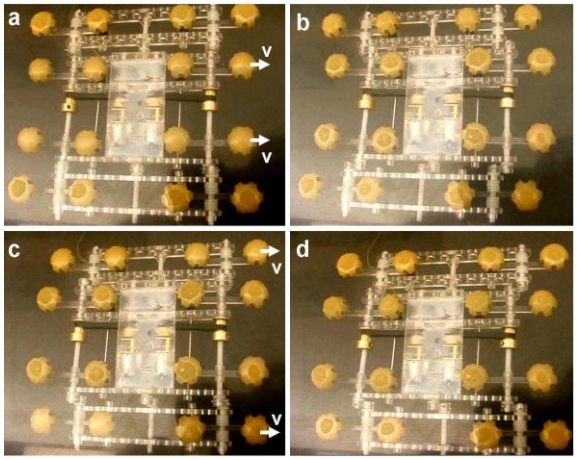

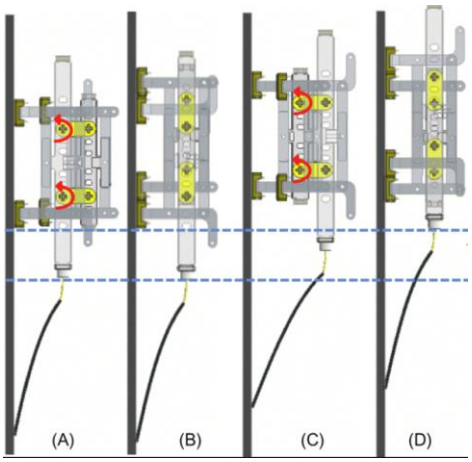

a) Side bodies are attached and the main body is moving at a speed of v to the right.

b) Main body gets attached to the surface.

c) Main body is attached and side bodies are moving to the right

d) Side bodies get attached to the surface.

(1) Photograph of the climbing robot during inverted walking on an acrylic surface [19]

(A) Gives the initial state, only the feet in the outer frame attach to the vertical surface;

(B) The inner body moves forward and finally all feet attach to the surface;

(C) Only the feet in the inner frame attach to the vertical surface;
(D) All feet attach to the surface

(2) Photograph of robot-walking locomotion by parallel four-bar linkage rotation [28]

Fig. 2.5. Process of transferring climbing of the translation robots

2.1.5 Combined locomotion

The merits of legged locomotion, tracked locomotion and wheeled locomotion mentioned before can be combined to achieve a wider application and a better contribution than individually. For example, combined systems include leg-wheel locomotion (illustrated in Figure 2.6, Figure 2.7 (1)) or wheel-track mechanism (illustrated in Figure 2.7 (2)). In [31] and in [14, 32, 33], the robots having legged mechanisms combined with 2-wheels and 6-wheels, can overcome high obstacles and also be navigated effectively. Jinwook Kim et al. [12] presented a novel robot with four wheels combined with two tracks that can climb a stair slope of up to 45 degrees with a step height of up to 240mm. Also, it moves at the maximum speed of 1 m/s for the track and 2 m/s for the wheels. Obviously, the combined locomotion mechanisms include two or more than two locomotion mechanisms so it has more complex structure and higher cost, as shown in Figure 2.8.

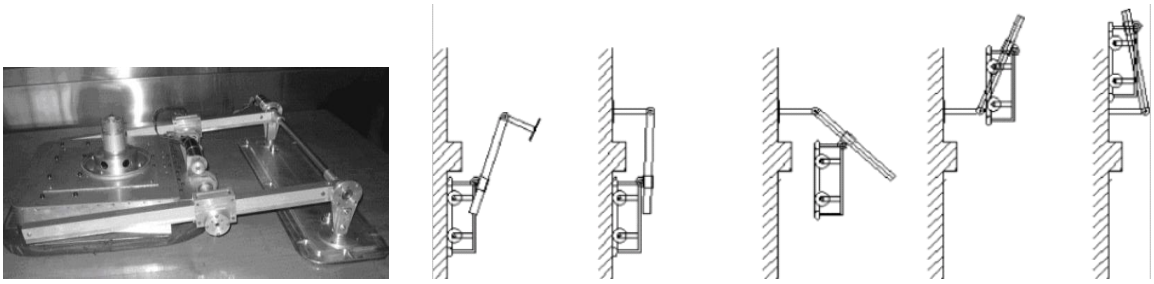

(1) A novel wall climbing robot (2) Robot's movement sequence to span a ledge

Fig. 2.6. A wheel-leg wall climbing robot [14]

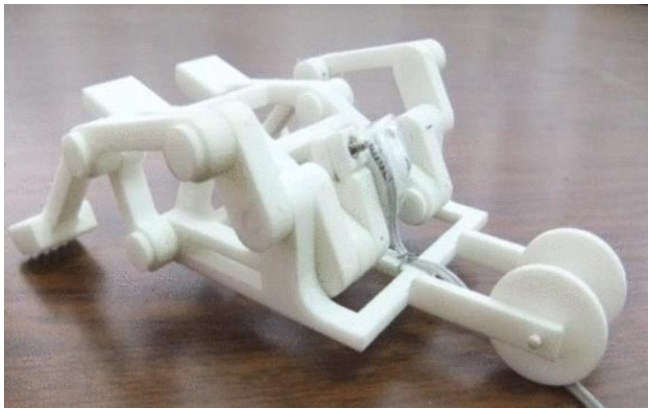

Fig. 2.7. A leg-wheel wall climbing robot [31]

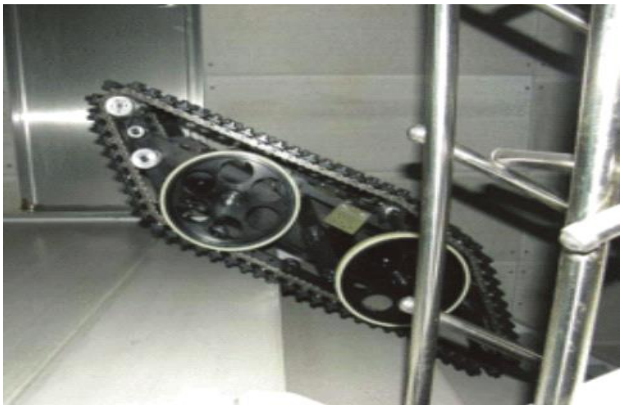

Fig. 2.8. A Wheel-Track hybrid robot [12]

Comparison of main locomotion mechanisms is shown in table 2.1:

Table 2.1 Comparison of main locomotion systems

Categories	Pros	Cons
Wheeled locomotion	Simple and flexible movement [8-11]	Small payload capacity for wall climbing applications, difficult to cross barriers [12]
Legged locomotion	High obstacles avoidance and mobility on different terrains [12]	Complicated structure and control, low speed [4, 8, 12, 17]
Tracked locomotion	Move fast and larger contact surfaces [8, 9, 25]	Difficult to cross barriers, complex structure [12]
Transferred locomotion	Simple structure [27]	Large size, slow speed [27]
Combined locomotion	Flexible and fast moving can be designed to easily cross barriers [14, 32, 33]	More complex structure and high cost

2.2 Adhesion system

Today there are many categories of adhesion, including:

- Magnetic adhesion
- Vacuum adhesion
- Passive vacuum adhesion
- Dry adhesion
- Wet adhesion

Design decisions about robots regarding locomotion mechanisms and adhesion mechanisms must be made to meet the requirements for any given application. Detailed comparisons of adhesion systems are given below.

2.2.1 Vacuum adhesion

2.2.1.1 Active vacuum adhesion

Active vacuum adhesion is one of the main adhesion techniques used in commercially available wall climbing robots sold online and in stores [3, 19, 34, 35]. This method has reliable adhesion ability and a simple mechanical structure as well as the advantage of working on uneven terrain surface of many different materials. However, active vacuum adhesion does not work well on rough or cracked surfaces, which result in air leakage, causing reduced suction forces [4, 5, 7-9]. In [9] air leakage is not the main concern for the ROMA II climbing robot because 5 pairs

of suction cups provide enough suction forces to avoid loss of adherence, as shown in Figure 2.9(1). Cleanbot II, having 52 suction pads, is designed to move continuously since they always guarantee adhesion [9]. Usually, sufficiently flat surfaces are provided for active vacuum adhesive robots, such as window glass [5, 9, 36] Often, robots using active vacuums are heavy because a pump is needed to provide continuous pressure [3, 30] , which can also cause a high noise level. This heavy robot is combined with the payload weight and requires sufficient suction to hold on to the glass. It is difficult to reliably maintain high suction, even for a short time [5, 8, 19] Thus, in [29] (illustrated in Figure 2.9 (2)), the supporting vehicle on the ground dramatically reduces the weight of the cleaning robot. Likewise, YiLi Fu et al. [14] developed the wheel-leg hybrid locomotion mechanism connected to three vacuum suction sucker to move fast, as well as span a certain barrier. In this design, the big suction cup is designed into the robot's frame to guarantee the efficient suction forces as well as reduce the whole size via fixing wheels inside itself [14].

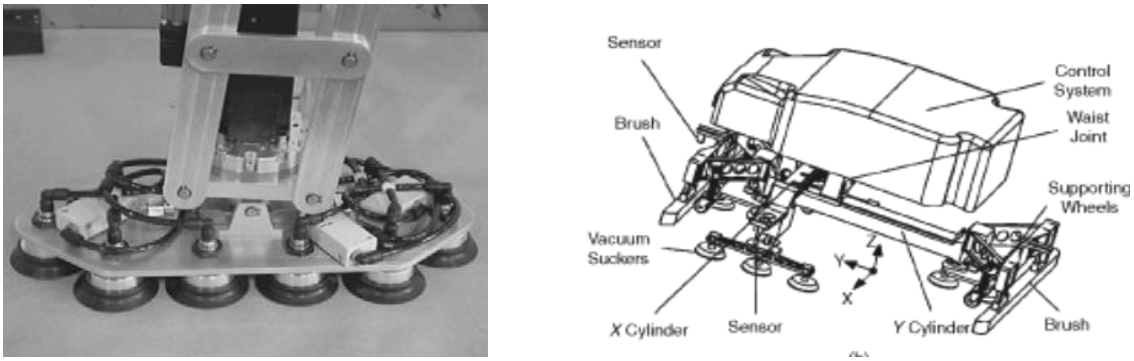

(1) ROMA II climbing robot [9] (2) Sky Cleaner 3 [29]

Fig. 2.9. Active vacuum adhesion

Wet adhesion typically was an active vacuum method with the adhesion of a lubricant to improve performance. Vacuum suction could not work on rough surfaces well because of air leakage. To solve this problem, a novel vacuum-based wet adhesion system was developed through improving the adhering ability [6, 37]. It has been tested using a specially developed robot WallWalker, where the friction in wet adhesion is half of that in dry adhesion. Moreover, the seal performance of suction pads is improved after adding lubricant between the pads and climbing surfaces, such as glass or concrete, as shown in figure 2.10 [37]. As a result, wet adhesion system can contribute to the climbing robot to potentially work on uneven surfaces. However, it requires the chosen lubricant having high features of not soiling the surfaces and not adhering to the driving wheels and not causing the robot to slip down a wall.

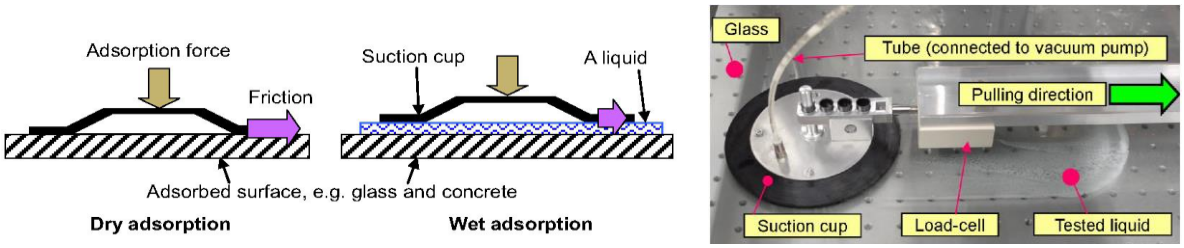

Fig. 2.10. The mechanism of vacuum-based wet adhesion Experiment

2.2.1.2 Passive vacuum adhesion

Passive vacuum adhesion is also given high consideration because its mechanism is simple and it is suitable for the same types of surfaces as active vacuum adhesion. Most importantly, it works well on smooth surfaces by merely providing appropriate pressure normal to the surface so an on-board vacuum pump is not required. Passive vacuum adhesion has the obvious advantages of low-no power consumption and light weight [4, 5, 8, 9]. These studies show passive vacuum suction cups (shown in Figure 2.11(1) and (2)) having elastic characteristics attached to the robotic mechanism. For example the novel robot in [5] has four suction pads (shown in Figure 2.11(3)) within the two tracks or belts and some suction pads under the chassis outside the tracks. The tracks or belts are flexible and deformable. They can be sucked into concave shapes relative to the surface when passive pressures occur between them, thereby acting like suction pads. Furthermore, this configuration can prevent the suction pads from seriously abrading.

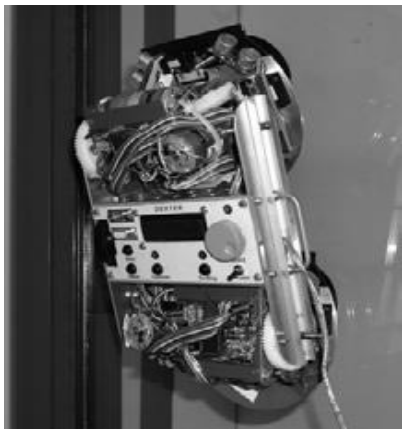

(1) DEXTER [9]

(2) Passive suction cup in DEXTER [9]

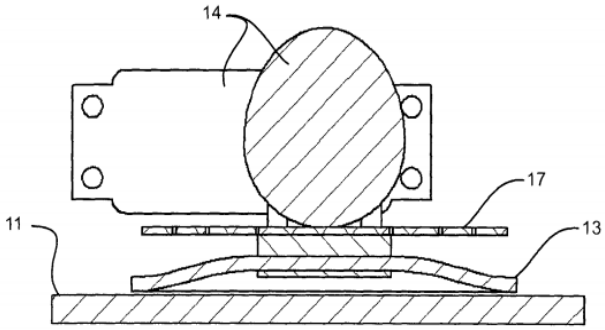

(3) The suction pad component [5]

Fig. 2.11. Passive suction adhesion

The two types of vacuum adhesions enable useful designs and high stability. However, they do not work well on dusty, rough or porous surfaces. Also, they may leave marks and wear abrasion is serious as they are always in contact with surfaces [5, 9, 14, 38], and often need to slide across the surface.

2.2.2 Magnetic adhesion

Magnetic adhesion can only work on ferrous material surfaces, whether smooth or rough. There is low-no power consumption [3, 8, 9, 13, 19], depending on whether electro- or permanent-magnets are used. This adhesion mechanism combined with wheeled or legged locomotion is used on robots for detecting surface faults or cracks on oil tanks [10, 15, 39], to weld on a ship hull, or to avoid various obstacles [9, 13, 32, 40] (shown in Figure 2.12). However, it is not suitable for non-ferrous surfaces, such as concrete, glass, and many stainless-steels. But there have been several kinds of glass cleaning robots, such as the Windoro window cleaning robot, which use magnetic adhesion. In this case, magnets are needed both on the inside and the outside module of the glass [9, 16, 41]. The two magnetic modules are programmed to clean and navigate separately and are actuated by wheels, but it is hard to separate them from each other when they are not in use [16].

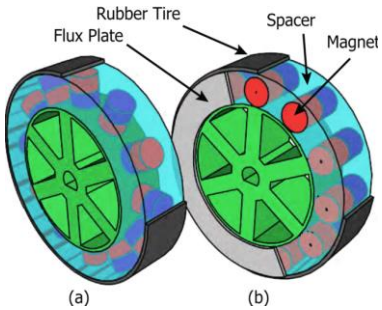

(1) Magnets in a teleoperated wall climbing robot for oil tank inspection [10]

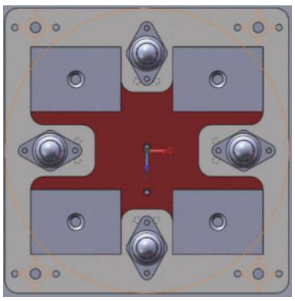

(2) A non-contactable and adjustable adhesion mechanism in a climbing robot for inspection [15]

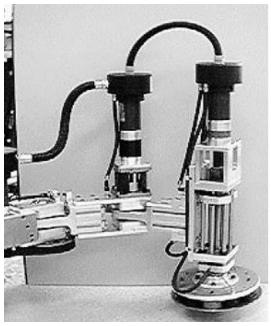

(3) Electric magnetic grippers in REST 1 for inspection, cleaning and welding on a ship hull [9]

Fig. 2.12. Magnetic adhesion

To solve the problem of difficult detachment, electro-magnetic adhesion was developed, which works very reliably and quickly on ferromagnetic surfaces [9, 13, 39] could also work for the window cleaning robot, if an inside module was used. However, electromagnetic adhesion requires more power consumption than a permanent magnet system.

2.2.3 Dry adhesion

Dry adhesion does not need energy to adhere tightly to the surface, or pressure to climb because it is mainly due to molecular forces, which result in its main advantage of very light weight. It is well known that geckos can attach to almost any surface, whether wet or dry, smooth or rough [35, 42, 43]. The study of geckos has been incorporated into the design of dry adhesives for wall climbing robots [20, 35, 42-46] . IBSS_Gecko_6 was presented as a bio-inspired legged climbing robot. In its design, a novel footpad attached by polyurethane adhesive can ensure the robot can climb and stay on a vertical wall [45] , shown in Figure 2.13(1). In [19, 34] , a legged palm-sized climbing robot was designed and experimentally shown to have the ability to climb robustly and vertically on both smooth and rough surfaces although it climbed better on smooth surfaces. With a weight of only 115g, on a smooth inverted surface, it can hold an up to 196g payload. The researchers chose flat tacky elastomer footpads to ensure that the robot would not to fall down. Then, this research team [47], using the methodology of Taguchi Methods, developed an optimal footpad for a climbing robot when working on a vertical acrylic surface having different curves. The optimized footpad shape improved the payload capacity by 46.9% over the previous dry adhesive in [19] , shown in Figure 2.13 (2). However, robots attached by dry adhesives usually have low payload due to their light weight, so that these robots have no the ability to accommodate other heavy additional equipment, such

as a cleaning system. Moreover, dry suction pads lose adhesion when used for a period of time, especially on dusty surfaces [3, 9, 46]. So, they need to have a regular cleaning to prevent these pads from falling down.

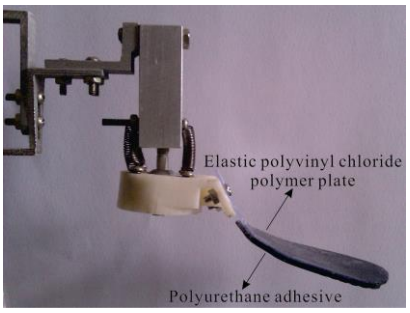

(1) Photograph of the new footpad with polyurethane adhesive [45]

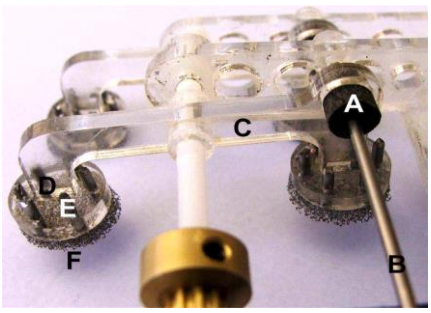

(2) Rocker foam(A) and Footpad foam(F) [19]

Fig. 2.13. Dry adhesion

Table 2.2 compares main common adhesion mechanisms:

Table 2.2 comparison of main adhesion systems

Categories	pros	cons
Active vacuum adhesion	Small size, simple structure, many types of surfaces [3-5, 7-9, 19, 34, 35], Reducing friction, working on uneven surfaces lubricant (wet adhesion) [37]	Loss of air pressure, appropriate ambient pressure, air leakage, a heavy air pump [4, 5, 7-9], high features of lubricant (wet adhesion) [37]
Passive vacuum adhesion	Small size, simple structure, no energy consumed, light weight, low cost, easy to adhere [4, 5, 7-9]	Air leakage, appropriate ambient pressure [4, 5, 7-9]
Magnetic adhesion	No power consumption (permanent magnet), more robust adhesion [3, 8, 9, 13, 19]	Power (electromagnet), slow and hard retraction, limited working surfaces [3, 8, 9, 13, 16, 19]
Dry adhesion	Almost any surfaces, more robust adhesion and fast velocity, no power consumption [35, 42, 43]	Difficult structure, degraded adherence on dirty surfaces, limited time use [3, 9, 20, 35, 42-46]

2.3 Actuation system

Small Robotic systems commonly use one of the three actuators described below: Electric motor, linear actuator and pneumatic cylinder [48]. However, it is rare to find the actuation systems described in previous research, despite the importance. On the one hand, the actuation system is vital to drive the adhesion and locomotion systems continually and/or precisely. On

the other hand, its specifications and performances can affect the precision, velocity and flexibility [31] of the robots various motions, as well as the cost and the adhesion for wall climbing robots. Additionally, more light weight wall climbing robots have increased mobility, payload and reliable adhesion with smaller, more efficient actuators [9, 19, 29, 31, 49, 50].

2.3.1 Electric motor

Rotational electric motor can be broadly divided into two main categories in robotic applications: stepping motors and servo motors [48]. Their constructions are illustrated in Figure 2.14[51, 52]. The difference is more a function of how they are used and controlled, rather than of physical construction. Stepping motors are open-loop and can be commanded to make rotational 'steps' with the resolution dictated by their construction[53] [54]. Stepping motors are often used in these applications where accurate open-loop, position and precise rotation are required, such as 3D printers and robotics [55] [23]. Stepping motions require a special driving circuit. The current for any motor is a function of the power and can be high. Normally, stepper motors are quite heavy and have a relatively low torque due to the fact that they are typically designed for high angular resolution and therefore have many permanent magnetic poles. However, Brushless DC (BLDC) motors (shown in Figure 2.14(2)) [56] can also be considered stepper-motors, with low angular resolution, but optimised of high-speed. BLDC motors have the advantages of no brushes[53], are very compact and have high efficiency and energy density [55, 57, 58].

Servo motors are closed-loop and can be commanded to a given position or velocity[53] [54]. They are widely used in modern robotic systems, especially synchronous servo motors [6, 59-62], such as driving the wheels, arms and legs of robots. Servo motors can drive other components continuously, especially synchronous servo motors, which can maintain a stable torque with a constant speed [62]. Two examples of applying servo and stepper motors shown in Figure 2.15, where a servo motor is used to drive the slide actuator for measuring absorption forces [6] and a stepper motor to drive the slider along a threaded rod [23].

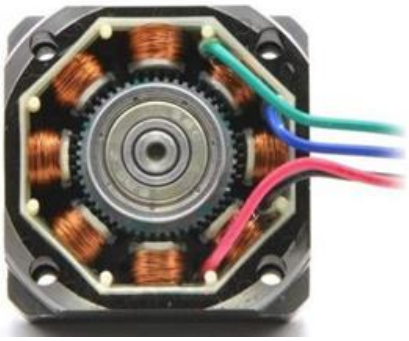

(1) Stepper motor [63]

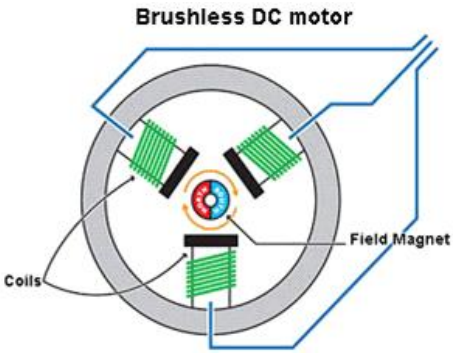

(2) brushless DC motor [56]

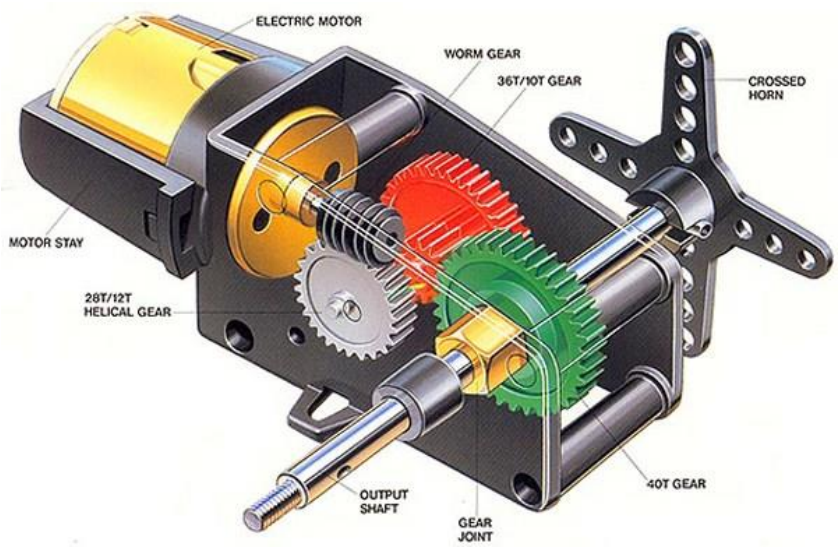

(3) Servo motor [64]

Fig. 2.14. Categories of electric motors

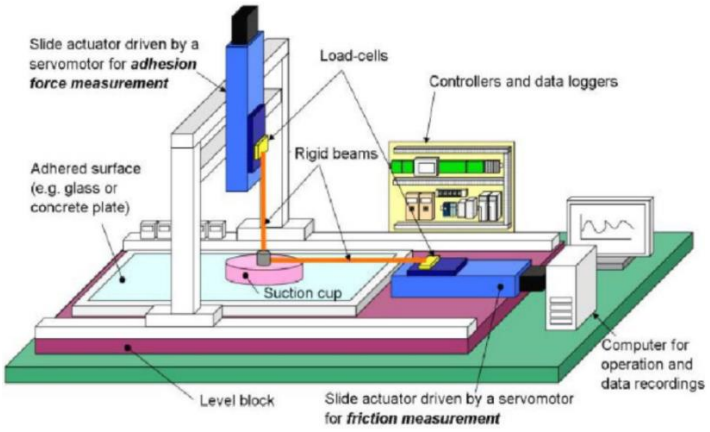

(1) The application of a servo motor [6]

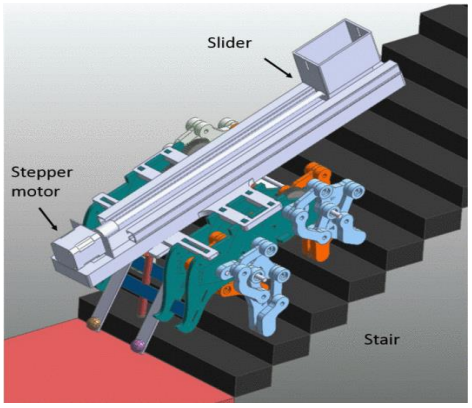

(2) The application of a stepper motor [23]

Fig. 2.15. Applications of stepper and servo motors

On the one hand, rotational electric motors are indispensable actuators for various mechanisms. Two examples of common working requirements are shown in Figure 2.16. The two DC motors

equipped are used to drive the main body and the side bodies to move parallel to each other [19, 31], shown in Figure 2.16(1). In [57], four electric motors are utilized to drive the four propellers to generate thrust forces, providing reliable adhesion. While attached firmly to the wall, the wall-cleaning robot can span different obstacles as well as clean the window which is with the help of another brushless DC motor, indicated in Figure 2.16(2).

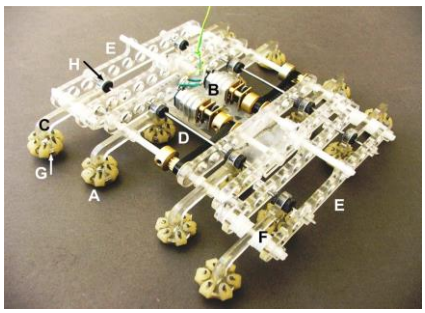

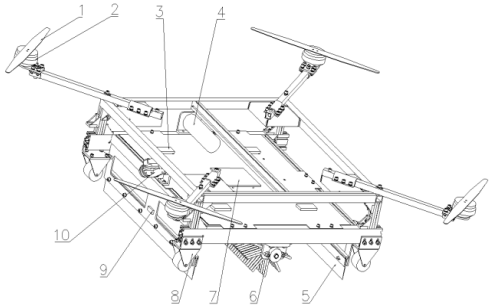

(1) The application of DC Motor (B) [19]

(2) The application of four electric motors 2 and a brushless DC motor 4 [57]

Fig. 2.16. Examples of common applications of electric motors

On the other hand, it is necessary to reduce the numbers or the size and weight of electric motors to increase the payloads, lower the cost, especially for wall climbing robots. The three robots, separately named LWbot (shown in Figure 2.17(1)) [31], O-M-Climber (shown in Figure 2.17(2)) [50] and AnyClimb-II (shown in Figure 2.17(3)) [28] all operate with only one motor via imitating bionic climbing principle or symmetric parallel four-bar linkages which greatly reduce the weight of these robots.

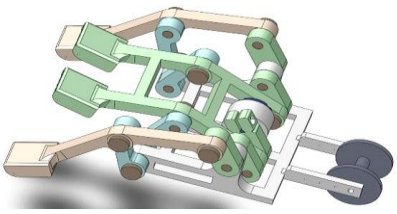

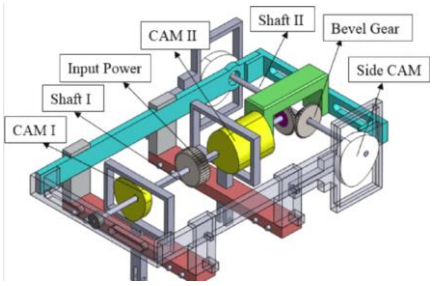

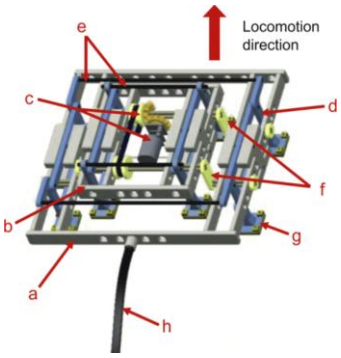

(1) Single motor in the CAD model of LWbot(100g) [31]

(2) Single motor in the 3D model of O-M-Climber [50]

(3) Single motor in the 3D model of AnyClimb-II [28]

Fig. 2.17. Examples of using a single motor to reduce the weights of robots

2.3.2 Pneumatic Cylinder

Linear motion can be accomplished by a pneumatic cylinder, which can be controlled manually or automatically with the help of an air compressor. The construction of a pneumatic cylinder is indicated in Figure 2.18(1) [65]. Adhesion can be achieved via suction disks [4, 29, 66, 67] or a propeller driven by some pneumatic cylinders. Houxiang Zhang et al. [29] and Dong Sun et al. [67] all installed suction pads on the ends of X and Y cylinders. The pads on each cylinder can be alternatively extended and retracted step by step under the control of pneumatic cylinders. This consideration enables a sliding motion and simplifies the structure, and results in lightweight and increased mobility, especially when using an air compressor on the ground. Also, pneumatic cylinders are attached into the four-bar mechanism of a one-legged jumping robot to drive and position its arms [68], illustrated in Figure 2.18(2). The jumping ability of this robot developed in 2014, has been improved to obtain a maximum output force of 1200N using the McKibben-type pneumatic muscle actuators, illustrated in Figure 2.18(3). The better jumping robot is lighter and jumps higher in [69]. However, the required compressor pump is one of the main disadvantages affecting the payload of wall climbing robots. So, an Electric Linear Actuator (ELA) is potentially better alternative to reduce the weight of these robots. Also, pneumatic cylinders have other disadvantages: high maintenance cost and high energy loss [70, 71].

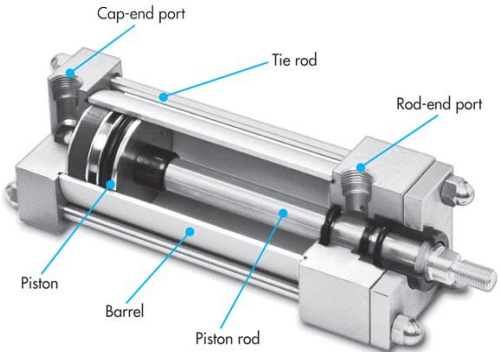

(1) Structure of pneumatic cylinder [65]

(2) Application of Pneumatic cylinders in robot [68]

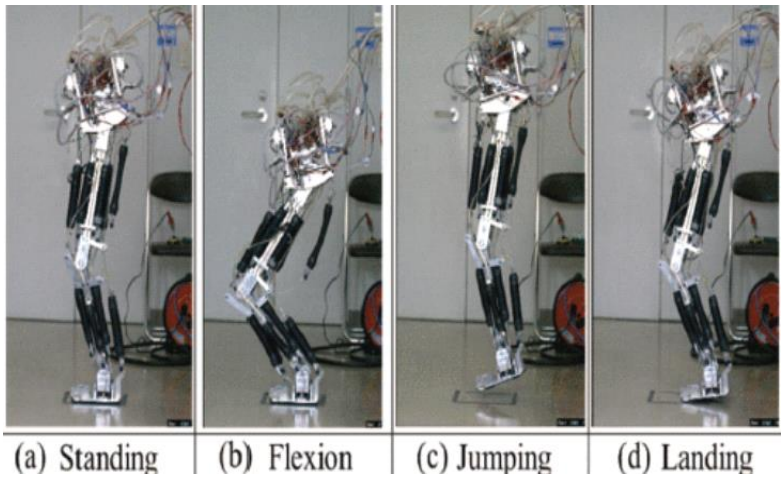

(3) Jumping motions of one-legged jumping robot driven by the pneumatic muscle actuators [69]

Fig. 2.18 Structure and applications of pneumatic actuators

2.3.3 ELA

To reduce the size of a robot, an electric linear motor can play a great role. ELAs have undergone development and now their structures(shown in Figure 2.19(1)) [72], working principles and application abilities [73-75] achieve the hoped for requirements, namely light-weight [76], high torque, continuously variable strokes, in many different kinds of industrial and domestic fields, for example, manufacturing in hospitals, packaging machines [73, 77-80].

In [76] a small linear actuator was devised to meet the requirement of light weight robot. By experiments investigating its characteristics, it can function but is not stable. Also, optimization of the motion of the robot is necessary and was conducted in simulation. Based on the unique characteristics of Cheetaroid [75] (shown in Figure 2.19 (2)): high-velocity moving, a special linear actuation system that is a direct-driven direct-current linear actuator was constructed. It has proved to have high power capacity and maximum actuation force, which can ensure the mobility of Cheetaroid that Byeonghun Na et al. have shown in experiments. In [15] a linear actuator is used to adjust non-contactable permanent magnets to the wall, as indicated in Figure 2.19(3). However, the life span of this actuator is affected by the static friction between the brushes and electrodes.

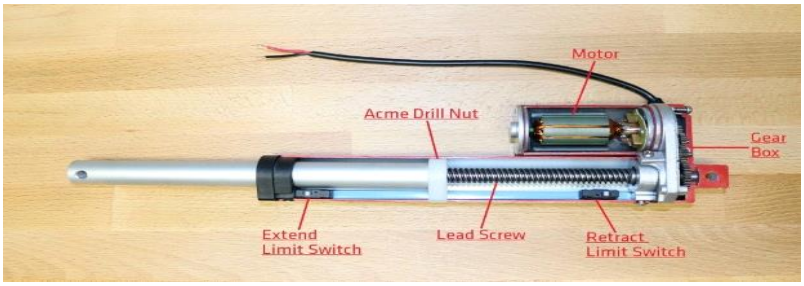

(1) Structure of ELA[72]

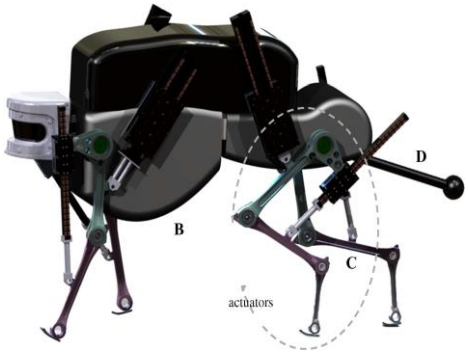

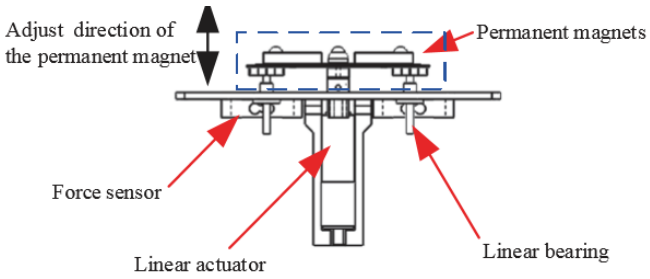

(2) Improve the mobility of Cheetaroid [75]

(3) Control the position of magnets [15]

Fig. 2.19. Structure and applications of ELA

Furthermore, LinMot (shown in Figure 2.20 (1)), which only consists of the stator and the slider, was developed to not include intermediary complements, such as gears, belts or spindles [80-82]. Additionally, LinMot linear motors, provide many great advantages. They are: superb controllability, high thrust forces, amazing and flexible velocity and multi-position [83] , as well as low energy loss and low operating cost, compared to pneumatic cylinders [70, 71, 82] but expensive to make currently. In the automation industry around the world, LinMot linear motors are being implemented into many sorts of equipment, such as Packaging Systems and vacuum supply [83-85], shown in Figure 2.20 (2) (3)).

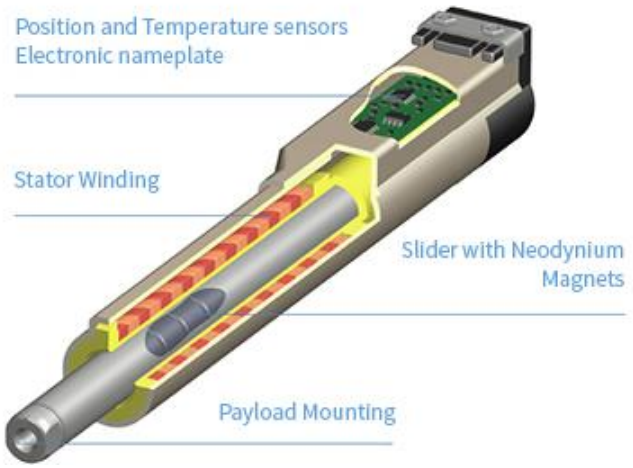

(1) Structure of LinMot linear motor [81]

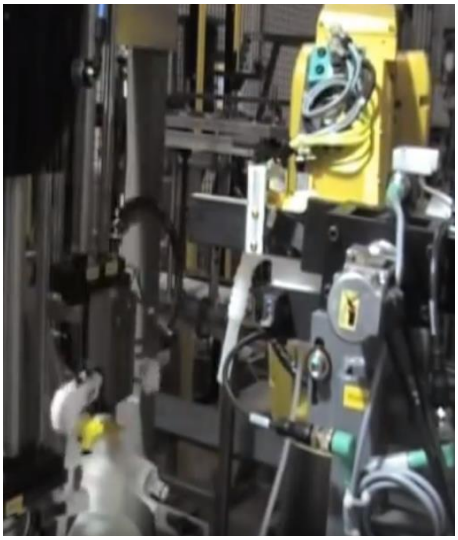

(2) Serve vacuum supply [83]

(3) Screw the lip on the bottle [84]

Fig. 2.20. Structure and applications of LinMot

Table 2.3 compares main common actuation mechanisms:

Table 2.3 Compares main common actuation mechanisms

Categories		pros	cons
Electric motor	Servo	Accurate positioning, high torque, fast control the speed, to keep a constant speed regardless changing loads, light weight [6, 53, 58-61, 86]	Special driving circuit, limited velocity range, keep a stable torque [58, 62, 86]
	Stepper	Simple structure, not requiring gear reduction, precise rotation [23, 55]	Consuming high current, special driving circuit, slow speed, low torque, high weight [55, 57]
Pneumatic cylinder		Light-weight, easy design, safety, fast control velocity, low initial system cost [67] [29, 67]	Requires pressurised air supply or pump. Maintenance cost, high energy loss [70, 71], many appurtenance
Electromechanical linear actuator		Light-weight, high thrust forces, fast and flexible velocity, low energy loss, low operating cost [70, 71, 75, 76, 82, 83]	High initial system cost (LinMot) [70, 71, 82]

2.4 Existing Window Cleaning Robots

Though the view of climbing robots, some research on window cleaning robots are abstracted to make comparisons, as shown in table 2.4:

Table 2.4 Compares main common actuation mechanisms

Robot	Dimension L×b×h (mm)	Weight (kg)	Payload (N)	Speed (mm/s)	Locomotion	Adhesion	Adhesion force(N)
WallWalker [6]	300×300×100	3	No	10	Wheeled	Vacuum (active)	70
Sky Cleaner 3 [29, 87]	1136×736×377	45	588	680	Translation	Vacuum (active)	-
NINJA-1,2 [9]	500×1800×400	45	-	160	Legged	Vacuum (active)	-
Skyscraper's glass cleaning robot [36]	380×540×150	6	6	1.33	Rotating-disc	Vacuum (active)	6kpa
Stickybot [9, 44]	600×200x60	0.37	-	40	Legged	Dry adhesive	-
Geckobot [9, 88]	190×110x20	0.1	-	50	Legged	Dry adhesive	-
A sixteen-legged palm-sized climbing robot [19]	120×110×20	0.115	20	4	translation	Dry adhesive	-
A window cleaning robot [67]	1220×1340×370	30	147	50	translation	Vacuum (active)	147
Windoro [89, 90]	200×200×85	3	-	-	Wheeled	Magnetic	-
DEXTER [91, 92]	365×220×130	3	-	-	Legged	Vacuum (passive)	-
Cleanbot II [26]	720×370×390	22	250	166	Tracked	Vacuum (active)	80kpa

As can be seen in Table 1.4, *Sky Cleaner 3* [29, 87], *a sixteen-legged palm-sized climbing robot* [19], and *a glass cleaning robot* [67] utilise a translation locomotion system. This system is the simplest among all locomotion systems. However, most of these robots using translation locomotion system are larger and heavier as well as have high payload capacity, except these robots using dry adhesion. Those robots, including *Stickybot* [9, 44] and *Geckobot* [9, 88], have the most complicated mechanical structures: legged locomotion systems but having lighter weight.

Active vacuum suction pads are mostly used because of the relatively simple structure, such as in WallWalker [6], Sky Cleaner 3 [29, 87] and NINJA-1,2 [9], et.al. Other robots use dry adhesive [19] [44] [44], passive vacuum [91, 92] or magnetic [89, 90] adhesion systems. Their velocities are either fast or slow, regardless of their structures, but affected by the weight of a robot.

2.5 Summary

Through a review of the literature, this chapter introduces the backgrounds of the three main systems of climbing robots: locomotion system, adhesion system and actuation system. Each of them is divided into various kinds of mechanisms as well as comparing their advantages and disadvantages.

Further, the actuation system is discussed to highlight its function in a climbing robot, such as affecting the payload capacities and adhesion forces. Some research shows the necessity of reducing the number of motors as well as choosing the appropriate specifications for a light weight and a high force/torque. Most importantly, some of existing window cleaning robots from literature are compared in their characteristics, such as payload capacity, locomotion and adhesion systems.

3 Mechanical Design of the Window Cleaning Robot

3.1 Introduction

A review of the literature shows a dramatic increase in the development of robotic technologies to meet an increasing need for climbing robots in different kinds of hazardous environments over the past 20 years [4]. Particular tasks for such climbing robots include cleaning high-rise buildings and examining oil tanks [1, 2] [4, 7-9, 13, 19, 29, 30, 40, 57, 66, 87]. Robots often can work with higher precision and less risk of injury than human operators performing the same task. However, challenges with climbing robots, especially window cleaning robots, also occur, such as limited working terrain, complicated structures of the robot, weight and limited ability to span obstacles. These limitations are gradually being solved with improved relevant technology. To address some of outstanding problems, a design scenario for a window cleaning robotic system is presented and focuses on the locomotive, actuation and necessary adhesive systems. Relevant design options are listed and compared to develop the optimal component for the corresponding sub-systems, as shown in Table 3.1.

Table 3.1 Morphological matrix for sub-systems

	1	2	3	4
Locomotion system	Wheeled 	Legged 	Tracked 	Translation 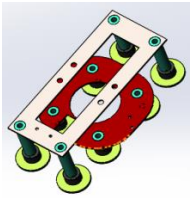
Leg extension system	Electric motor 	Pneumatic cylinder 	ELA 	

leg extension arrangements	Module 1&2 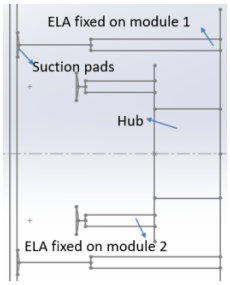	Module 1 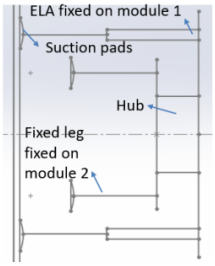	module2 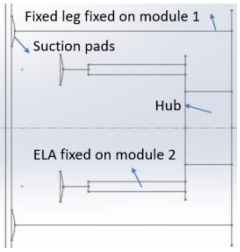	Between the modules 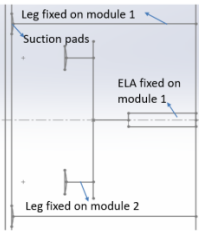
Vacuum adhesion	Active 	Passive 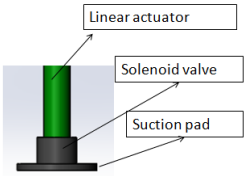	Magnetic 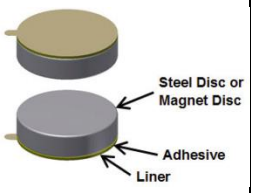	Biomimetic 
Rotational mechanism	A rack and pinion 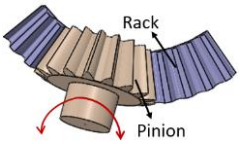	Special hub 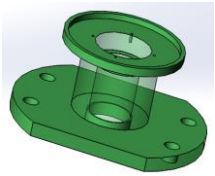		
Bearings arrangements	1st arrangement of bearings 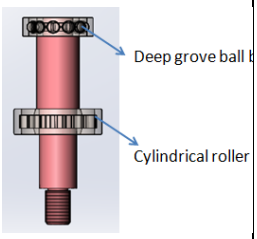	2nd arrangement of bearings 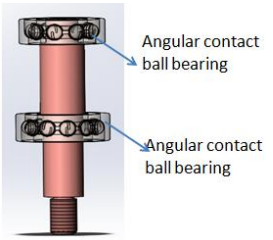	3rd arrangement of bearings 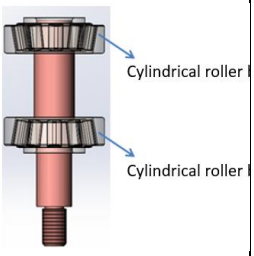	
Contribution of solenoid valve & suction pads	2 solenoid valves & 8 suction pads 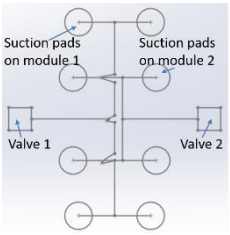	8 solenoid valves & 8 suction pads 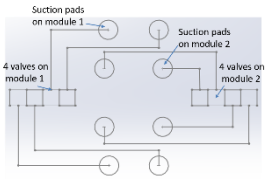	8 valves& 8 suction pads 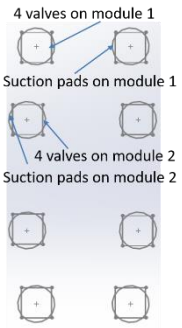	

First, some specific requirements of a window cleaning robot are listed and considered, based on the common considerations of a wall climbing robot.

3.2 Design Requirements

The general considerations of are considered below.

1) Reliable locomotion on various surfaces, regardless of their flatness and composition. In particular, the ability to span different kinds of obstacles is important [13];

2) Reliable adhesion and smooth separation ability, to guarantee the working safety and improve efficiency of climbing robots. Also, sufficient adhesion force to support auxiliary equipment [93, 94] [14];

3) Sufficiently light weight to enable mobility, reliable adhesion, acceptable payload and low power requirements [13, 29, 49].

4) Long life span. A robust robotic structure should ensure this aspect. Also, reducing the wear abrasion of suction pads to keep climbing robots on surfaces even when they are sliding.

5) Simple mechanical structure and control systems to enhance overall reliability of the system and reduce costs.

6) Low fabrication cost.

Further, with respect to a window cleaning robot, there are a number of key technical issues to be emphasized.

First, building a simple and light weight robot is the key to this robotic design. So the following are proposed:

1) To simplify the robotic structure, while still allowing it to overcome obstacles, the preferred locomotion mode will be discussed;

2) Minimising the numbers of actuators, including electric motors, vacuum pumps and linear actuators, will help reduce the weight.

Second, maximising adhesion forces and preventing damage to window glass due to repeated adhesion and separation over a long period are also vital. The factors mentioned above affect the adhesion forces as well as materials, sealing and resistance to wear of suction cups.

Third, the design and choice of every element is vital. In particular how to specify the critical components, how to mount them and how to ensure that there is no interference of the parts of the robot during motion.

Finally, for a window cleaning robot, it is important to minimise any tracks left on the glass by the adhesion system. To achieve this, decreasing the stickiness of adhesive materials or keeping the suction pads from touching surfaces while sliding is essential.

3.3 Conceptual Ideas of Mechanical Design

3.3.1 Assumptions and Assumption

In this project, some assumptions about working circumstance are first given below before considering how to design the locomotion, adhesion and actuation systems:

1) The robot will be designed to work on flat window glass (minimum radius of curvature, $r_{glass} > 3.0m$);

2) The working terrain is defined as a vertically oriented, rectangular window;

3) Working conditions for the robot will be dry and clean glass surfaces;

4) Obstacles to span are assumed to be less than 50mm in height and 20mm in width;

4) The friction coefficient of the rubber adhesion pads on glass is assumed $\mu_f = 1.0$ [95-97].

5) On pressing against a glass surface, the rubber adhesion pads are assumed to expel 60-75% of the air volume to form a vacuum.

6) The actuators on the robot will follow a trapezoidal velocity trajectory (displacement will be linear with parabolic blend.

To clean a rectangular window pane, the robot will follow a path such as that shown in Figure 3.1. This path requires the robot to be able to translate and rotate by 90 degrees.

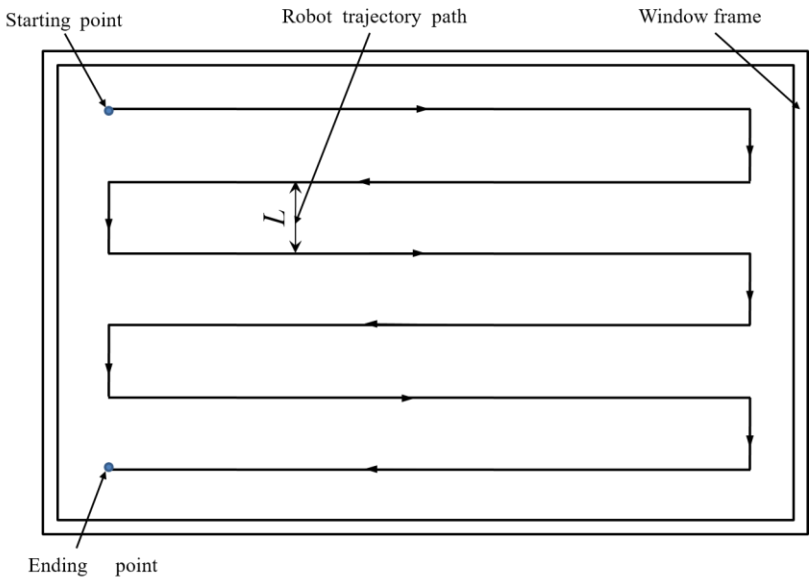

Fig. 3.1. Proposed working area and trajectory on a rectangular window

3.3.2 Preferred Robotic System

In Chapter 2, various kinds of locomotion, adhesion and actuation systems were introduced. However, to decide the best robotic structure, translation locomotion, passive vacuum adhesion and ELA systems will be compared to the others in their individual families. All comparisons and decisions about these preferred systems are based on the characteristics required for this robot to climb on window glass,

3.3.2.1 Preferred Locomotion System

In this part, the two-frame translation mechanism, rather than a wheeled, tracked, or legged mechanism, is chosen because of its simple structure as well as reliable adhesion. Legged mechanisms are ruled out due to the complex design and control with multiple gaits. Wheeled mechanisms, which are a popular robotic structure, will not be chosen even though they are fast and generally very flexible. The main reason is that this system must either incorporate the adhesion pads on the wheels (with a small contact area), use sliding adhesion pads (leaving marks on the window), or use two complementary magnetic modules inside and outside the window. Tracked locomotion would have more reliable adhesion to the surface when suction pads are installed under the tracks or belts due to larger adhesion surfaces. Tracked locomotion can even keep suction pads within the deformable tracks and belts from seriously abrading[8]. However, developing a tracked locomotion system that could reliably navigate obstacles would

result in a robot that was more complex than translation locomotion and heavier than wheeled and legged locomotion systems. Thus, a translation locomotion mechanism for the window cleaning robot is proposed using two modules that can translate and rotate relative to each other, as shown in Figure 3.2.

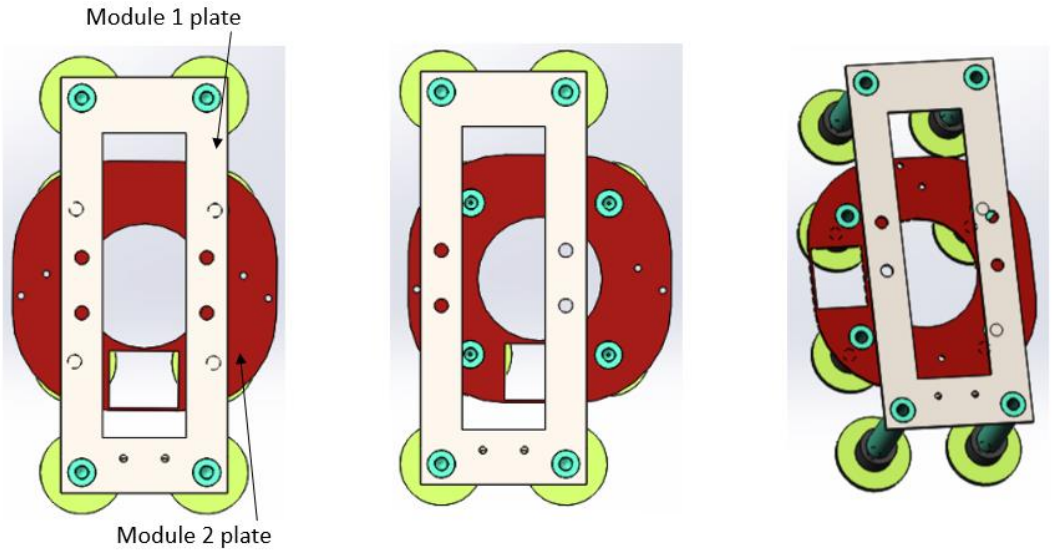

Fig. 3.2. Concept sketch for a translation locomotor consisting of two frames, each with an independent set of suction pad

3.3.2.2 Preferred Adhesion System

Wall climbing robots must robustly adhere to the window glass at all times. To achieve that, large numbers of adhesion devices, such as permanent or electrical magnets, active or passive vacuum suction pads and biomimetical stickers, have been studied and developed to apply to wall climbing robots.

Permanent or electrical magnets can be used for adhesion to the window glass. Complementary sets of magnets are placed inside and outside the window, with the attraction between the sets providing the adhesive force. However, this requires a rather complex system as both sets of magnets must move together, and is limited to relatively thin glass due to the rapid attenuation of the magnetic force through glass. Another alternative adhesion device is biomimetic stickers. The downsides of this mode of adhesion is that it can only provide a small force and the stickers need to be frequently cleaned to maintain performance as these systems are sensitive to the contamination from the environment.

Most current window glass robots use active vacuum adhesion, which can offer sufficient adhesion forces as well as a relatively simple structure. However, they are relatively heavy due to the requirement for an on-board pump. Passive vacuum adhesion is easily activated by using a simpler mechanism to physically press the adhesion pad onto the window glass. As these pads are pressed to the surface, they expel the air in the sealed areas and produce a lower pressure inside than the surrounding atmosphere, resulting in an adhesion force normal to the surface that is proportional to the pressure difference and pad area. However, it is hard to pull passive suction pads away from the window glass. In the following, the active and passive adhesion systems compared for this design.

1. Passive Vacuum Mechanism

A passive vacuum mechanism has the obvious merit of not needing a vacuum pump. Instead, the elastic materials use deformation to generate a vacuum and physically adhere onto the window glass. However, high performance is difficult to achieve as well as robust adhesion forces. Also, detaching the suction pads from the window can be difficult as the vacuum forces need to be overcome. In the following, a passive vacuum adhesion mechanism will be proposed to reduce these drawbacks.

To ensure robust adhesion, many suction pads will be independently attached to the glass, rather than a single, large pad. This configuration means that the robot can maintain reliable adhesion forces even though some of the pads may fail to adhere to the window glass. These pads are fabricated from polyurethane, which has the advantage of withstanding higher elastic loads memory, better resistance to abrasion and air leakage, in comparison to rubber [98]. Furthermore, electro-mechanical solenoid valves will be used to solve the problem of difficult detachment of the adhesive pads. Ports of these valves are connected between the sealed areas of the suction pads and the atmosphere. By activating the solenoid valve, air is allowed into the sealed areas so that the air pressure difference is removed, allowing the pad to be easily detached from the glass. To reduce the risk of the robot falling down due to inadequate adhesion, these valves will be attached directly to each individual suction pad, as shown in Figure 3.3 and Table 3-1 (8 valves & 8 suction pads).

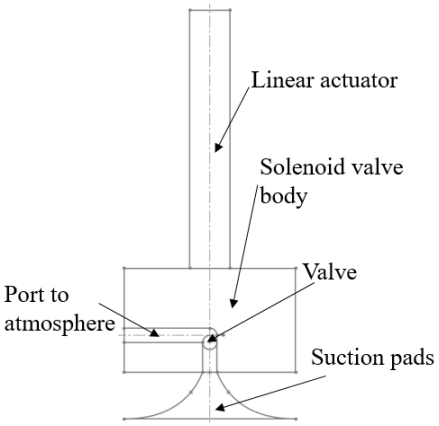

Fig. 3.3. Diagram of the assembly of the suction pad, valve and actuator

2. Active Vacuum Adhesion Mechanism

Active vacuum adhesion has been widely used in window glass cleaning robots (Table 2.4) due to the high adhesion forces that can be achieved. However, there is a significant disadvantage of needing an on-board vacuum pump. To solve this problem, a compressor pump can be mounted on a supporting vehicle on the ground to reduce the weight of the cleaning robot itself [29]. However, a potential problem with this centralised vacuum system is that if one suction pad does not adhere properly, the vacuum to the other pads may be compromised, leading to failure. Another option is a decentralized vacuum system that uses many smaller pumps directly installed on the suction pads to independently control them. Further, multistage low-pressure ejectors replace conventional single-stage ejectors improving the effective working of vacuum supply [98].

Comparing the two vacuum adhesion systems, the passive vacuum adhesion mechanism has lower manufacturing cost and lighter weight than the active vacuum adhesive with the trade off of reduced performance. However, these limitations can be overcome with careful design. Consequently, the passive vacuum adhesive will be the preferred choice for this design.

3.3.2.3 Actuation System

Actuators are required to achieve the necessary motions for this robot. Common actuators for this type of application are rotational electric motors, pneumatic cylinders or electromechanical linear actuators. In the context of this robot’s requirements for motion, the different types of actuators are compared.

The two main modules must move linearly relative to each other, parallel to the window glass. However, the modules must also rotate relative to each other by 90 degree to enable the robot to change direction and follow the desired trajectory, as shown in Figure 3.4.

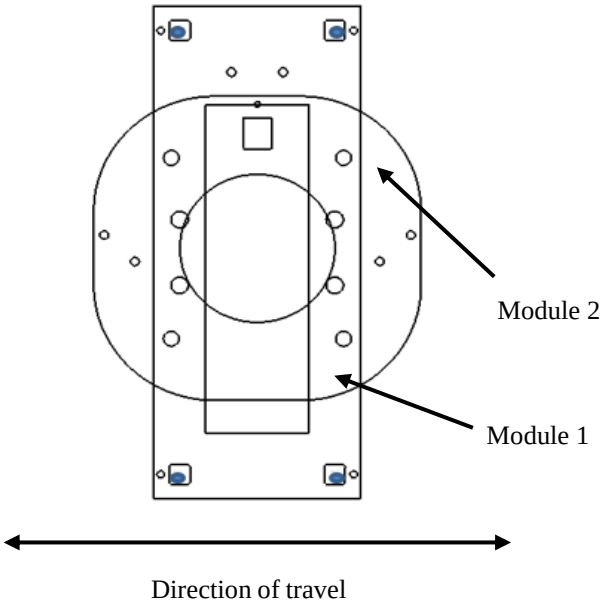

(1) Two main modules move linearly relative to each other

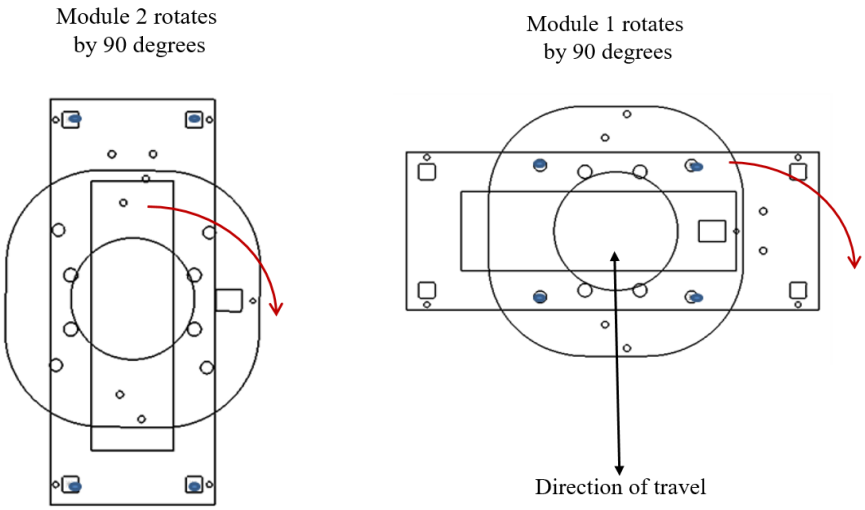

(2) Two modules rotate relative to each other by 90 degree and then do above linear motions

Fig. 3.4. Linear translation and rotation of proposed robot

To successfully achieve this type of motion, the linear actuator system needs to be engaged/disengaged. The simplest way to achieve this requirement would be to use a rack and pinion system driven by an electric servo motor. One motor will be mounted on the module 1

to drive the pinion that will drive the rack installed on the module 2. There is also a need to actuate the rotation of one module relative to the other. Given the rotational motion, an electric servo motor is the obvious choice. Electric servo motors provide the necessary torque and speed in a very small package, with high positional accuracy.

For the linear motion needed to engage/disengage the suction pads with glass during motion, and step over obstacles, there are several options of actuators. An electric motor can transfer a rotary motion into a linear motion with a rack and pinion, but this will complicate the robotic structure. Electromechanical linear actuators have the advantage of higher torque and low weight. Pneumatic cylinders are commonly used with the applications requiring linear motions, but require an air supply.

Pneumatic cylinders and electromechanical linear actuators, are both candidates which can achieve a flexible, quick and long stroke. They will be further compared below and the preferred one will be selected.

1. Pneumatic Cylinder

If a compressed air pump was proposed to serve the active vacuum adhesive, pneumatic cylinders could be used to achieve linear motion with little added complexity. If the pump remains on the ground and is connected to the robot via a tether, weight of the robot itself will be reduced, but the tether may add significant weight itself. Also, in addition to the pneumatic cylinder itself, a pneumatic system would require an air accumulator, air supply and solenoid valves for control.

2. Electromechanical Linear Actuator

The passive vacuum adhesion, without the need of a compressor, is proposed to attach in this robot. An ELA (ELA) is thus the appropriate actuator for a passive vacuum adhesion system as it requires no air supply. Further, for equivalent performance (considering stroke, force and weight), ELAs are typically less expensive, simpler to control, and lighter. That is because ELAs do not require any additional component as pneumatic cylinders. As a result, an ELA would be the more suitable actuator than a pneumatic cylinder.

After evaluating the options, the best choice for translation locomotion system, using passive vacuum adhesion and ELAs with solenoid valves to enable easy engagement/disengagement of suction pads with the glass. This system should be relatively light, simple and inexpensive yet able to complete the required task of moving around a rectangular window.

3.3.3 Development of Translation Locomotion System

In general, this window cleaning robot needs to perform linear motions, 90^0 rotational motions and step over obstacles. Considering the technical issues, the mechanical structures required to achieve each kind of motion will be described after applying the best robotic structure.

3.3.3.1 Linear motion mechanism

For this robot, the linear motion refers to the sliding process parallel to a pane of a window glass. To achieve this, each of the two modules will translate a certain distance via a rack and pinion device. Four independent suction pads per module provide adhesion and ensure that one module remains fixed relative to the glass, while the other moves, as shown in Figure 3.5. The working principle of the linear motion is described as follows:

1) Motor 2, connected with the pinion is fixed on the module 2 plate. The rack and the slider are mounted on the module 1 plate.
2) Motor 2 first rotates the pinion clockwise to drive the module 1, after the suction pads of the module 1 are retracted from the window glass. Throughout this motion, the module 2 is firmly adhered to the window glass, as shown in Figure 3.6 (1).
3) The suction pads of module 1 are engaged, while those of module 2 are disengaged and retracted before it will repeat same linear motions, as shown in Figure 3.6 (2).

Note: One motor can achieve the individual translation of both modules, reducing the number of motors required by other designs that use two sets of actuators. However, the pinion must be retracted to separate it from the rack through another actuator, during interfering the rotational motions, as shown in Figure 3.7.

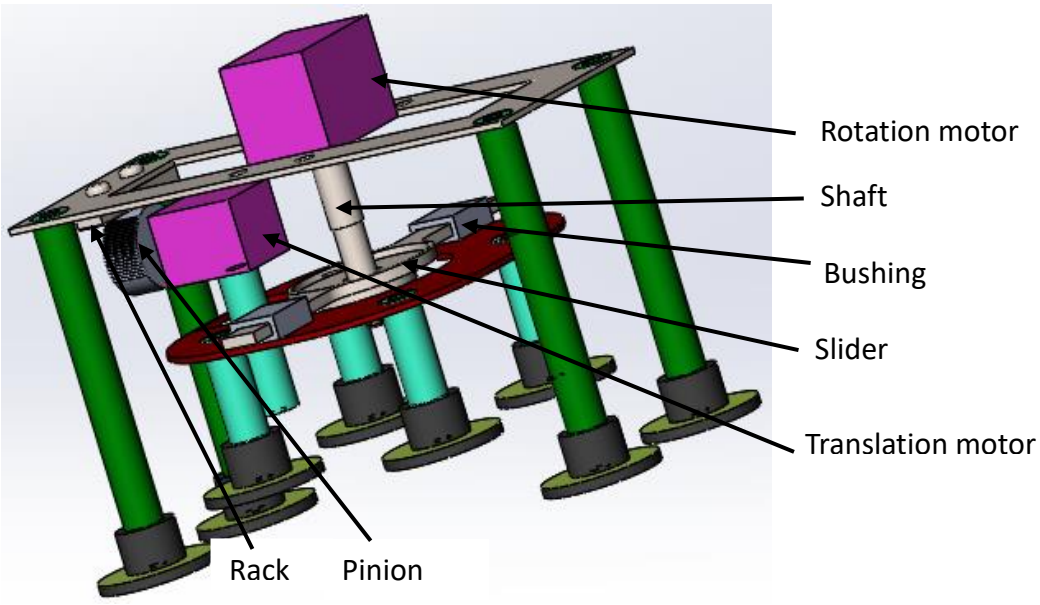

Fig. 3.5. Diagram of the linear motion mechanism

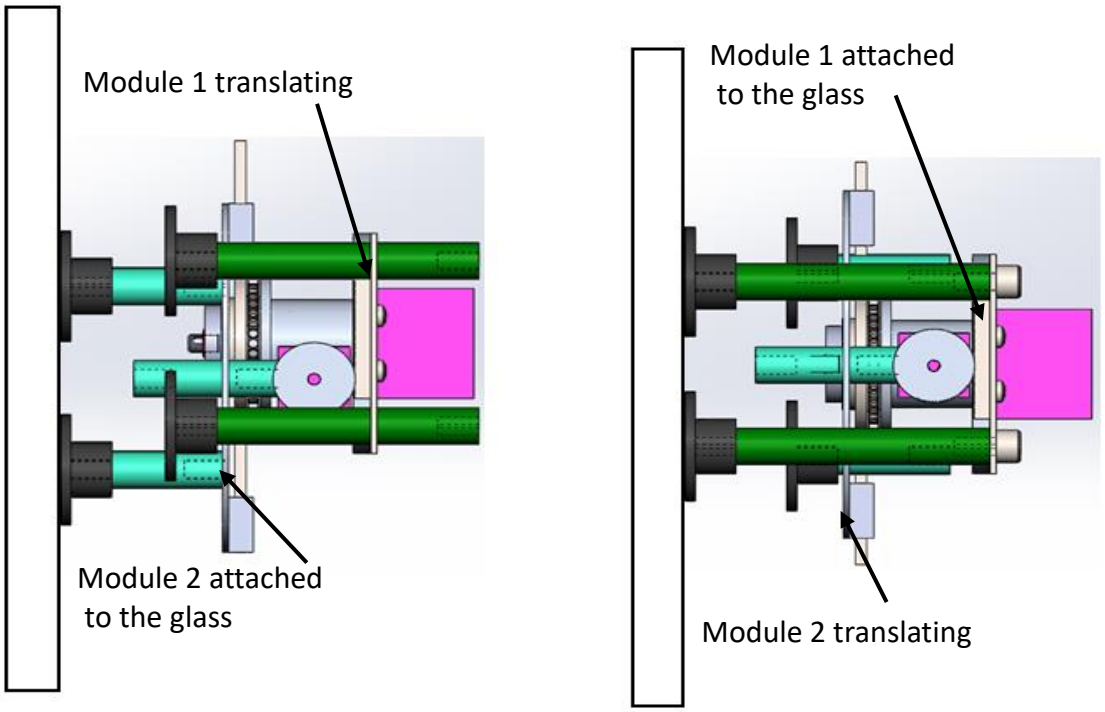

(1) Module 1 is driven after its suction pads detach from the window glass

(2) Module 2 is driven after its suction pads detach from the window glass

Fig. 3.6. Working process of the linear motion mechanism

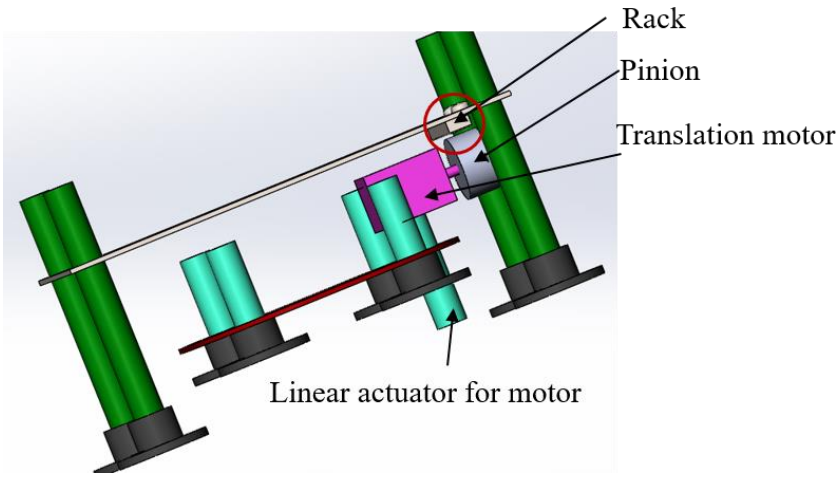

Fig. 3.7. Separate the pinion from the rack

The slider mechanism below shown in Figure 3.8 ensures precise movement and rigidity of the whole structure. The allowable displacement is determined by the length of slider and the positions of the two bushings. With this design, the robot can translate 20mm per step, as shown in Figure 3.9.

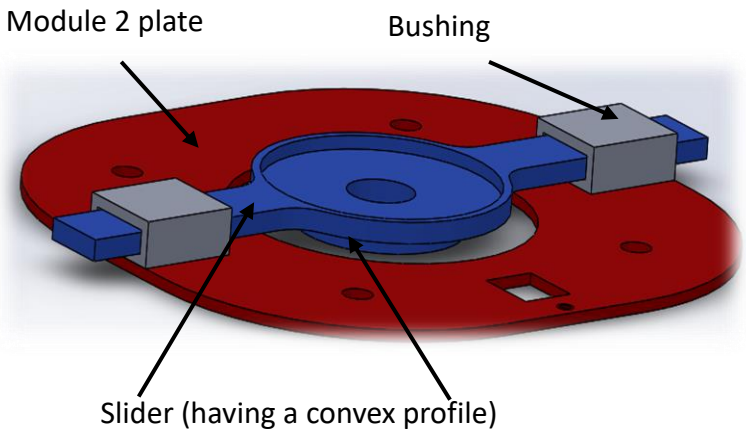

Fig. 3.8. Elements of affecting the displacement

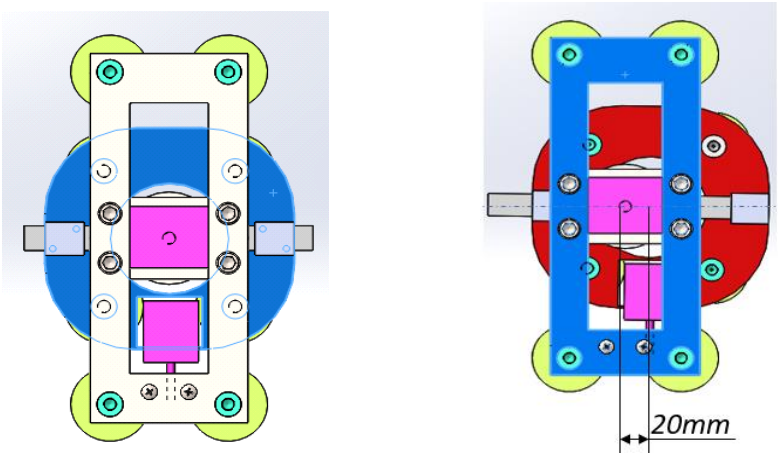

(1) Shape of the unchanged module 2 (10mm) (2) Shape of the changed module 2 (20mm)

Fig. 3.9. Comparisons of unchanged and changed modules

3.3.3.2 Rotational Motion Mechanism

The rotational motion mechanism is designed to allow to drive each module to successively rotate at 90 degrees. To do this, one module must detached from the glass, and the rack and pinion should be separated before initiating the rotation, as shown in Figure 3.7.

1. Rotational hub system

A hub has been designed (Figure 3.10) to enable the relative rotation of the two modules. As shown in Fig 3.11, the rotational mechanism mainly consists of the rotation motor, the hub, the rotational shaft and the slider. The hub is fixed on the module 1 plate via the four capscrews as well as the rotational shaft that mates the shaft of the motor through the hole (shown in Figure 3.12 (1)). Regarding the working process of this robot, the rotational shaft connecting the two modules has to sustain its weight at all times. Therefore, each end of this shaft requires bearings that are capable of carrying radial loads. These bearings are located by a lock nut and lock washer to fix the shaft onto the slider. The hub system transfers rotation motion to another module via the slider/bushing assembly

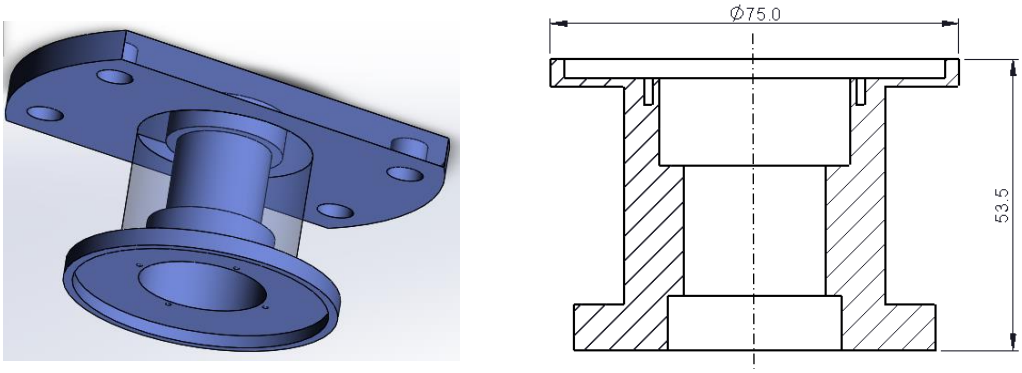

(1) Diagram of the 3D hub (2) Section view of the 2D hub

Fig. 3.10. Diagram and section view of the 3D hub

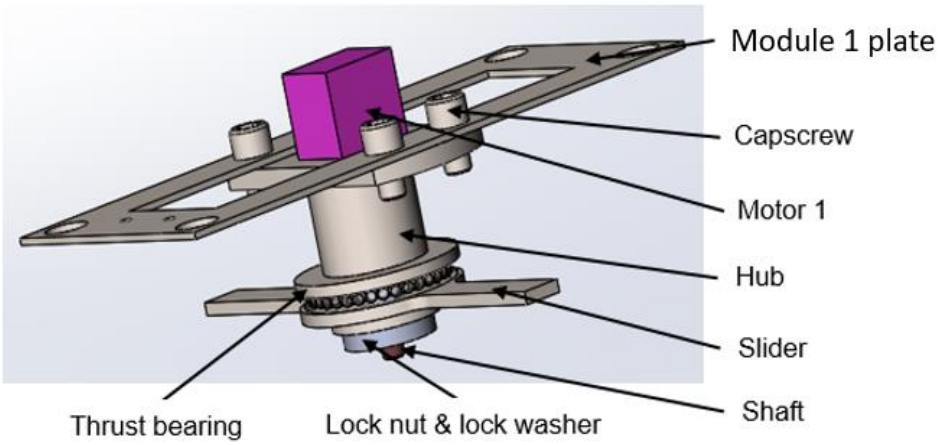

Fig. 3.11. Rotational mechanism having a special hub

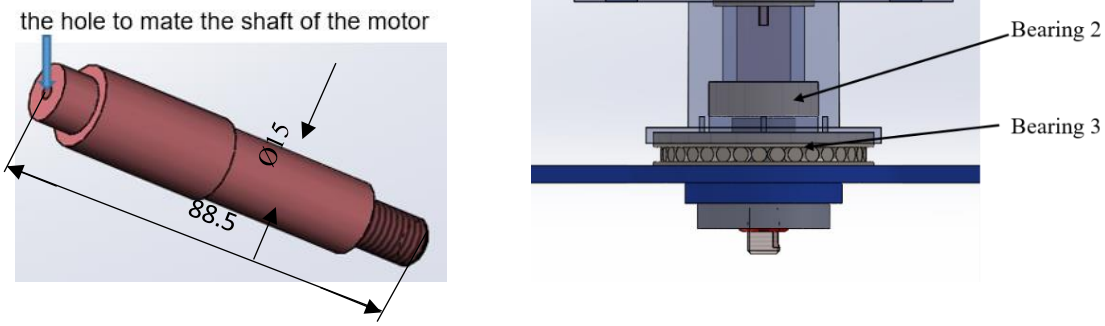

(1) Shaft (2) Bearing arrangements for the shaft

Fig.3.12. Rotational shaft and bearing arrangements

To protect the slim main shaft, selecting appropriate bearings is important. Their positions, combinations and types considerably affect the motion precision, the ability to endure loads

and the life of the spindle [99]. Usually, a shaft is supported by at least two bearings withstanding axial and radical forces at its opposite ends. One end is fixed by fixing or locating bearings, which bear both radial and axial loads. This bearing fixes the relative axial displacement between shaft (spindle) and bearings. Meanwhile, at the end of the shaft, there are free-end or non-locating bearings that only accommodate radial loads. These bearings can move axially so the thermal elongation and contraction of the shaft can be relived[100, 101]. In this robotic structure, three different kinds of bearings arrangement are proposed for 2 bearings to support the shaft within the hub, as indicated in Figure 3.12 (2). In the following section, the three potential bearing arrangements (as shown in Figure 3.13) will be discussed with respect to the key aspects, such as accuracy, withstanding forces, and cost, as shown in Table 3.2 [99] [102]. Additionally, one thrust bearing is needed to allow module 2 to rotate relative to the hub.

First, a common arrangement of a single row deep grove ball bearing and a straight cylindrical roller bearing is proposed [100], applied respectively to the bearing 1, 2. The former bearing can sustain large radial forces and small axial forces especially at higher revolution speeds. The lower cylindrical bearing is suitable for high radial loads at low speeds. That is because the rollers have linear contacts rather than ball bearings which have point contacts [99]. Also, cylindrical roller bearing can permit axial displacements because they are of separable design[101].

Second, two angular contact ball bearings could be used. These bearings carry similar radial and axial loads, but compared to deep grove ball bearings, can support larger axial loads. They are lighter but can carry smaller radial loads than cylindrical bearings. These bearings are usually arranged rigidly in back to back mode to take up titling moments [103]. Also, they are good for the situation where the two bearings are close (L<400mm) with applied moment loads. In this design, the length of the shaft is 90mm approximately and thus this is a good selection [101] [103].

Finally, two taper roll bearings could be used. They have the similar application and arrangement to angular contact bearings but they can carry large loads due to their linear contacts. Also, they are optimal for the accommodation of larger combined loads and further they have a larger axial load capacity, having a larger contact angle [100]. However, they are

relatively heavy, which is not suitable for the requirements of a light weight climbing robot. They also need a locknut and lock washer to provide the required preloads.

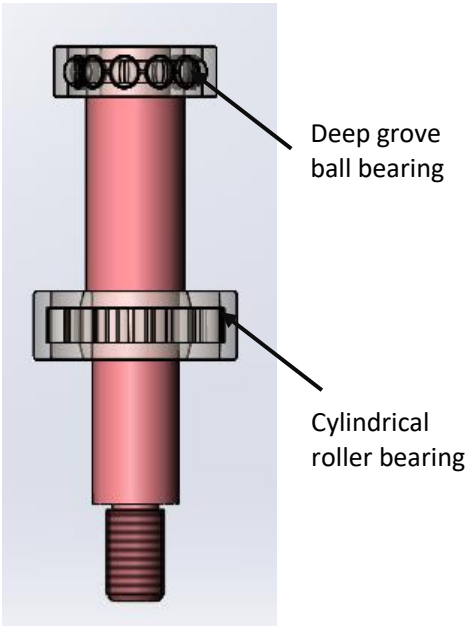

(1) The 1st arrangement of bearings

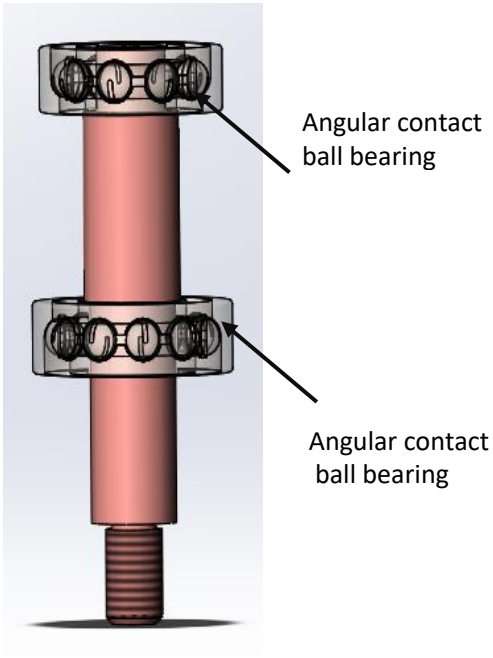

(2) The 2nd arrangement of bearings

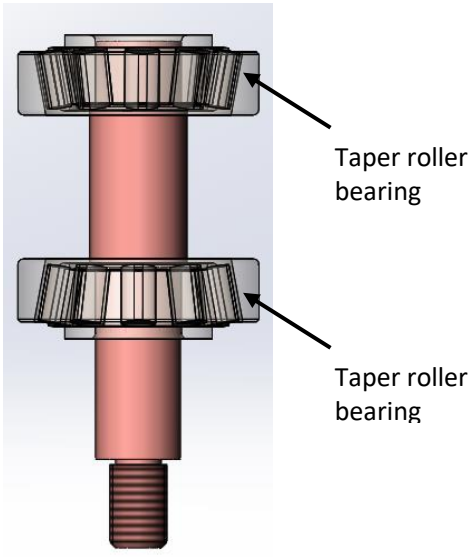

(3) The 3rd arrangement of bearings

Fig.3.13. Three potential bearing-shaft arrangements

Table 3.2 Comparisons of the three arrangements of bearings

	1st arrangement of bearings (deep grove ball bearing and a straight cylindrical roller bearing)	2nd arrangement of bearings (angular contact ball bearing)	3rd arrangement of bearings (taper roll bearings)
Accuracy	Intermediate [102]	Good [102]	Intermediate [102]
Weight	Intermediate	Light	Heavy
Load capacity	Common loads [99]	Middle combined loads [99]	Heavy combined loads [99]
Cost	Low	Low	High

After comparing these scenarios of arranging bearings, the back to back angular contact ball bearings or the back to back taper roll bearings would be the best choices. Once other aspects of the design have been finished, the specific bearing sizes can be selected for calculated loads conditions. If the loads are light, the former arrangement is the preferred one. Otherwise, the latter bearing arrangement is suitable. A thrust bearing should be selected to engage the two modules, as shown in Figure 3.11.

2. Curved Rack Rotational Mechanism

An alternative system to drive the rotational mechanism is a curved rack and pinion (indicated in Figure 3.14). With the rack and pinion each mounted to one of the modules. The pinion can be connected an electric motor to drive one of the modules to rotate relative to the other. However, this is a fairly imprecise system and unnecessary complicated.

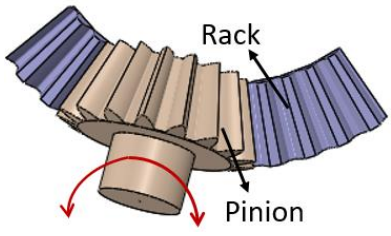

Fig. 3.14. Curved rack and pinion

As a result, in comparison to the structure of the special curved rack and pinion, the structure of the special hub is simpler and stronger. The hub will incorporate with the motor's body

which can be arranged to rotate around the fixed shaft, achieving the required functions. Further, choosing the suitable bearings can protect the rotational shaft and improve its rigidity.

3.3.3.3 Leg Extension/Retraction Motion Mechanism

With legs within the two modules engaging and disengaging with window glass, each module of this robot can thus walk on the even window glass. However, during the robot climbing process, it is common to encounter various obstacles, such as ledges, frames around windows. Based on prior references, legged, wheeled and tracked robots, which have flexible motion mechanisms can easily step over different barrier heights. However robots working on glass windows cannot avoid obstacles as easily as terrestrial robots. That is because glasses are fragile so they cannot carry heavy loads. In this project, avoiding obstacles motions are also completed via the movements of extending/retracting these same legs by ELAS. This leg motions are accomplished by the extension/retraction mechanism (shown in Figure 3.15).

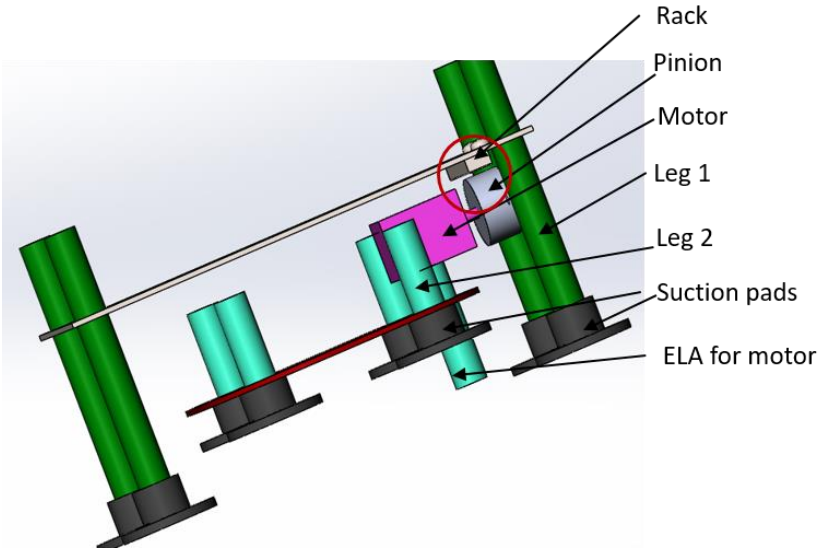

Fig. 3.15. Elements of the interference avoidance motion mechanism

Retracting the suction pads from the glass to enable a step, and avoid any obstacle, is the main function of this subsystem. To achieve this function, the required mechanism only needs 1 DOF (degree of freedom). In this case, the four options of leg extension/retraction are proposed as follows.

1) 8 ELAs, solenoid valves and suction pads, as shown in Figure 3.16 (1). This mechanism can accomplish the obstacle avoidance motion however it is redundant as only 1 DOF is required. So 4 of the ELAs are unnecessary to achieve the desired motion.

2) 4 ELAs are mounted onto one of modules while four fixed legs will be mounted onto another one. The ELAs can be mounted on either of the two modules (Figure 3.16 (2) and (3)). The configuration with the ELAs on module is the most space efficient as the ELAs have a minimum length, so placing them on this module that is the furthest from the glass minimised the standoff distance of the robot.
3) Further, to reduce the number of actuators, one ELA could be placed between the two modules as in Figure 3.16 (4). However, in this case, the positioning will affect the functioning of the hub.

Thus, the leg extension arrangement in Figure 3.16 (2) is preferred for this design as it requires the ELA having a fixed minimum length.

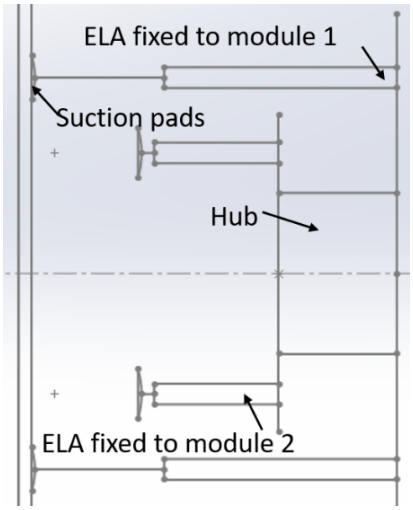

(1) ELA Fixed to Module 1 and 2

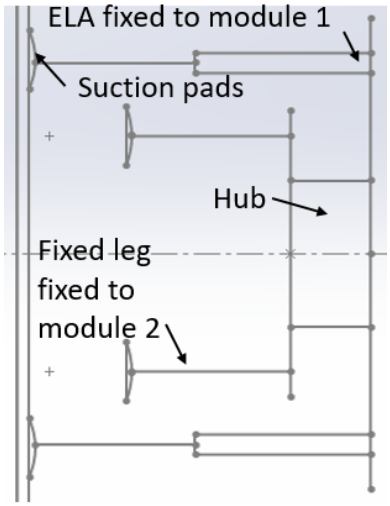

(2) ELA Fixed to Module 1 and Fixed Legs on Module 2

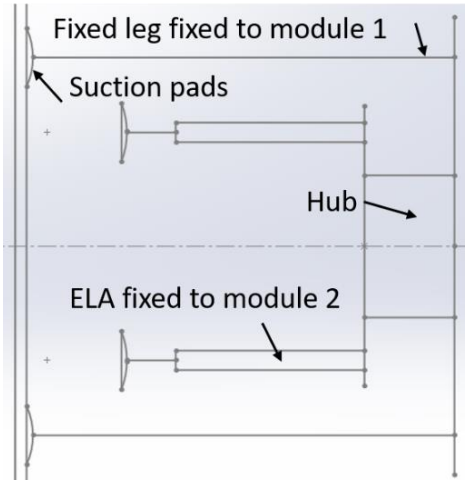

(3) ELA Fixed to Module 2 and Fixed Legs on Module 1

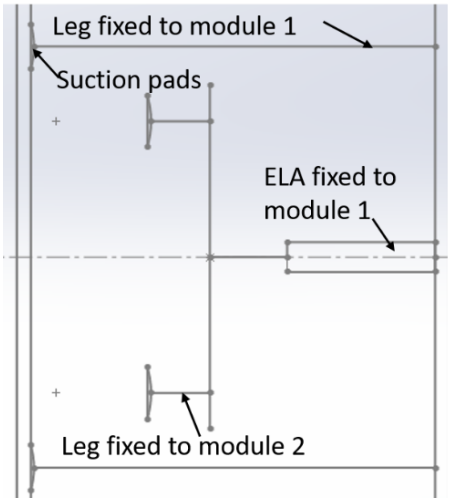

(4) ELA Fixed between Module 1 and 2

Fig. 3.16. Options of Leg Extension Arrangement

During these attachments and detachments movements, the attachment is easier than the detachment. This is because the adhesion forces will be easily created by physically pressing the suction pads attached to the locomotive system onto the smooth surface. Detaching these pads is difficult to physically achieve. However, retracting them will occur quickly by connecting the normally closed 2-position electromechanical solenoid valves with them, as shown in Figure 3.17. The valves will only be turned on when the suction pads are retracted from the window glass otherwise they are closed. When the valves open, they create a path from the suction pads to atmosphere, relieving the vacuum.

Further, there are several options of how to install the solenoid valves to the suction pads.

(1) Each module has only one solenoid valve to control the four suction pads, as shown in Figure 3.18 (1). However, the robot will have a high risk of falling from the window glass if one of the suction pads fails attach properly as these suction pads all share one connection, so will be vented to atmosphere.

(2) Attaching more small suction pads decreases their diameters, as shown in 3.18 (2). However, attaching one valve to control them in each module, if one of these fails to stick, all of them fail as there is a path from all suction pads to atmosphere (as per point (1)). With a larger number of pads, there is a higher chance that one will not attach properly, and that the entire system will fail.

(3) Another alternative is to add solenoid valves to individually control each of the four suction pads, but located distant from the pads as shown in Figure 3.18 (3). The downside is bulk attached to legs and weight of valves but small light valves are available for low pressure. Also, a manifold is where several pipes join not just a bank of valves.

(4) These solenoid valves are directly installed between the ELAs and suction pads, all above disadvantages can be avoided, as shown in Figure 3.18 (4). Thus, this last scenario is proposed.

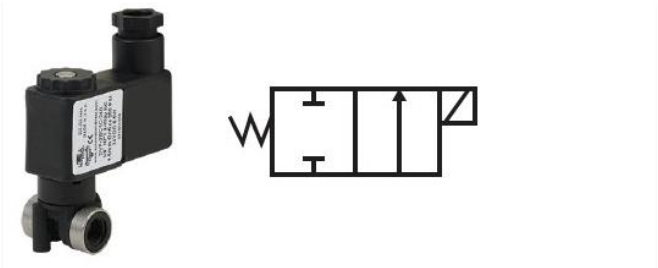

Figure 5B: 2-way, 2-position, normally closed direct-acting solenoid valve, spring return

Fig. 3.17. Two way, two position, normally closed solenoid valve

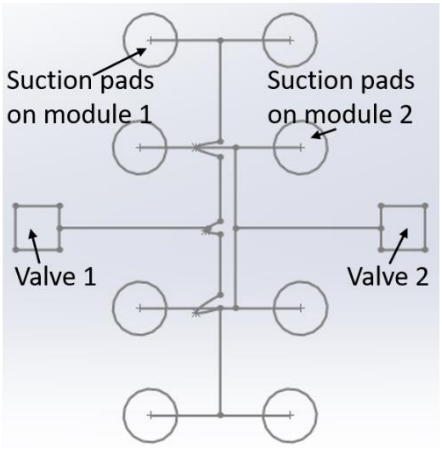

(1) 2 solenoid valves controlling 8 suction pads

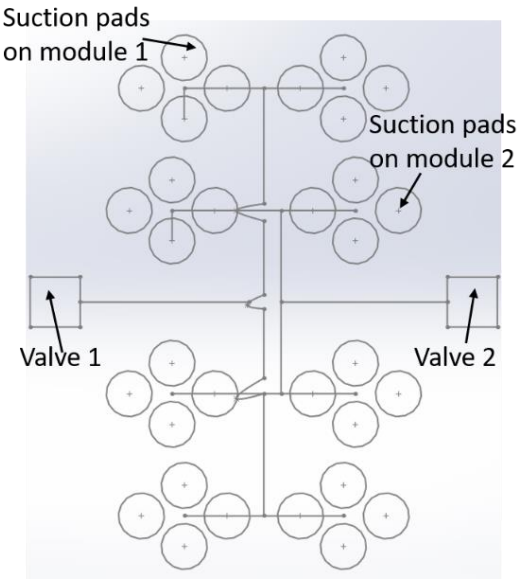

2) 2 solenoid valves controlling 32 suction pads

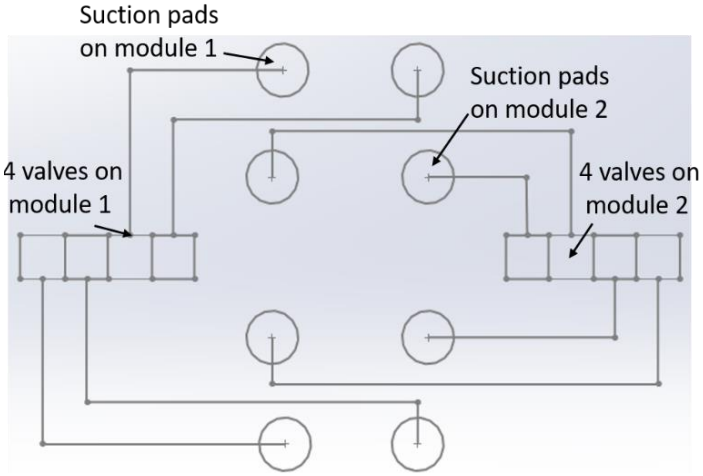

(3) 8 solenoid valves distantly controlling 8 suction pads

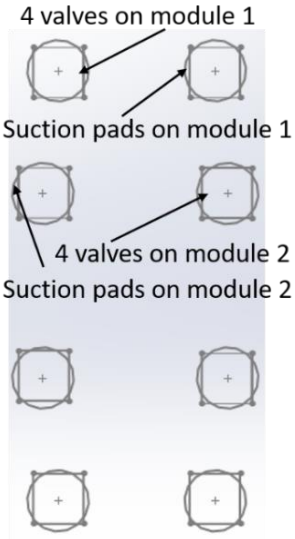

(4) 8 solenoid valves controlling 8 suction pads

Fig. 3.18. Options of leg extension arrangement

3.3.3.4 Interference Avoidance Motion Mechanism

The function of the interference avoidance mechanism is to change the direction of motion of the robot. To allow the two modules to rotate, the pinion must disengage from the rack, which can be accomplished by the use of an ELA. This mechanism mainly includes a servo motor, an ELA and the pinion gear, as shown in Figure 3.15. In this design, one of modules rotates with respect to the other only after the rack and pinion separates. The required displacement is small,

only greater than the height of the rack teeth. Under the demands of a light weight robot, an ELA, which will be attached to pillar 3, is as suitable choice of actuator with 10mm of the maximum stroke.

3.4 Conclusions

So far, all the mechanical design concepts for this window cleaning robot have been discussed and then decisions made according to the design requirements. The proposed robot will be designed using the simple translation locomotion system. The linear motions will be achieved by using a DC servo motor to drive a rack and pinion gear. The rotational motions will be accomplished by a hub and a DC servo motor. The two motions above are all assisted by the leg extension/retraction motion using 4 ELAs to attach or detach the passive suction pads from window glass. Also, the interference avoidance motion needs to perform before the rotational motions. Next, further calculations from kinematic and dynamic analysis will help choose suitable actuators and adhesion suckers and decide the final robotic structure.

4 Analysis of Robotic Structure

The robot consists of the two modules to achieve the three main motions described in Chapter 3. For this design, the linear motion parallel to the window glass and the rotational motion perpendicular to the window glass have to occur in condition with the leg extending/retracting motion. To ensure the reliability of these robotic, kinematic analysis such as velocity and acceleration calculations, and dynamic analysis such as adhesion and motor forces, are important.

4.1 Kinematic and Dynamic Analysis for Adhesion Forces

To ensure that the robot can remain attached to the window while it moves analysis of the minimum required adhesion forces are necessary. This analysis must extend beyond the static case, to include forces that result from the accelerations of the robot modules as they move. One important configuration of the robot is shown in Figure 4.1.

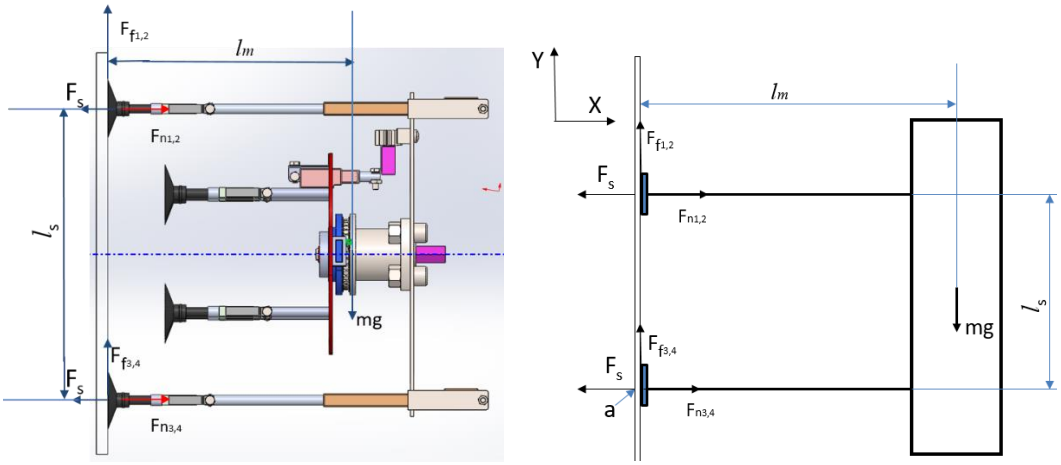

(1) Potential robotic structure (2) Simplified free body diagram

Fig. 4.1. Analysis of kinds of forces for preventing the robot falling down

In the static analysis, the suction pads of each module adhere to the window glass. In the worst case, the resultant section forces of the top legs are affected by three main factors. And these results are from the application of Static Equilibrium Conditions, as shown in Equations (4.1-4.3).

$$\Sigma F_x = 0 \qquad (4.1)$$

$$\Sigma F_y = 0 \tag{4.2}$$

$$\Sigma T_a = 0 \tag{4.3}$$

Where

$\sum F_{x,y}$ are all forces acting on a body in the horizontal(x)/vertical(y) direction for equilibrium states, *N*;

$\sum T_a$ are all torques about a point for equilibrium states, *Nm*;

The theoretical adhesion force is the same for both suction pads, but the resultant force exerted by the robot on the top legs will be different than the bottom legs. The reason is that the mass of the robot is some distance from the point of attachment of the glass, so the top legs must resist the moment trying to roll the robot off the window. Based on the above Static Equilibrium Condition, Equations (4.4-4.6) are correspondingly obtained below:

$$(F_{s1,2} - F_{n1,2}) + (F_{f3,4} - F_{n3,4}) = 0 \tag{4.4}$$

$$mg = F_{f1,2} + F_{f3,4} \tag{4.5}$$

$$mgl_m = (F_{s1,2} - F_{n1,2})l_s \tag{4.6}$$

Where

F_s is the suction force of each leg, *N*;

F_n is the normal force of each leg, *N*;

F_f is the friction force of each leg, *N*;

m is the mass of the robot, *kg*;

l_m is the distance between the centre of the robot and the window glass, *m*;

l_s is the vertical distance between the adhering suction pads, *m*.

Then, assuming Coulomb friction in a stationary condition, the friction forces of these suction pads can be indicated in Equations (4.7), (4.8).

$$F_{f1,2} = \mu F_{n1,2} \tag{4.7}$$

$$F_{f1,2} = \mu F_{n3,4} \tag{4.8}$$

μ is the coefficient of static friction and is assumed $\mu=1$. Substituting Equations (4.7), (4.8) into Equations (4.5), then Equation (4.9) is achieved.

$$F_{n1,2} + F_{n3,4} = mg \tag{4.9}$$

Next, substituting Equations (4.9) into Equations (4.4), then Equation (4.10) is achieved.

$$F_{s1,2} + F_{s3,4} = mg \tag{4.10}$$

In the worst-case, as the robot rotates off the glass, the resultant reaction of the normal forces on the top legs is $F_{n1,2}=0$. Generally, the adhesion forces on each of the two top legs are same. Substituting this value into Equation (4.6), the required adhesion forces on each top one should achieve the value from Equation (4.11).

$$F_s \geq \frac{mgl_m}{2l_s} \tag{4.11}$$

There are four possible configurations to consider for performing this calculation. These states depend on the state of the robot (module 1 or module 2 suction pads attached), and the orientation of the robot, as shown in Figure 4.2.

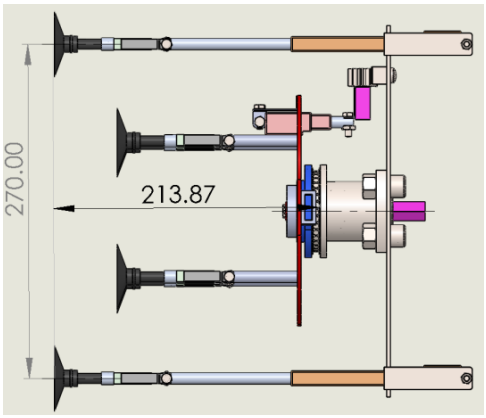

(1) 1st state of suction pads

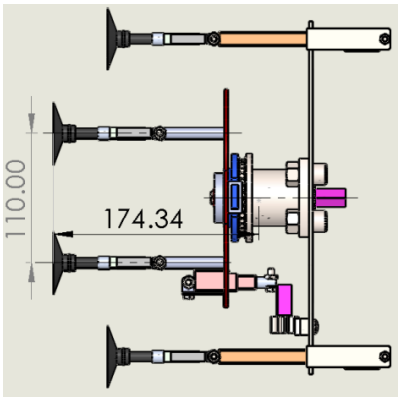

(2) 2nd state of suction pads

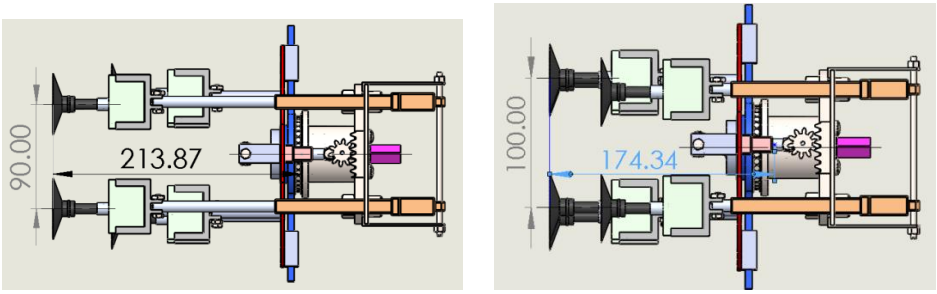

(3) 3rd state of suction pads (4) 4th state of suction pads

Fig. 4.2. Four states of the suction pads

Note: The Canter of Mass is determined from the 3D model in Solidworks.

where

$$m=2.25kg$$

$$g=9.8N/kg$$

Consequently, comparing the above four configurations (as shown in Figure 4.2), the different values of l_m and l_s are shown in Table 4.1, as well as the four outcomes for the minimum adhesion forces:

Table 4.1 Four outcomes of the adhesion force

State of suction pads	l_m(mm)	l_s (mm)	F_s (N)
(1)	*213.87*	*270*	*8.7*
(2)	*174.34*	*110*	*17.5*
(3)	*213.87*	*90*	*26.2*
(4)	*174.34*	*100*	*19.2*

Comparing to the other states, the 3rd state in Figure 4.2 has the maximum adhesion forces. The reason is that it presents the minimum distance of the suction pads l_s and the maximum distance l_m between the centre of the robot and the glass. Thus, the maximum adhesion force is obtained:

$$F_s>26.2N$$

4.2 Kinematic Analysis in the Leg Extension/retraction Motion

4.2.1 Leg Extension/Retraction Motions of Suction Pads

In this project, ELAs will be used to actuate the legs of module 1 as mentioned in Chapter 3. The four ELAs, having the maximum stroke of 100mm enable the robot to overcome barriers up to 50mm high. These actuators will be mounted onto module 1 to reduce the required length of the fixed legs attached to module 2, as shown in Figure 4.3. By extending or retracting these 4 ELAs simultaneously, the 8 legs (2 groups of 4) can be extended/retracted to engage/disengage with the window glass.

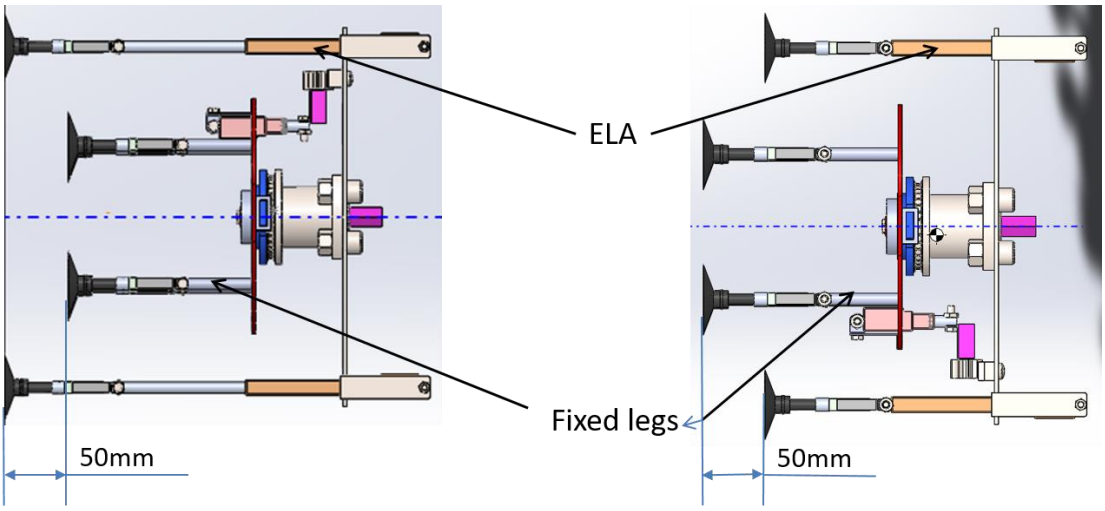

(1) Suction pads of module 2 are retraced while suction pads of module 1 are adhering to the window glass

(2) Suction pads of module 1 are retraced while suction pads of module 2 are adhering to the window glass

Fig. 4.3. The status of the suction pads during extension/retraction motion

The L12 Series ELA from Actuonix (Actuonix Motion Devices, Canada), with a stroke of 100mm, is a suitable actuator. This ELA uses DC motor and lead screw to achieve linear motion. Figure 4.4 and Table 4.2 show a diagram and the specifications of this actuator.

Fig. 4.4. 100mm L12 actuator size of Actuonix's L series

Table 4.2 Electric linear actuators mounted on module 1

Max Force	80*N* (lifted)
Max Side Load	15N(extended)
Input voltage	12VDC
Max Input Voltage	13.5V
Stall Current	185mA
Speed	4.5*mm/s* (36N)
Stroke	100mm
Closed Length	152mm(hole to hole)
Operation temperature	.10°C ~ +50°C

The specification of an electric linear actuator will be influenced by the height of the steps that the robot must move to span obstacles without collision. To span higher obstacles, the actuators must have longer shafts. However, the longer the stroke of the actuator is, the lower the maximum side loads are that can be tolerated. Therefore, it is necessary to consider whether or not the ELAs are strong enough to hold the side forces. In this robotic structure, its weight causes a total side load 22.05*N*, on the four legs in per module. Thus, each leg is required to support side loads of at least *7.84N*. The Actuator L12 actuator, has the max side load of *15N* at its maximum extension (Table 4.2). This side load capacity is enough to support the weight of the robot.

In Table 4.1, the minimum adhesion force (*Fs>26.2N*) for each suction pad has been determined. Suction pads for this robot need to provide minimum adhesion force, and operate with the lifting direction parallel to the glass. The available space for the pads dictates a maximum diameter of *50m*. Based on properties of adhesion material found in literature [98], passive suction pads can be designed, as shown in Figure 4.5. It is assumed *75%* air of the sealed area can be cleared.

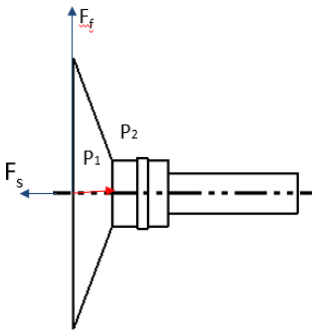

Fig. 4.5. Status of the suction pads

Generally, the pressure difference within a suction pads multiples its areas touching the adhering surface equal to the adhesion force. This relationship is show in Equation (4.12).

$$F_s = (P_2 - P_1)A \tag{4.12}$$

F_s is the adhesion force on the suction pads in N;

P_2 is the standard atmosphere in bar;

P_1 is the vacuum atmosphere in bar;

A is the sealed area in square meter.

where

$$P_2 = 1bar$$

$$P_1 = 0.25bar$$

$$A = 0.00196m^2$$

Then, the value of the suction force is achieved.

$$F_s = 147.19N$$

This suction force is equal to the normal force N. So, the shear force on this suction pad can be calculated via Equations (4.7), (4.8),

Thus, this suction pad can provide the friction force below.

$$F_f = 147.19N$$

The value is considerately greater than the weight of the robot 22.05N. For this robot, the total friction forces of the suction pads in each module are used to hold its weight. As a result, each suction pad has enough ability to hold the robot on the window glass, and thus it is reliable. The design for each suction pad is shown in Figure 4.6.

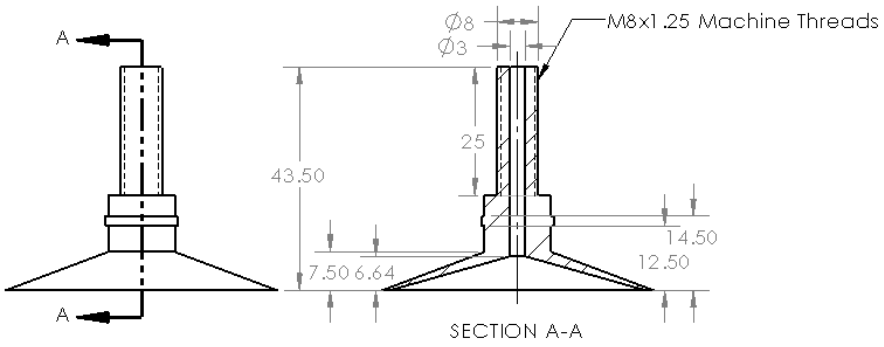

Fig. 4.6. Diagram of designed suction pads

As mentioned before, one solenoid valve will connect with each of the 8 pads by one adapter to easily break the vacuum within them. A high-speed, 2 port SMC solenoid valve SX10 Series is proposed. The dimensions are shown in Figure 4.7. It is screw mount type as well as always closed. Meanwhile, the adapter is shown in Figure 4.8 as the bracket is used to connect the solenoid valve with the ELA (T 4.2).

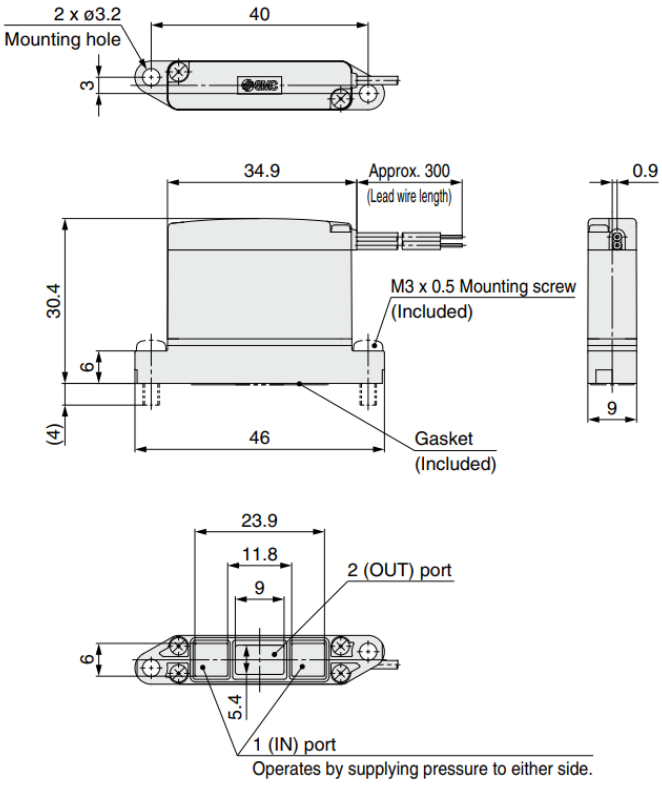

Fig. 4.7. Diagrams and dimensions of the SMC (SX10 Series) solenoid valve

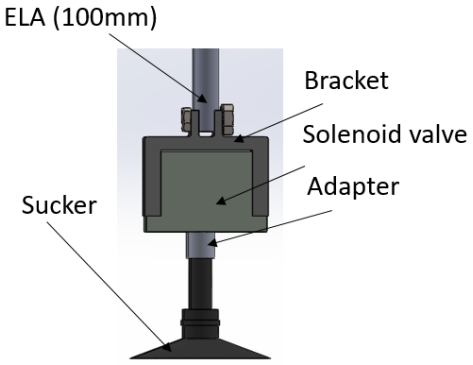

Fig. 4.8. Assembly of the ELA, solenoid valve and suction pads

4.2.2 Leg Extension/Retraction Motions of Pinion

A rack and pinion will drive the relative motion of the modules to move linearly, parallel to the window glass. However, to avoid interferences, the rack and pinion will have to separate before the robot rotates. This is because they are coupled so as to drive the linear motion of this coupling prevents the two modules from rotating relative to each other. Retracting the pinion to a certain distance can be achieved by an ELA. The distance should be greater than the teeth depth of the pinion. However, the depth has to be confirmed to choose the specification of the ELA after designing the rack and pinion. It will be approximately 10mm to allow the use of a short ELA.

4.3 Forces Analysis in the Linear and Rotational Motions

The linear and rotational motions are assumed to occur with a displacement that is linear with parabolic blends, resulting in a trapezoidal velocity profile [104]. An example of a displacement profile is shown in Figure 4.9. This graph has the two parabolic blends at its two ends with a linear section between them. Note, Q is the generalized coordinate for displacement which represents linear displacement x and angular displacement θ. Therefore, $\dot{Q}$ and $\ddot{Q}$ represent generalized velocity and acceleration and their plots are shown separately in Figures 4.10, 4.11.

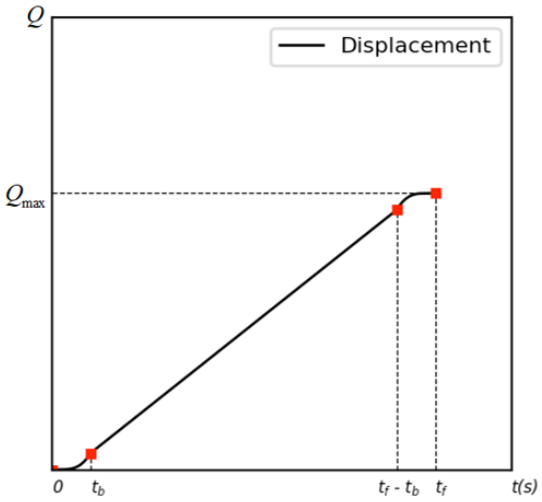

Q-Displacement of the robot , *m or* ^{0}; Q_{max}-The maximum displacement is equal to, *m or* ^{0};

t_f-the whole moving period, *s*; t_b-The start point of changing into the oblique line, *s*

Fig. 4.9. Linear with parabolic blend displacement profile

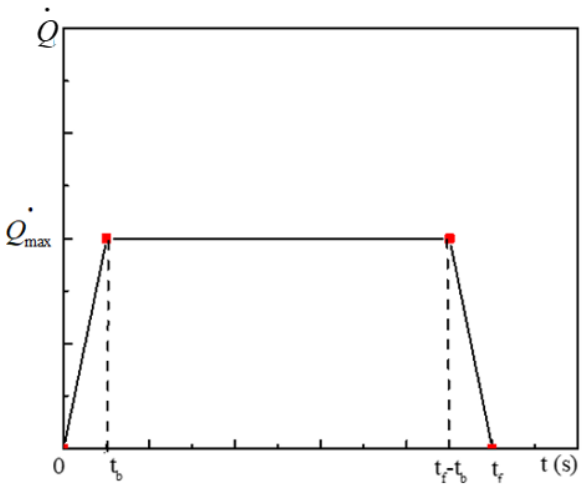

$\dot{Q}$ -Velocity of the robot , m/s or ^{0}/*s*; $\dot{Q}_{max}$ -The maximum velocity is equal to, m/s or ^{0}/s;

t_f-The whole moving period, *s*; t_b-The start point of achieving the maximum speed, *s*

Fig. 4.10. Plot of the velocity of linear with parabolic blend displacement

Considering the enclosed area at the maximum velocity $\dot{Q}_{\max}$ shown in the plot of the velocity (in Figure 4.10 [104]), the equation of the displacement of this profile is obtained in Equation 4.13:

$$Q = \frac{\dot{Q}_{\max}}{2} \cdot t_b + \dot{Q}_{\max} \cdot (t_f - 2t_b) + \frac{\dot{Q}_{\max}}{2} \cdot t_b \qquad (4.13)$$

$\dot{Q}_{\max}$ is the maximum velocity during the whole motions, *m/s or* ^{o}*/s;*

Q is the displacement of the whole motions, *m* or ^{o};

t_f is the whole moving period, *s*;

t_b is the specific point of accelerating the maximum velocity, *s*.

Further, the maximum velocity can be determined in Equation (4.14)

$$\dot{Q}_{\max} = \frac{Q}{t_f - t_b} \tag{4.14}$$

Then we can obtain Equations (4.15), (4.16) and (4.17) of velocity ($\dot{Q}$) during the three phases.

$$\dot{Q} = \frac{\dot{Q}_{\max}}{t_b} \cdot t \qquad (0 \le t < t_b) \tag{4.15}$$

$$\dot{Q} = \dot{Q}_{\max} \qquad (t_b \le t < (t_f - t_b)) \tag{4.16}$$

$$\dot{Q} = -\frac{\dot{Q}_{\max}}{t_b} \cdot (t - t_f) \qquad ((t_f - t_b) \le t < t_f) \tag{4.17}$$

Also, the three corresponding acceleration Equations (4.18-4.20) are obtained below and its graph of the three periods is shown in Figure 4.11

$$\ddot{Q} = \ddot{Q}_{\max} \qquad (0 \le t < t_b) \tag{4.18}$$

$$\ddot{Q} = 0 \qquad (t_b \le t < (t_f - t_b)) \tag{4.19}$$

$$\ddot{Q} = -\ddot{Q}_{\max} \qquad ((t_f - t_b) \le t < t_f) \tag{4.20}$$

$\ddot{D}$ is the acceleration of the robot, m/s^2 or $^{o}/s^2$;

$\ddot{D}_{\max}$ is the maximum acceleration of the robot, m/s^2 or $^{o}/s^2$.

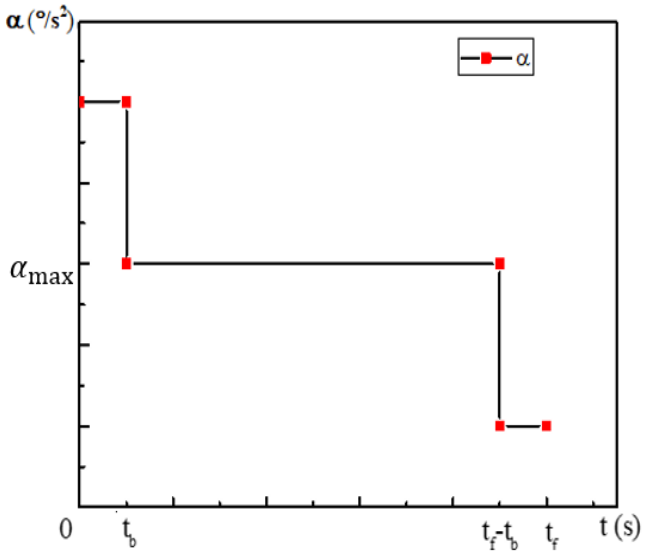

Fig. 4.11. Plot of the acceleration

Torque of moment and Force can be calculated by Newtons Second Law (shown in Equation (4.21), using the values of the acceleration, moment of inertial and mass. In the following, there are the corresponding calculations of the dynamic forces to choose the available actuators in rotational and linear motions.

$$T = I \cdot \ddot{\theta} \qquad F = ma \qquad (4.21)$$

4.3.1 Rotational Motions

To enable the robot to change direction, the modules can rotate relative to each other. This rotational motion requires a torque, which must be reacted by the suction pads at the glass. It is important to know that this torque will not cause the robot to fall off the window. When module 2 (shown in Figure 4.12) rotates, the suction pads of module 1 are attached to the glass, as shown in Figure 4.13. Likewise, when module 1 (shown in Figure 4.14) rotates, the suction pads of module 2 attached to the glass, as shown in Figure 4.15.

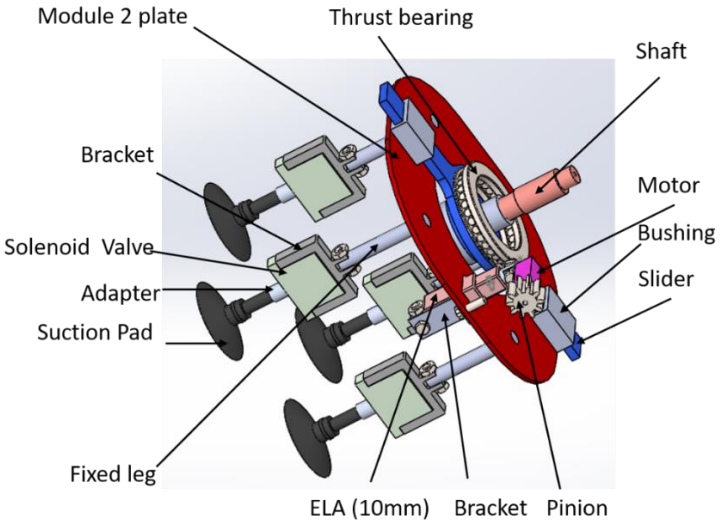

Fig. 4.12. Diagram of the rotating components of module 2

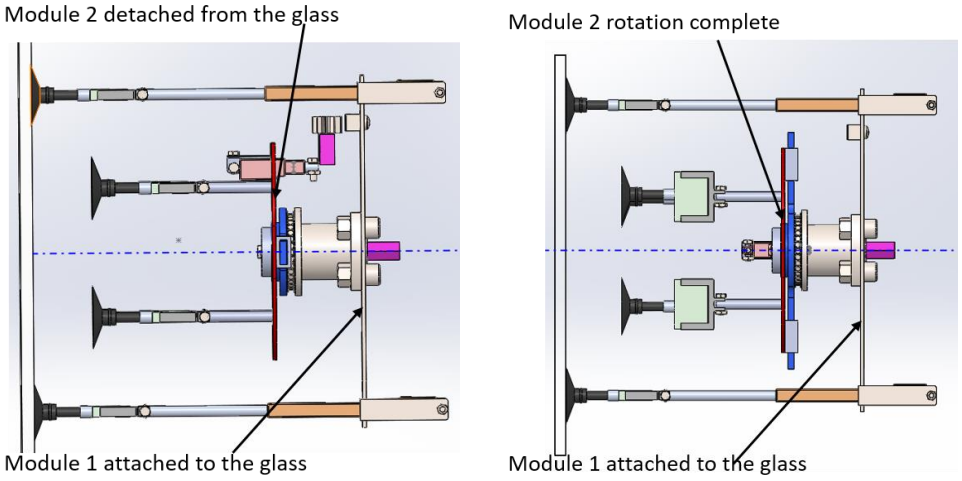

(1) Module 1 is adhering to the window glass when module 2 is about to rotate

(2) Module 1 is adhering to the window glass when module 2 has completed rotation

Fig. 4.13. Rotational motion of module 2 with module 1 attached to the glass

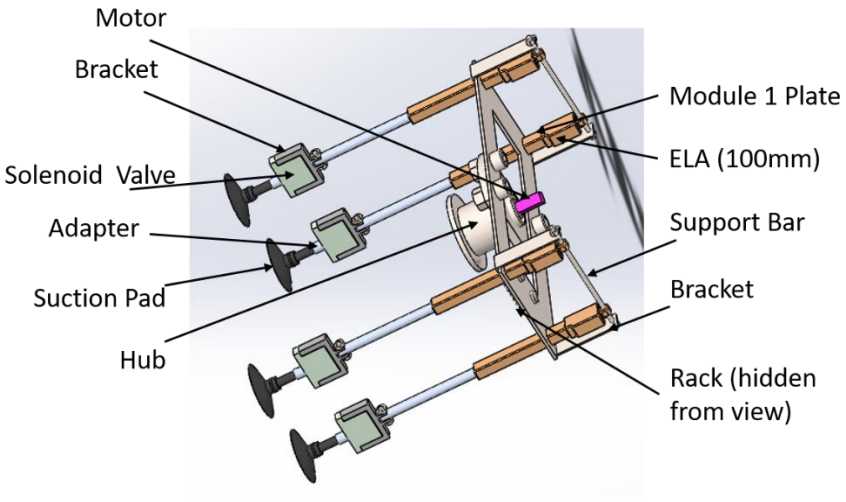

Fig. 4.14. Diagram of the rotating components of module 1

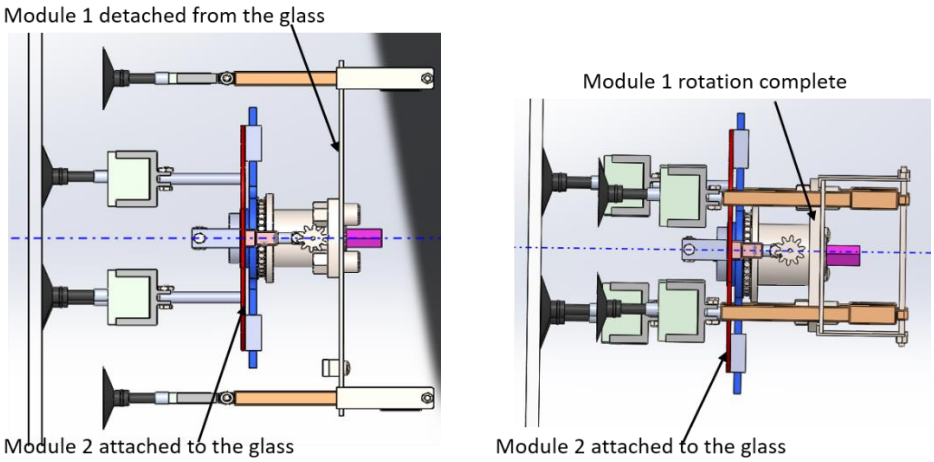

(1) Module 2 is adhering to the window glass when module 1 is about to rotate

(2) Module 2 is adhering to the window glass when module 1 has completed rotation

Fig. 4.15 Rotational motion of module 1 with module 2 attached to the glass

These rotations occur under the assumed displacement and velocity, with the below further assumptions:

- Each module rotates 90° over 1s;
- *Blend time* t_b is equal to 0.1s.

The plot of the displacement is shown in Figure 4.16. Note, θ is same to Q in Figure 4.9.

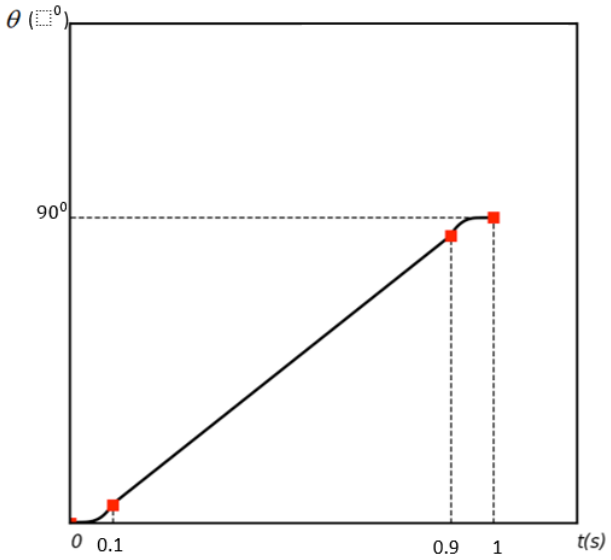

Fig. 4.16. Displacement plot of each module rotates 90° over 1s

These assumptions apply for rotations of both modules. Based on Equations (4.15-4.20), their angular velocity and the angular acceleration Equations are achieved below:

$$\dot{\theta} = 10\dot{\theta}_{\max} \cdot t \qquad (0 \le t < 0.1) \qquad (4.22)$$

$$\dot{\theta} = \dot{\theta}_{\max} \qquad (0 \le t < 0.9) \qquad (4.23)$$

$$\dot{\theta} = -10\dot{\theta}_{\max} \times (t-1) \qquad (0.9 \le t < 1) \qquad (4.24)$$

$$\ddot{\theta} = 10\dot{\theta}_{\max} \qquad (0 \le t < 0.1) \qquad (4.25)$$

$$\ddot{\theta} = 0 \qquad (0 \le t < 0.9) \qquad (4.26)$$

$$\ddot{\theta} = -10\dot{\theta}_{\max} \qquad (0.9 \le t < 1) \qquad (4.27)$$

$\dot{\theta}$ is the velocity of the robot, equal to $\dot{Q}$, $^o/s$;

$\dot{\theta}_{\max}$ is the maximum velocity of the robot, equal to $\dot{Q}_{\max}$, $^o/s$.

$\ddot{\theta}$ is the acceleration of the robot, equal to $\ddot{Q}$, $^o/s^2$;

$\ddot{\theta}_{\max}$ is the maximum acceleration of the robot, equal to $\ddot{Q}_{\max}$, $^o/s^2$.

Equation (4.14) can be combined with $\theta = 90^0$, $t_f = 1s$ and $t_b = 0.1s$ to yield the value of the maximum angular velocity:

$$\dot{\theta}_{\max} = 100^o / s$$

Adding this value into Equations from (4.22) to (4.27), then Equations of the angular velocity (4.28)-(4.30) and acceleration (4.31-4.33) for each module rotating 90° over 1s can be achieved below:

$$\dot{\theta} = 1000^o \cdot t \qquad (0 \le t < 0.1) \qquad (4.28)$$

$$\dot{\theta} = -1000^o \qquad (0 \le t < 0.9) \qquad (4.29)$$

$$\dot{\theta} = -1000^{o} \times (t-1) \qquad (0.9 \le t < 1) \qquad (4.30)$$

$$\ddot{\theta} = 1000^{o} / s^{2} \qquad (0 \le t < 0.1) \qquad (4.31)$$

$$\ddot{\theta} = 0 \qquad (0 \le t < 0.9) \qquad (4.32)$$

$$\ddot{\theta} = -1000^{o} / s^{2} \qquad (0.9 \le t < 1) \qquad (4.33)$$

The plot of the angular velocity is obtained in Figure 4.17. The enclosed area is the total displacement $\theta_{total} = 90^{0}$. Note, $\dot{\theta}$ in this paragraph are same to $\dot{Q}$ in Figure 4.10.

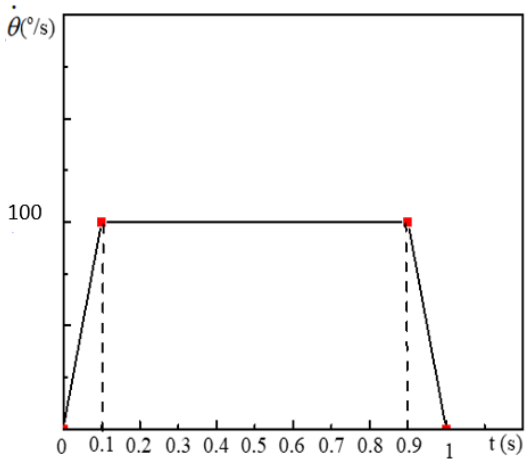

Fig. 4.17. Angular velocity plot of each module rotates 90° over 1s

The plot of acceleration is obtained, as shown in Figure 4.18. Note, $\ddot{\theta}$ in this plot is same to $\ddot{Q}$ in Figure 4.11.

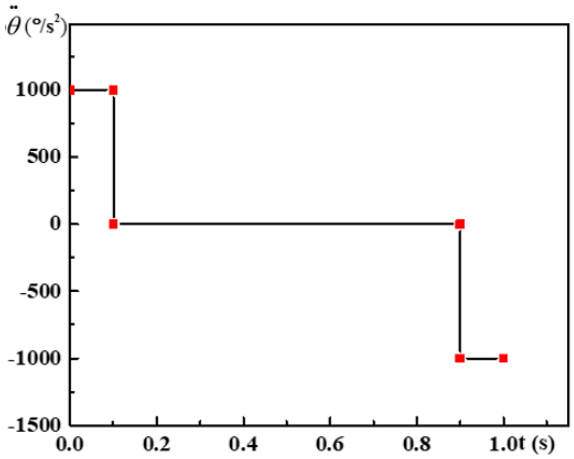

Fig. 4.18 Angular acceleration plot as each module rotates 90° over 1s

In Equation (4.21), the torque is determined by the moment of inertia when $\ddot{\theta}$ is a constant so. Each rotating module has different values of the moment of inertia. The values of moments of inertial (I_{xx}) for per rotating module is determined from Solidworks developed in Solidworks (Dassault System, version 2018), as shown in Table 4.3. These values are substituted into Equation 4.21, with the angle acceleration $\ddot{\theta} = 1000^o / s^2$.

Thus, the torque (T) of each rotating module is calculated, as shown in Table 4.3.

Table 4.3 Values of the moments of inertia and torques of each rotating module

	Moments of inertia (I_{xx}) about the axis of the rotation ($kg.m^2$)	the torque of the robot(T), $N \cdot m$;
Module 1	0.017	0.29
Module 2	0.004	0.063

Comparing the two required torques, the greater one is *0.29N.m,* which can be used to help select an appropriate motor. Based on the calculated maximum angular velocity $\dot{\theta}_{\max} = 100^o / s$, the revolution speed of the motor output shaft needs to be maximum ideal required.

$$n = 1.75rad/s = 16.67rpm$$

The power is decided by the torque and angle velocity by using Equation (4.34).

$$P = T \cdot \dot{\theta} \tag{4.34}$$

Where the velocity and the torque values are substituted into this equation to yield the power.

$$P = 0.56w$$

The values of torque, the speed of revolution and power suggest a servo motor having reduction gearbox. As a result, the preferred motor is in Figure 4.19 and its specification in Table 4.4 below:

Fig. 4.19. The structure of 298:1 micro metal gearmotor HPCB 12V with extended motor shaft for encoder

Table 4.4 Specification of 298:1 Micro Metal Gearmotor HPCB 12V with Extended Motor Shaft

Size:	10 × 12 × 26 mm
Weight:	9.5 g
Shaft diameter:	3 mm
Gear ratio:	297.92:1
No.load speed @ 12V:	110 rpm
No.load current @ 12V:	0.06 A
Stall current @ 12V:	0.75 A
Stall torque @ 12V:	0.32 N·m
Max output power @ 12V:	1.0 W
Motor type:	0.75A stall @ 12V (HPCB 12V . carbon brush)

Performance at maximum efficiency is below:

Max efficiency @ 12V:	26 %
Speed at max efficiency:	87 rpm
Torque at max efficiency:	0.072 N·m
Current at max efficiency:	0.21 A
Output power at max efficiency:	0.65 W

4.3.2 Linear Motions

4.3.2.1 Choosing an Actuator for the Linear Motion

Module 2 (as shown in Figure 4.20) moves when its suction pads detach from the window glass, but the suction pads of Module 1 requires attached to the window glass, as shown in Figure 4.21. Likewise, Module 1 (as shown in Figure 4.22) moves when its suction pads detach from the window glass, but the suction pads of Module 2 remain attached to the window glass, as shown in Figure 4.23.

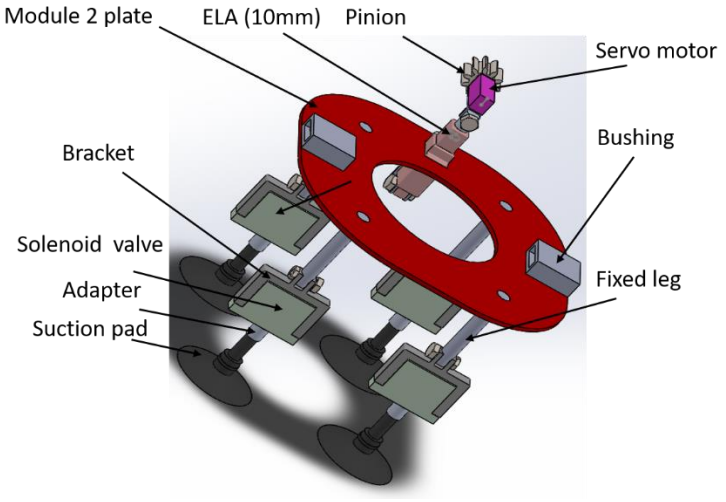

Fig. 4.20. Diagram of the moving components of module 2

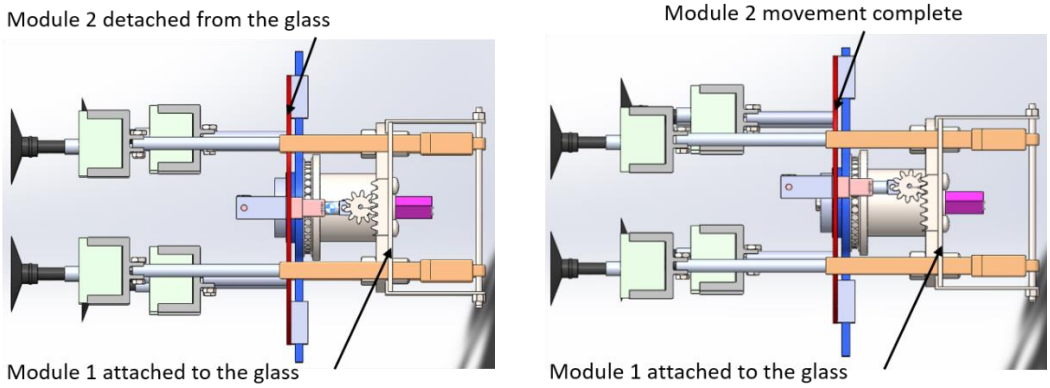

(1) Module 1 adheres to the window glass while module 2 is about to rotate

(2) Module 1 is adhers to the window glass while module 2 has completed 20mm translation

Fig. 4.21. Diagram of translational motion for module 2

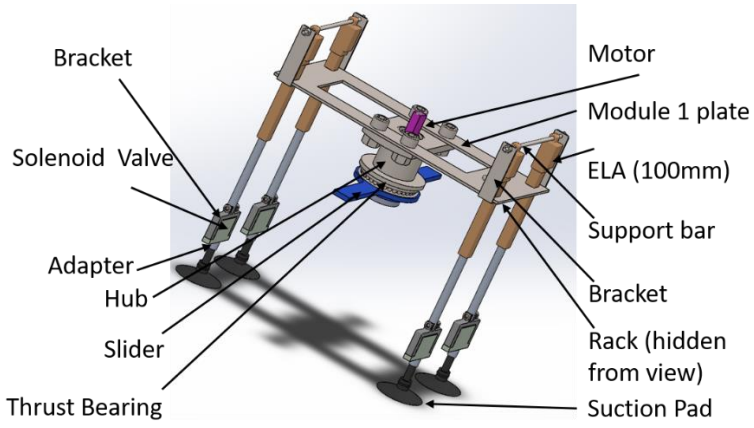

Fig. 4.22. Diagram of the moving components of module 1

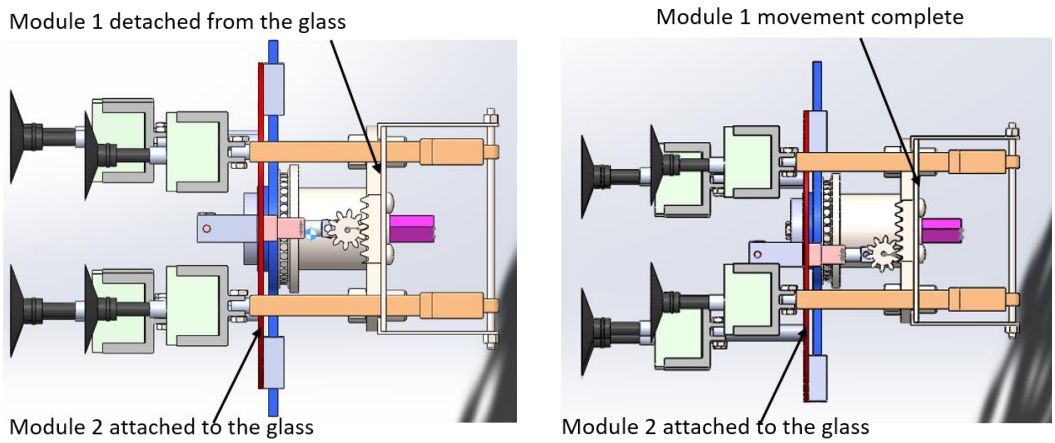

(1) Module 2 adheres to the window glass while module 1 is about to move

(2) Module 2 adheres to the window glass while module 1 has completed 20mm translation

Fig. 4.23. Diagram of translational motion for module 1

These moving motions perform the same assumption about displacement and velocity. Also, their specific assumptions are taken as follows:

- Each moving module moves *20mm* over *1s* as well as *40mm* over *2s*;
- *Blend time* t_b is equal to *0.1s*;
- The pinion is assumed to have the radius r_p*=10mm,* module m*=2* and pressure angle φ_p*= 200* .

The plot of the displacement is shown in Figure 4.24. Note, x is same to Q in Figure 4.9.

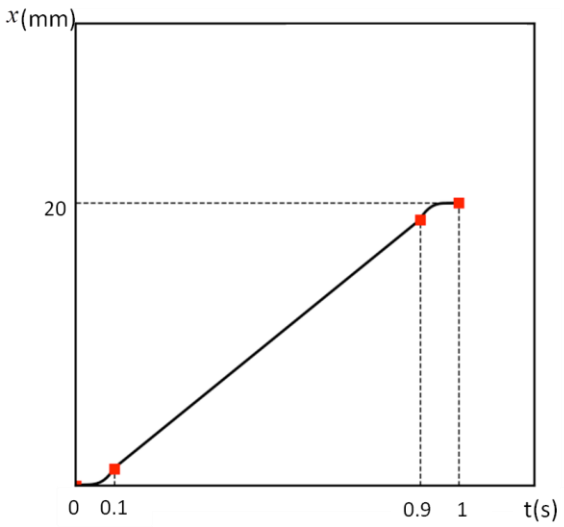

Fig. 4.24. Displacement (20mm) plot of the linear motions of the robot

The plot of linear velocity is shown in Figure 4.25 and the enclosed area is the displacement Q. Note, $\dot{x}$ and $\dot{x}_{max}$ in this plot are same to $\dot{Q}$ and $\dot{Q}_{\max}$ mentioned before.

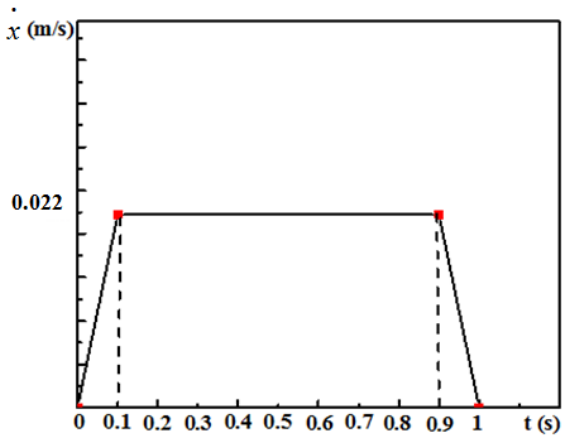

Fig. 4.25. Linear velocity plot of the linear motions of the robot for 20mm

Based on Equation (4.14), combining with $x = 20mm$, $t_f = 1s$, $t_b = 0.1s$, the value of the maximum linear velocity is yielded:

$$\dot{x}_{max} = 0.022\ m/s$$

Then, substituting this value into these equations (4.15-4.20), the equations of the linear velocity (4.35-4.37) and the linear acceleration (4.38-4.40) for each component moving *20mm* over *1s* can be achieved below:

$$\dot{x} = 0.22t \qquad (0 \le t < 0.1) \qquad (4.35)$$

$$\dot{x} = 0.022 \qquad (0.1 \le t < 0.9) \qquad (4.36)$$

$$\dot{x} = -0.22(t-1) \qquad (0.9 \le t < 1) \qquad (4.37)$$

$$\ddot{x} = 0.22 \qquad (0 \le t < 0.1) \qquad (4.38)$$

$$\ddot{x} = 0 \qquad (0.1 \le t < 0.9) \qquad (4.39)$$

$$\ddot{x} = -0.22 \qquad (0.9 \le t < 1) \qquad (4.40)$$

$\dot{x}$ is the velocity of the robot, equal to $\dot{Q}$, *m/s*;

$\dot{x}_{max}$ is the maximum velocity of the robot, equal to $\dot{Q}_{max}$, *m/s*.

$\ddot{x}$ is the acceleration of the robot, equal to $\ddot{Q}$, m/s^2;

$\ddot{x}_{max}$ is the maximum acceleration of the robot, equal to $\ddot{Q}_{max}$, m/s^2.

The plot of acceleration is obtained, as shown in Figure 4.26. Note, $\ddot{x}_n$ in this plot is same as $\ddot{Q}$.

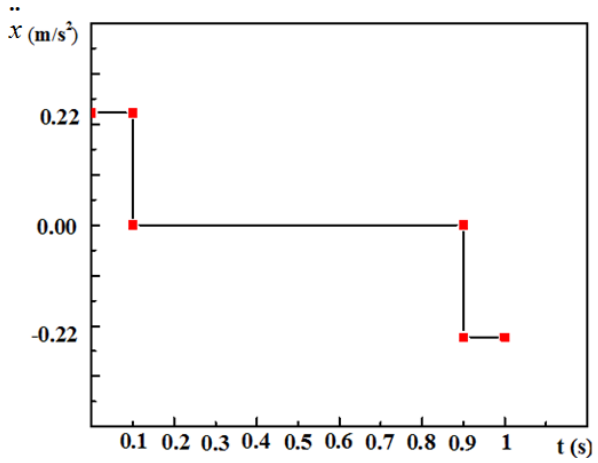

Fig. 4.26. Linear acceleration plot of the linear motions of the robot

This robot undertakes two different step size. First, it starts from its centre and travel *20mm* over *1s*. Next, it moves up to *40mm* over *2s* due to its symmetric structure. Finally, it moves *20mm* over 1s to go back to its centre before the robot's rotation motion. These two motions of different displacements are assumed to have the same maximum acceleration value and similar plot shape of the displacement and velocity. However, their maximum velocities are a slightly different due to the time spent at maximum velocity (the robot travels *40mm* at the velocity of *0.021m/s* and the acceleration of *0.21m/s*^{2})

The linear motions are driven by the rack and pinion. During robot climbing up on the glass at a certain acceleration, the adhesion forces of these adhered suction pads should be enough to support the robot, both weight and acceleration, as shown in Figure 4.27.

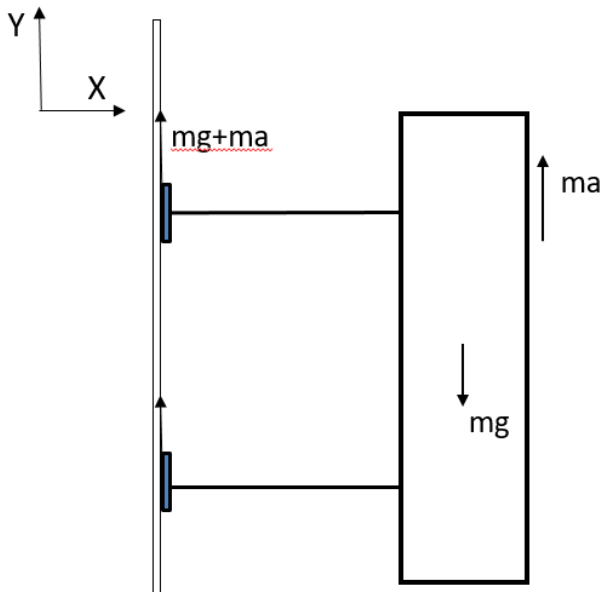

Fig. 4.27. Diagram showing forces on robot when climbing

To specify the motor, the torque can be calculated from these forces that need to be generated through the pinion. Then Equation (4.41) about these factors which are the weight and acceleration of the robot and the radius of the chosen pinion is yielded.

$$T_{1,2} > (m_{1,2}g + m_{1,2}a)r \tag{4.41}$$

Where

$T_{1,2}$ is the required torque of actuating the module 1/2, *Nm*;

$m_{1,2}$ is the mass of the module 1/2, *kg*;

r_p is the pinion radius, *m*.

Actuating each module needs different torques because of their individual mass, which are measured in Solidworks, as shown in Table 4.5.

Where

G=9.8N/kg

$a=0.22\ m/s^2$

$r_p=10mm$

The required torque is obtained, as shown in Table 4.5.

Table 4.5 Values of the masses and torques of each moving module

	Mass (kg)	Torque required at pinion($N \cdot m$)
Module 1	1.730	0.17
Module 2	0.514	0.05

Generally, the torque of the suitable motor should be decided by the greater torque required to move module 1. This module is ideal and does not account for any losses due to friction etc. Therefore, the motor should be sized to provide a torque larger than this value.

$$T > 0.17Nm$$

In this design, a rack and pinion will realize the linear motions of the internal and external moving module. The gear ratio affects the choice of the motor.

First, to obtain the gear ratio, Equation (4.42) is introduced. It shows that Module is the ratio of the reference diameter of the gear divided by the number of teeth. The number of the teeth is decided by choosing a module of the gear.

$$m_p = \frac{d_p}{Z_p} \tag{4.42}$$

Where

d_p is the diameter of the pinion, m;

m_p is the module of the pinion;

Z_p is the number of the teeth.

Where

$$d_p = 20\ mm$$

$$m_p = 1$$

Thus, the number of the pinion teeth Z_p is obtained

$$Z_p = 20$$

The velocity of the rack v_r is equal to the above linear velocity $\dot{x}$ of the robot,

Where

$$v_r=0.022 m/s$$

Then, adding d_p =20 *mm* into Equation (4.43), where the relationship between the pinion diameter and the rack's linear velocity is shown.

$$n_p = \frac{v_r}{\pi d_p} \tag{4.43}$$

The value of the rotational speed of the pinion n_p is obtained

$$n_p=2.20 rad/s=21.02 rpm$$

Note, the length of the rack is greater than the assumption of the moving distance (*20mm* over *1s* and *40mm* over *2s*) of each moving module, that is

$$L_r > 40$$

The rack has the same module and pressure angle as the pinion. Substituting $m_r=m_p=1$ into equation (4.44), where the length of the rack equals to the product of its module multiplying its teeth number.

$$L_r = m_r z_r \tag{4.44}$$

L_r is the Length of the rack, *m*;

mr is the module of the rack;

Z_r is the number of the teeth of the rack.

Choosing

$$L_r=50$$

The number of the rack teeth is obtained

$$Z_r=50$$

Given the required $T_1>0.17Nm$, $n_p=21.02rpm$, the *298:1* Micro Metal Gearmotor HPCB 12V with Extended Motor Shaft is suitable to process the linear motions, its specification is presented in Table 4.4. It is the same servo motor, used to manage the rotational motions.

4.3.2.2 Choosing an Actuator for Interference Avoidance Motion

The rack and pinion actuate the linear motions parallel to the window glass however they have to separate to allow the robot to rotate. This required an interference avoidance motion, which is proposed to be achieved by an ELA. The teeth depth of the pinion affects choosing the ELA. Equations (4.45) and (4.46) shows that the outside and root diameters of a pinion are all affected by its pitch diameter and module.

$$D_o = d_p + 2m_p \quad (4.45)$$

$$D_r = d_p - 2.5m_p \quad (4.46)$$

D_o is the outside diameter of the pinion, *m*;

D_r is the root diameter of the pinion, *m*;

d_p is the pitch diameter of the pinion, *m*;

m_p is the module of the pinion;

Where,

$m_p = 1$

$d_p = 20\ mm$

Then, the values of the outside and root diameters are calculated:

$D_o = 22mm$

$D_r = 17.5\ mm$

The pitch depth is the value of the difference between the outside and root diameter of the pinion. It is *2.25mm* that the pinion should be retracted greater than, which makes sure their completely separation. The Actuonix's L series of ELA, as shown in Table 4.6, having the maximum stroke of *10mm*. Additionally, its maximum side load is *50N* enough to support the weight of the servo motor and the pinion: *14g* (determined by Solidworks). Therefore, this ELA is suitable and then it is designed to connect with the above motor, as shown in Figure 4.28 (1). Next, the rack and pinion are attached onto the module 1 &2 plates and 1st frame to mate, as shown in Figure 4.28 (2).

Table 4.6 Electric linear actuators mounted on the module 2 plate for pinion interference avoidance

Max Force	22N (lifted)
Max Side Load	50N(extended)
Nominate Input voltage	6VDC
Max Input Voltage	7.5V
Stall Current	460mA
Speed	25mm/s (no load)
Stroke	10mm
Closed Length	62mm(hole to hole)
Operation temperature	-10°C ~ +50°C

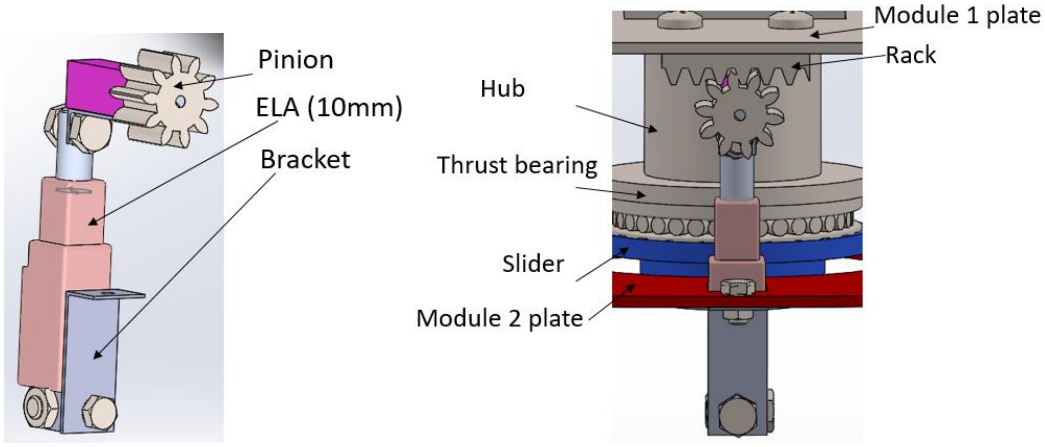

(1) Assembly of the ELA (10mm) and the pinion (2) Positions of the mated pinion and rack

Fig. 4.28. Assembly and position of the pinion and rack

As a result, all of non-standard elements in this robot have been designed as well as standard parts chosen after the kinematic and dynamic analysis and calculations.

4.4 Payload Capacity

In Equation (4.11), the required adhesion force is achieved, but only the net weight of the proposed robot is considered. However, the special designed suction pad needs to hold both the robot itself and any extra equipment required to clean windows. The weight of this equipment is the potential payload. Based on the assumed suction pads, each pad can provide an adhesion force of 147.19N (Section 4.2.1). So, the total available adhesion forces

F_s=588.76N for four attached suction pads. Then, including payloads, the Equation (4.47) to calculate the payloads is yielded:

$$F_s > \frac{1}{4} g(m + m_p)(\frac{1}{\mu} + \frac{l}{l_s}) \quad (4.47)$$

F_s is the suction force of the robot, *N*;

m is the mass of the robot, *kg*;

M_p is the payloads of the robot , *kg*;

l is the distance between the centre of the robot and the window glass, *m;*

l_s is the vertical distance between the adhering suction pads, *m.*

Comparing the four states of these suction pads (as shown in Figure 4.2), when the suction pads of the module 2 adhere to the window glass, l_m shows the maximum distance and simultaneously l_s presents the minimum one. Their values are below (in Table 4.1):

l_s=*90.00mm*

l_m=*213.87mm*

Where

m=2.25kg

μ=*1*

Then, the maximum available payloads that this robot can carry are obtained:

m_p=68.93kg

However, there is another factor that needs to be considered, the 4 ELAs need to hold the robot and its payload oriented vertically and each ELA has the maximum side load of *15N*. So, the 4 ELAs can withstand a combined maximum side load of *60N*. After considering the mass of this robot *about 2.3kg*, the remaining capacity for payload is about *3.7kg*. Consequently, considering the safety criteria, this robot has a payload capacity of *3.7kg.*

4.5 Final Robotic Structure

The final mechanical robotic structure of this window glass cleaning robot is presented in Figure 4.29 and its exploded view in Figure 4.30. It is accomplished through designing non-standard elements where necessary and choosing standard ones where possible, informed by kinematic and dynamic analyses. During this design, the preferred choices, about the rotational mechanism, the position of the ELAs and so on, are decided after comparing them to others options.

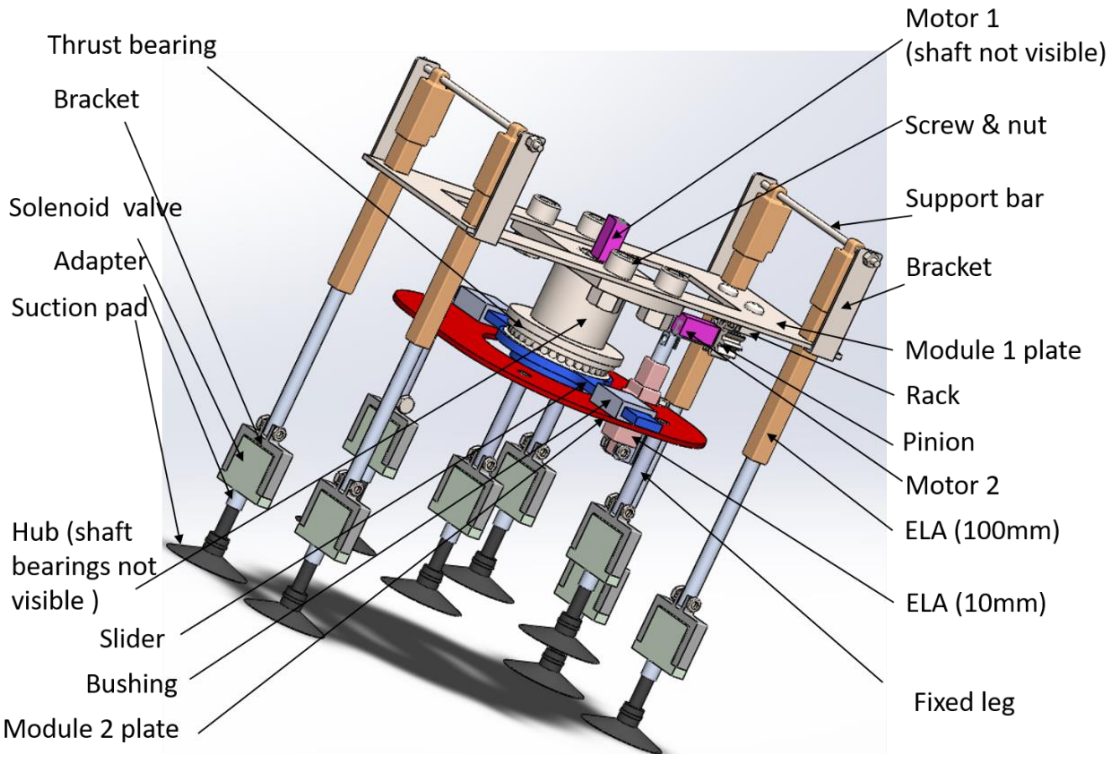

Fig. 4.29. Whole robotic structure of this project

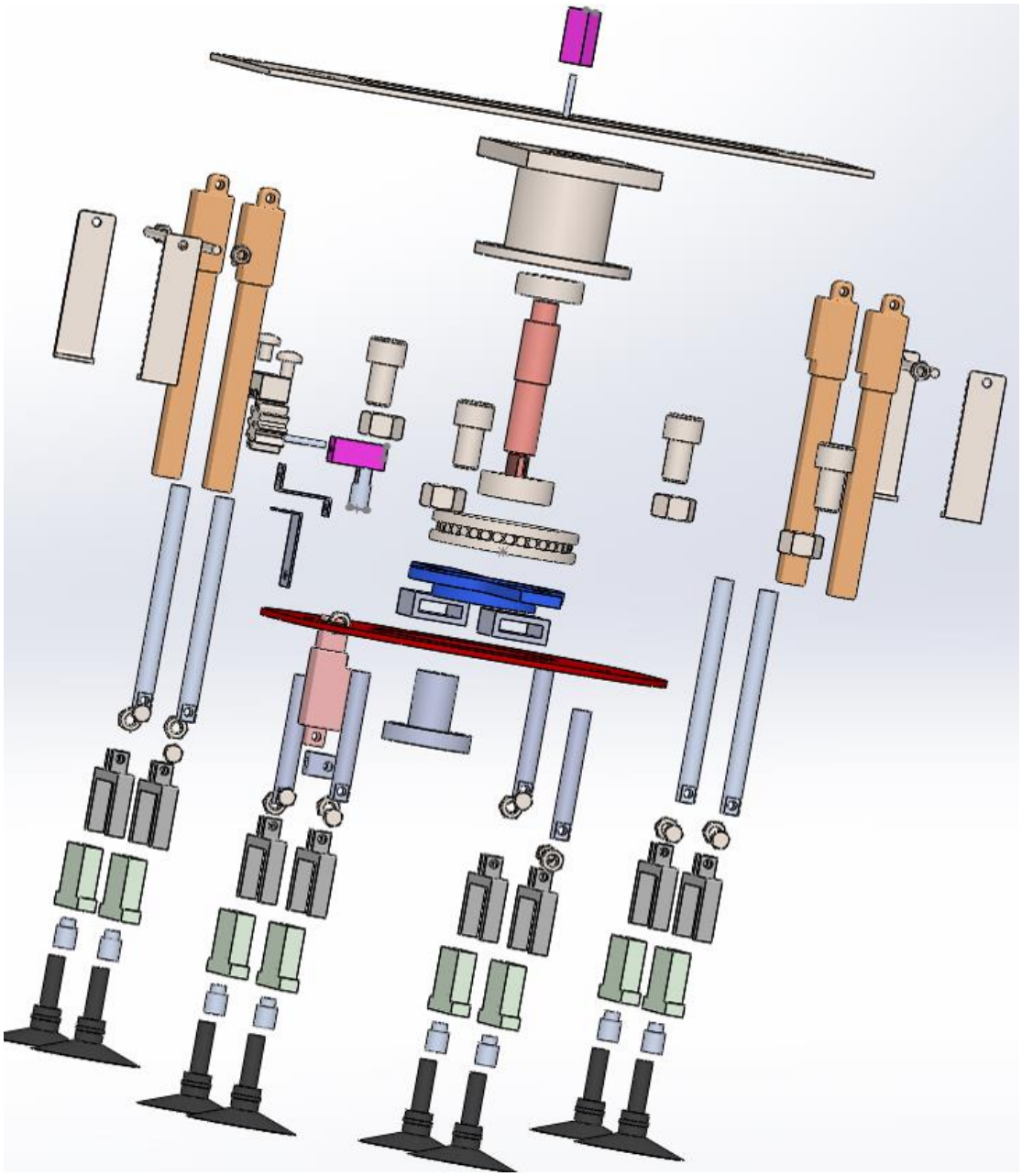

Fig. 4.30. Exploded view of the whole robotic structure

Furthermore, to show how the robot work, the sequence formulations for linear motions and rotational motions with leg extension/retraction motions are listed in Table 4.7, Table 4.8.

Table 4.7 Sequence for linear motions

Step	Diagrams of working processes	Discription of the working process
1	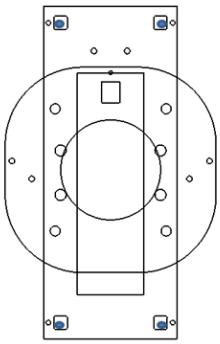	The four suction pads of the module 1 adhere to the window glass via manual forces. All the ELAs are extended. Also, the other four suction pads of the module 2 are detached from the glass 50mm and the rack and pinion are mated together. Note: all the solenoid valves are closed.
2	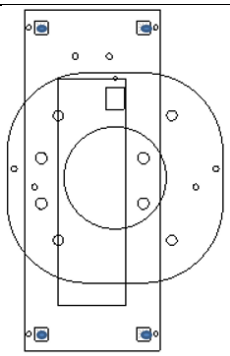	Module 2 is driven by the rack and pinion, to linearly move 20mm over 1s from the left to the right. During the process, the maximum velocity is 0.022m/s, using a trapezoidal velocity profile.
3	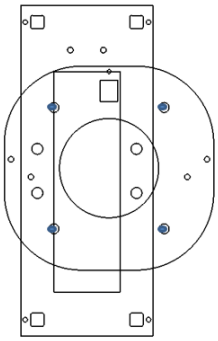	The four suction pads of module 1 are totally retracted by the ELAs with the speed of 4.5mm/s. A retraction of 50mm is made until the suction pads of module 2 adhere to the glass. The solenoid valves of module 1 are open to release the suction pads. Retraction of ELAs is continued. The suction pads of module 1 are withdrawn 50mm from the window glass (total movement 100mm).
4	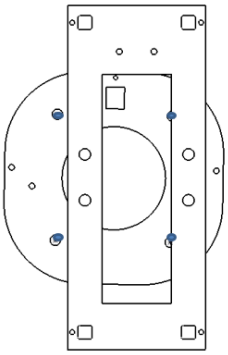	Module 1 is driven to make a 40mm linear movement in 2s. (Similar to Step 2).

5	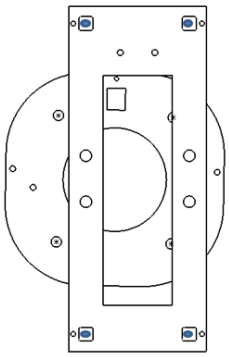	The four suction pads of module 1 are totally extended by the ELAs with the speed of 4.5mm/s. An extension of 50mm is made until the suction pads of module 1 attach to the glass. The solenoid valves of module 2 are open to release the suction pads. Extension of ELAs is continued. The suction pads of module 1 are extended 50mm from the window glass (total movement 100mm).
6	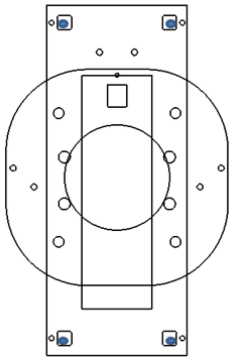	Module 2 is driven to make a 40mm linear movement in 2s. (Similar to Step 2).
Notice	1. The linear motions complete according to the displacement and velocity profiles described in Section 4.3.2. 2. Black blue points represent the adhering states of the suction pads. 3. In the following, the repeated motions happen from the 2nd to 6th step.	

Table 4.8 Sequence for rotational motions

step	Diagrams of working processes	Discription of the working process
1	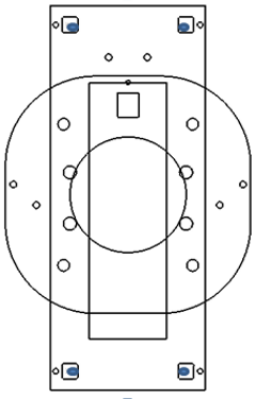	The four suction pads of the module 1 are totally extended by the ELAs with the speed of 4.5mm/s。 An extension of 50mm is made until the suction pads of module 1 adhere to the glass. The solenoid valves of module 2 are open to release the suction pads. Extension of ELAs is continued (total movement 100mm). The suction pads of module 2 are withdrawn 50mm from the window glass. Meanwhile, a retraction of 4.5mm, with the speed of 19mm/s, is made by the ELA, having the maximum stroke of 10mm. The pinion is thus unmated from the rack before the rotational motion of module 2.

2	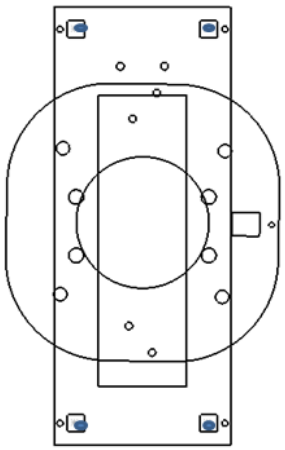	Module 2 is driven to rotate 90^0 over 1s by the servo motor. During the process, the maximum angular velocity is 100^0/s using a trapezoidal velocity profile.
3	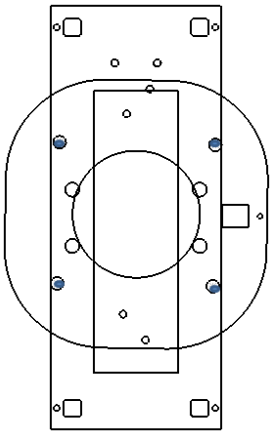	The four suction pads of the module 1 are totally retracted 100mm by the ELAs with the speed of 4.5mm/s. A retraction of 50mm is made until the suction pads of module 2 adhere to the glass. The solenoid valves of module 1 are open to release the suction pads. Retraction of ELAs is continued. The suction pads of module 1 are withdrawn 50mm from the window glass (total movement 100mm).
4	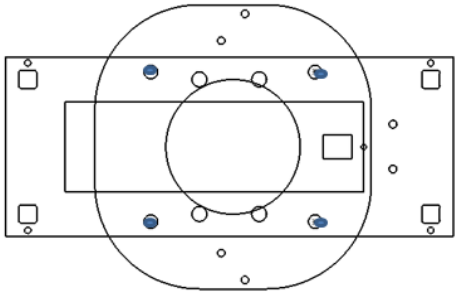	Module 1 is driven to rotate 90^0 over 1s. (Similar to Step 2).
Notice	1. The rotational motions according to the displacement and velocity profile described in Section 4.3.2. 2. Black blue points represent the adhering states of the suction pads. 3. In the following, the repeated motions happen from the 1st to 4th step.	

Finally, the whole working process of Hubbot, including the four motions above, can be presented more clearly using the timeline, as shown in Figure 4.31. Different colours represent different kinds of working phrases respect to their individual working periods. Obviously, the extending and retracting phrases of ELAs are great longer than the other ones, which is the serious drawback of this design.

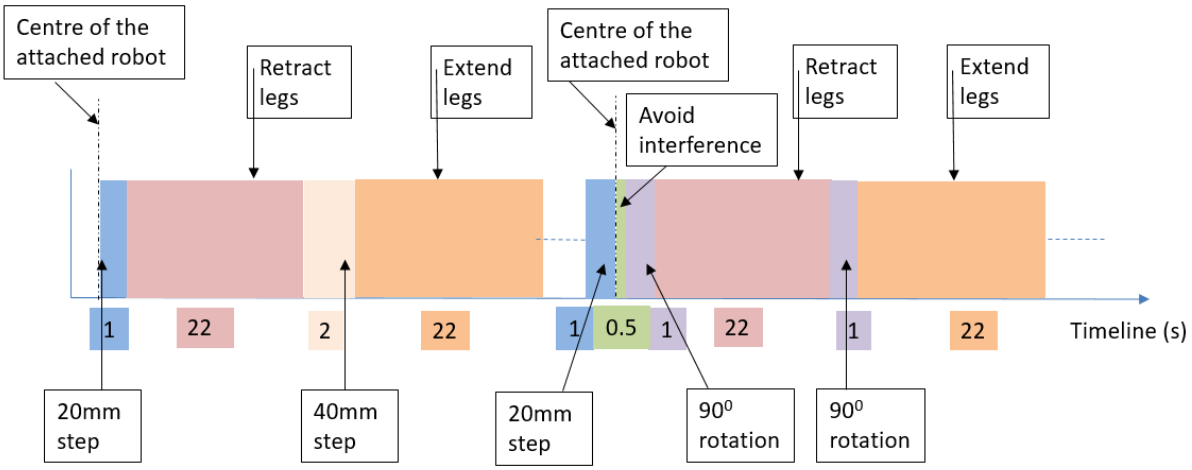

Fig. 4.31. Timeline of the whole working process of Hubbot

4.6 Estimated Costs of Hubbot

After selecting the whole structure of this robot, its costs can be approximately estimated in Table 4.9.

Table 4.9 Estimated Costs of Hubbot

Number	Element	Price(NZD)	Quantity
1	Germotor(298:1 Micro Metal Gearmotor HPCB 12V)	30.52	2
2	Electric Linear Actuator (100mm L12 Actuator Size of Actuonix's L series)	137.35	4
3	Electric Linear Actuator (10mm L12 Actuator Size of Actuonix's L series)	137.35	1
4	Solenoid Valve(SMC solenoid valve of high speed 2 port valve SX10 Series)	61.05	8
5	Bearing 12x32x10mm (SKF-Angular contact ball bearing d= 12 DIN 628-7201B-8)	30.13	1
6	Bearing 15x35x11mm (SKF-Angular contact ball bearing d=15 DIN 628-7202B-10)	28.38	1
7	Bearing(cylindrical roller thrust bearing-D=70 8110 GB 4663-94)	84.94	1
8	Hub*	90.00	1
9	Main Shaft*	130.00	1
10	Module 1 plate*	35.00	1
12	Module 2 plate*	35.00	1
13	Slider*	120.00	1

14	Bushing*	60.00	1
15	Suction pad*	90.00	8
16	Fixed pin*	40.00	4
17	Lock Washer (SKF-MB0)	1.00	1
18	Lock Nut(SKF- KM0)	1.00	1
Total price		2379.64	
* cost estimates from UC workshop staff			

Also, the costs of the other parts, such as Battery, CPU and Motor driver need to be approximately estimated. They are listed below.

1) Battery: Turnigy Nano-Tech 2100mAh 2S1P 20C LiFePo4 Transmitter Pack $40 (NZD);
2) CPU: Arduino Teensy $43 (NZD);
3) Motor driver: L298N $2 (NZD).

As a result, the total cost of this robot is about NZD 2380, which is inexpensive

4.7 Summary

Through a series of kinematic and dynamic analyses, the required torques and velocities and accelerations for linear and rotational motions are determined based on the assumed displacement: linear with parabolic blends. Then, the two available DC servo motors were selected as well as the appropriate suction pad was specified. Also, the two ELAs, individually having the strokes of 100mm and 10mm were selected to perform leg extension/retraction and interference avoidance motions. Further, the working process of this robot is introduced by sequence for the four motions as well as its working timeline. In addition, this robot's payload capacity and total cost were estimated.

5 Comparisons of Existing Window Cleaning Robots and Hubbot

5.1 Introduction

In chapter 3, some existing window cleaning robots were introduced and compared (Table 1.5). These robots are compared with Hubbot. The criteria for these comparisons are listed in Table 5.1.

Table 5.1 Success Criteria of Window Cleaning Robots

Success criteria	Reasons
Safety	Low risk of dropping from window glass, reliable adhesion ability
Simple structure	Short design and construction period, low cost in manufacture, easy assembly and repair
Light weight	Low risk of breaking window glass, low energy power consumption, portable operating, guarantee of reliable adhesion, increased payload and velocity
Capability for cleaning	Few or no marks left, cleaning fast
High speed	High working efficiency
Obstacle traversal	Meet the market requirements to flexibly span different obstacles
Environmental considerations	Little or no noise to disturb building occupants, no pollution
Cost	Low operation and maintenance costs, low energy requirements

Table 5.2 shows important information about each of these existing robots and Hubbot. Table 5.3 evaluates and compares the other window cleaning robots against Hubbot.

Table 5.2 Robot Statistics of These Existing Robots and Hubbot

Robot	Dimension L×b×h (mm)	Weight (kg)	Payload (kg)	Speed (mm/s)	Locomotion	Adhesion	Adhesion force (N)
1. 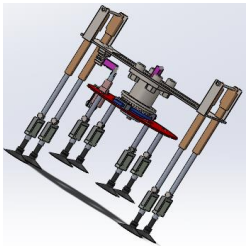 Hubbot	300×190 ×336	2.25	3.7	22 (linear)	Translation	Vacuum (passive)	588

Robot	Dimension L×b×h (mm)	Weight (kg)	Payload (kg)	Speed (mm/s)	Locomotion	Adhesion	Adhesion force (N)
2. 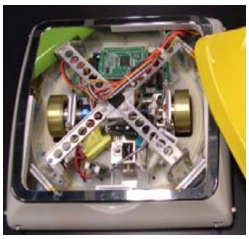 WallWalker [6] [9]	300×300 ×100	3	-	10	Wheeled	Vacuum (active)	70
3.  Sky Cleaner 3 [9, 29, 87]	1136×736 ×377	45	60	680	Translation	Vacuum (active)	-
4.  NINJA-1,2 [9]	500×1800 ×400	45	-	160	Legged	Vacuum (active)	-
5. 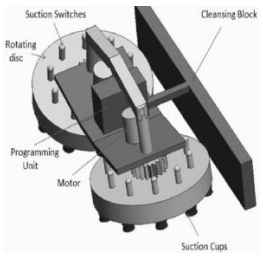 Skyscraper's glass cleaning Automated robot [36]	380×540 ×150	6	0.6	1.33	Rotating-disc	vacuum (active)	6kpa

Robot	Dimension L×b×h (mm)	Weight (kg)	Payload (kg)	Speed (mm/s)	Locomotion	Adhesion	Adhesion force (N)
6. 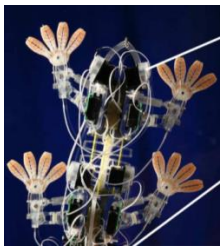 Stickybot [19, 44]	600×200 x60	0.37	-	40	Legged	Dry adhesive	-
7. 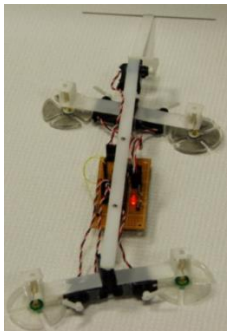 Geckobot [9, 19, 88]	190×110 x20	0.1	-	50	Legged	Dry adhesive	-
8. 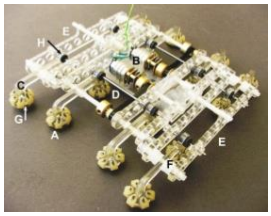 A sixteen-legged climbing robot [19]	120×110 ×20	0.115	2	4	translation	Dry adhesive	-
9. 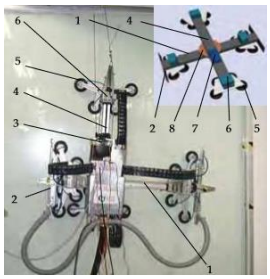 A cleaning robot [67]	1220×1340×370	30	15	50	translation	Vacuum (active)	450

Robot	Dimension L×b×h (mm)	Weight (kg)	Payload (kg)	Speed (mm/s)	Locomotion	Adhesion	Adhesion force (N)
10.  Windoro [89, 90]	200×200×85	3	-	-	Wheeled	Magnetic	-
11. 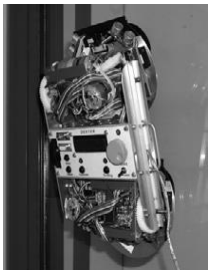 DEXTER [9, 91, 92]	365×220×130	3	-	-	Legged	Vacuum (passive)	-
12. 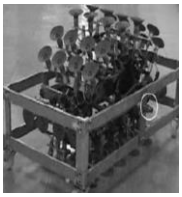 Cleanbot II [9, 26]	720×370×390	22	25	166	Tracked	Vacuum (active)	80kpa

Table 5.3 Evaluation Matrix of These Existing Robots and Hubbot

Number	Robot	Success Criteria							
1	Hubbot	Safety	Simple structure	Light weight	Capacity for cleaning	High speed	Obstacle traversal	Environmental considerations	Cost
2	WallWalker	=	−	−	+	−	−	−	+
3	Sky Cleaner 3[29, 87]	+	−	−	=	+	−	−	+
4	NINJA-1,2 [9]	=	−	−	=	+	−	−	+
5	Skyscraper's glass cleaning automated robot [36]	+	+	−	+	−	−	−	+
6	Stickybot [19, 44]	−	−	+	−	+	−	=	−
7	Geckobot [19, 88]	−	−	+	−	+	−	=	−
8	a sixteen-legged palm-sized climbing robot [19]	−	−	+	−	−	−	=	−
9	a climbing robot for cleaning glass surface with motion planning [67]	−	−	−	=	+	−	−	+
10	Windoro [89, 90]	+	−	−	+	−	−	=	−
11	DEXTER [9, 91, 92]		−	+	−	−	−	=	−
12	Cleanbot II [9, 26]	+	−	−	−	+	−	−	−
	Note:	1. Each performance indicator t in Table 1.5 is ranked against Hubbot. 2. "+" indicates better performance than Hubbot. 3. " − " indicates worse performancethan Hubbot. 4. "=" indicates a robot equivalent to Hubbot.							

Table 5.4 Results of the Evaluation Matrix in Success Criteria

Number	Robot	Better than Hubbot $\sum^{+}$	Same as Hubbot $\sum S$	Less than Hubbot $\sum^{-}$
1	WallWalker	2	1	5
2	Sky Cleaner 3[29, 87]	3	1	4
3	NINJA-1,2 [9]	2	2	4
4	Skyscraper's glass cleaning automated robot [36]	4	0	4
5	Stickybot	2	1	5
6	Geckobot [19, 88]	2	1	5
7	A sixteen-legged palm-sized climbing robot [19]	1	1	6
8	A climbing robot for cleaning glass surface with motion planning [67]	2	1	5
9	Windoro [89, 90]	2	1	5
10	DEXTER [9, 91, 92]	1	2	5
11	Cleanbot II [9, 26]	2	0	6
Note:		1. $\sum^{+}$ represents the sum of the better results in Table 5.2. 2. $\sum^{-}$ represents the sum of the worse results in Table 5.2. 3. $\sum S$ represents the sum of the same results in Table 5.2.		

In the Table 5.4, Hubbot shows its considerable advantages in most of the 8 success criteria except the three factors, including high speed, obstacle transversal and cost. It has more than 60 percent better outcomes in success criteria than the other 8 robots, except Sky Cleaner 3, NINJA-1,2 and the Skyscraper's glass cleaning robot. In the following, further analysis of the requirements, such as safety, parameters, motion mechanisms, actuation mechanisms, will be discussed with their individual contributing factors.

5.2 Discussion of Success Criteria

5.2.1 Safety Comparisons

Among all the success criteria, safety should be taken as a primary consideration. Window cleaning robots should have no or minimal risk of dropping from window glass. Reducing the weight of a robot and providing sufficient adhesion forces are the most important considerations in this respect. It is well known that the lighter the robot is, the easier it is to provide reliable adhesion forces. The two robots in [67], [9, 26] individually weigh of 30kg, 22kg. This is much heavier than Hubbot (2.25kg) in Table 5.1. The heavier one applies 16 active adhesion pads to achieve the adhesion force 450N, less than the value of Hubbot: 588N, which is about 1.5 times that of the heavier robot. However, Hubbot only uses 4 passive suction pads, with a diameter of 50mm. Further, Cleanbot II [9, 26], with 52 adhesion pads, provides the suction forces via a vacuum compressor, with a vacuum pressure of 80kpa. However, Hubbot provides an adhesion force of 588N under a negative vacuum pressure of 75kpa. Further, passive vacuum adhesion mechanism has less environmental impact due to low noise and power consumption.

5.2.2 Comparisons of Parameters

Important robots parameters include overall geometry, mass, and forces. Each of these parameters is important and they are related each other. They also affect the overall safety, cost, and quality of the robot.

The Stickybot (0.37kg) [19, 44], Geckobot (0.1kg) [19, 88] and the robot (0.115kg) in [19] are considerably lighter than Hubbot (2.25kg) because of their smaller volumes, as shown in Table 5.2. Therefore, their energy requirements are lower and they require smaller adhesion forces. These forces can be supplied by biomimetic adhesion pads, which are expensive. In addition, they have a very small payload capacity. Also, dry adhensives require a clean surface and need to be cleaned frequently to ensure reliable adhesion.

Sky Cleaner 3 [29, 87], NINJA-1,2 [9] and the cleaning robot [67] with weights of 45kg, 45kg and 30kg, respectively are considerably heavier than Hubbot (2.25kg) due to their larger volumes. Therefore, these robots have a higher energy requirements and greater adhesion forces. They also have a higher risk of falling than Hubbot. Also, the speed of these heavier

robots may be affected by their greater weight. In addition, their payload capacities (approximately 600N and 150N) respectively are higher than Hubbot's (about 3.7kg). However, the payload of Hubbot could be improved by using an ELA with higher side load capacity.

5.2.3 Comparisons of Motion Mechanisms

Window cleaning robots need to be able to move and also span obstacles. These robots may use wheels [6] [89, 90], rotating-discs [36], tracks [9, 26] or legs [9] [19, 44] [19, 88] to move. The robots in [29, 87] [19] [67], have a translation mechanism, which is the simplest locomotion system. Therefore, Hubbot uses this system to move.

5.2.3.1 Motion Mechanisms of the Existing Window Cleaning Robots

Many window cleaning robots have different kinds of motion mechanisms, and they are all more complex than Hubbot. They are easily to design due to their flexible motion characteristics. However, they have difficulty spanning obstacles. For example, Cleanbot II, using tracked locomotion with 52 adhesion pads, is designed to move across an obstacle less than 6mm in height. This will not meet the requirements because many windows have obstacles higher than 6mm. Likewise, legged robots with biomimetic pads have a similar problem. In addition, they have the most complicated mechanical structures due to multiple degrees of freedom. They are intricately designed to enable the robots to attach or detach from the sliding surfaces and flexibly rotate. On the other hand, translation locomotion systems can easily actuate suction pads via a pins connected with pneumatic actuators. However, they always need to attach an extra rotational mechanism, such as the waist joint actuated by a pendulum cylinder [29, 87] and a steering wheel by the cylinder [9, 26]. Thus, translation locomotion mechanisms have their own complex, which can be looked as a proxy for high costs.

5.2.3.2 Motion Mechanisms of Hubbot

In this project, Hubbot can complete the required motions by an improved locomotion system. First, it can step over barriers of height up to 50mm by means of the four ELAs. They are mounted on the outside frame (module 1) while the four fixed legs are screwed onto the inside frame (module 2). Each ELA and leg is connected with a solenoid valve and suction

pad. The suction pads on each frame can attach to or detach from window glass by actuating the four ELAs. This function enables the linear and rotational motions of this robot.

The linear motions operate via a rack and pinion actuated by a DC motor. The pinion is fixed on the outside frame (module 1) and the rack is on the inside one (module 2). The rack and pinion must be completely separated to avoid interference during the rotational motions. The reason is that Hubbot uses a hub and a motor to enable the two modles to rotate relative to each other. The motor is mounted on the external module while the rotational shaft is screwed into the internal module. This simple design enables Hubbot's rotation motions via a servo motor and does not cause interfere with the rack and pinion.

In conclusion, compared to the other listed window cleaning robots, Hubbot has a simple mechanical structure to realize the same motions. Meanwhile, this simpler structure reduces the initial cost

5.2.4 Comparison of Actuation System

5.2.4.1 Actuation Mechanism of the Existing Window Cleaning Robots

In Chapter 3, reducing the robot's weight to improve its payload capacity and decrease power consumption was considered in the design requirements of a robot. Weight depends primarily on the number of actuators, especially heavy actuators such as stepper motors, and pneumatic and hydraulic cylinders. For existing window cleaning robots reviewed, most of them use electric motors, whose weights can make up a high percentage of the robot's total weight. For example, Stickybot and Geckobot [19, 88] have weights respectively 0.37kg and 0.1kg respectively, but they are equipped with 4 and 8 electrical motors respectively. Additionally, Sky Cleaner 3 [29, 87], driven fully via 12 pneumatic cylinders, has a working body weight of 45kg. However, it is supported not only by a following unit on the top of the building but also by the supporting vehicle on the ground that is not connected to the main moving body, considerably reducing its weight. Therefore, these cylinders probably make this robot very heavy. Apart from that, an ELA has the same advantages, namely high force lifted and continuously variable stroke. Most importantly, it can achieve the desired light weight without a pump. Nevertheless, none of these robots reviewed use this mode of motor.

5.2.4.2 Actuation Mechanism of Hubbot

Hubbot reduces the weight of the structure by using ELAs and decreasing the number of actuators

First, using ELAs rather than pneumatic actuators to drive the adhesion pads reduces the weight of the robot. The four ELAs each have a maximum stroke of 100mm and a total weight to 0.224kg for the 4 ELAs, which lowers the weight of Hubbot 2.25kg. They improve the payloads of this robot due to their own light weight and by removing the requirement of a board vacuum pump. In addition, their individual maximum lifting force and side load (extended) is 80N and 15N respectively, thus ensuring the robot's safety.

Further, Hubbot reduces the weight of the robot by using two micro servo motors. This enables complete rotational and linear motions with the assistance of interference avoidance motions. One servo motor, successively drives the linear motions of the internal and external modules via a rack and pinion. The other servo motor controls the rotational motions through a hub. These locomotion modes considerably reduce the number of motors required by other designs that use two sets of actuators to separately drive two modules.

However, Hubbot as proposed and analysed can only achieve a maximum linear velocity of 22mm/s as the linear motion is actuated by the rack and pinion. Its speed is lower than the other listed robots, except the robots in [36] [19]. This is a disadvantage of Hubbot, but during a prototype testing the speed may be able to be increased.

To conclude, the low number of actuators required by the three locomotion mechanisms in Hubbot, enable its great characteristics, including spanning high obstacles. And, they enable a light weight robot that carries high payloads.

5.2.5 Economic Comparisons

Hubbot using ELAs instead of pneumatic actuators is more economic in the long term. Most of reviewed window glass cleaning robots use active vacuum adhesion pads, actuated by pneumatic actuators. Pneumatic actuators have several advantages: simple structure, low manufacturing cost, high torque and flexible stroke. However, pneumatic actuators have higher maintenance costs than ELAs, which still have the other merits of pneumatic

actuators. Further, ELAs can be assembled more easily than pneumatic actuators due to not requiring a pump and storage of compressed air.

Hubbot uses passive vacuum, and has a simpler mechanism, lower energy consumption and power efficiency and lighter weight than, either active vacuum or magnetic adhesion. This mode of vacuum adhesion reduces energy usage in Hubbot. DEXTER also applies an adhesion cup, 75 mm in diameter with a strap which can be pulled to break the vacuum by a servo motor or solenoid valve. However, Hubbot directly implements a single solenoid valve with a suction pad through a specially designed adapter. These mechanical structures are simpler than those of DEXTER. Further, this structure has no needs of pipes, T-joints and manifolds to connect the solenoid valves to the suction pads. To some extent, it is easy to assemble the assembly.

In Chapter 4, the total cost of this robot is estimated approximately about NZD 2380, which is inexpensive, and likely less expensive than the existing window cleaning robots.

5.2.6 Comparisons of Cleaning Capacity

The proposed assembly is actuated by the ELA (100mm). It enables the suction pads of Hubbot to reduce abrasion and avoid marks left on the window glass. That is because these suction pads in each module are retracted and detached from the window glass during linear and rotational motions. Robots whose dry adhesion stickers are attached by a legged locomotion mechanism, or active adhesion pads in a wheeled or tracked mechanism, always leave marks. That is because their adhesion pads slide on the window glass during operation. The problem is worse if the pads are made from the tackier elastic materials. Thus, the adhesion mechanism of Hubbot performs better than the other ones in respect to quality criteria.

In addition, Hubbot provides an adhesion force of 588N using the specially designed four suction pads. Each adhesion pad has an adhesion force of 147N and can hold about four times the weight of Hubbot with an approximate weight of 22N. This guarantees that Hubbot will stay on the window glass even when only one suction pad is adhering to the window glass. The two servo motors and four ELAs all have high operating precision and so control the required motions precisely.

5.3 Summary

On the whole, Hubbot achieves a higher success criteria than the other listed window cleaning robots. Its advantages and disadvantages are presented above. It has a simpler mechanical structure and assembly, and a lighter weight as well as more reliable suction. It can carry higher payloads and step over higher obstacles. Also, regarding quality criteria, it leaves fewer marks and is capable of precise motions. However, it has higher initial cost and is slower.

6 Conclusions and Recommendations

This research has investigated the feasibility of building *Hubbot* – a novel window glass cleaning robot, which addresses the weight, manufacturing cost, and window frame traversability issues which were identified as problems affecting other window cleaning robots. This chapter summarizes the design and expected performance of *Hubbot*, then described the conclusions of the project before discussing the recommendations for future work.

6.1 Performance achieved by Hubbot

6.1.1 Performance Measured against Design Requirements

Climbing robots work on different kinds of surface, having no, low or high obstacles. Their general working requirements were presented in previous research. To design *Hubbot*, the specific requirements of window glass cleaning robots were outlined and several design options were considered. The most important design requirements of this robot are:

- having a simple structure and a light weight;
- Maximising adhesion forces;
- Choosing and designing of every appropriate element;
- Minimising any tracks left on the glass.

Investigation of previous research suggested that a translation locomotion system was the simplest for window glass cleaning robot, when compared to legged, tracked or wheeled locomotion. The locomotion system makes manufacture and assembly easy and thus *Hubbot* can be more economic using translation locomotion system other than the others. *Hubbot* consists of two modules, each with a set of legs connected to suction. The suction pads of *Hubbot*, are designed to be retracted and detached from the window glass during their individual movements. This design reduces the abrasion of the pads and avoids marks left on the window glass that can occur within other designs. *Hubbot* has a considerable market advantage in terms of being able to produce mark free glass without the complexity of needing to clean up after the robot.

6.1.2 Performance of Motion Mechanisms

In previous literature all window glass cleaning robots moved in different motion modes (moved using different locomotion systems). *Hubbot's* motion can be characterised by the four main types: linear motion, rotational motion, leg extension/retraction motion and interference avoidance motion.

In comparison to the other translation robots, *Hubbot* uses the four different motion mechanisms. In previous research robots with two modules used two actuators to perform linear motions, such as a pair of rack and pinion gears or pneumatic cylinders. The two modules in the existing translation robots rotate using one actuator. However an extra rotational mechanism is added, such as a waist joint by a pendulum cylinder. These motion mechanisms did not reduce the number of actuators and rotational motion mechanisms but increased the complexity of the structure. However, *Hubbot* is designed with a new linear motion mechanism, using a rack and pinion to separately drive each module by a small servo motor. Rotational motion is achieved using a hub with a motor which is to provide relative rotation between the two modules. Similar to the other existing translation robots, *Hubbot* also needs to retract the suction pads of each module to perform linear and rotational motions. However, it uses ELAs to actuate the suction pads instead of pneumatic actuators other published designs have used, which reduces not only the weight of the robot but also maintenance costs.

As discussed in Chapter 2, translation locomotion mechanisms are often very heavy. That is because they are big and are actuated by heavy electric motors or pneumatic cylinders. For example, Sky Cleaner 3 [29, 87], driven by about 12 pneumatic cylinders, has a volume of 1136×736×377 mm3 and weighs 45kg. Hubbot, actuated by two servo motors and 4 ELAs, has a volume of 300×190×336 mm^3 and weighs just 2.25kg. So, Hubbot, using four motion mechanisms reduces the number of motors, which decreases its weight and improves its payload capacity.

6.1.3 Performance Regarding Adhesion Mechanisms

As discussed in Chapter 2, many window glass cleaning robots use active vacuum adhesion mechanisms. Other times, magnetic and biomimetic etc. adhesion mechanisms are used. It

was found that active and passive vacuum mechanisms have the same advantage of simple structure and large adhesion forces. However, active system are heavier due to the need for on-board pump. *Hubbot* was developed to use a passive vacuum adhesion mechanism. Weighing just 2.25kg, passive vacuum system can easily provide enough adhesion forces to stably operate on window glass. The 4 passive suction pads, each with a diameter of 50mm, in each module, achieved a total adhesion force of about 588N. However, the robot (30kg) in [67] uses 16 active suction pads to achieve the adhesion force about 450N, less than that of *Hubbot*.

Research also showed that magnetic, and biomimetic adhesion mechanisms have a more complicated structure than passive vacuum ones. Further, magnetic adhesion meant that the inner and outer parts are difficult to detach from each other and the biomimetic one needs frequent cleaning of the adhesion system. The Hubbot uses a solenoid valve attached to the suction pads to break vacuum easily and no extra cleaning required for the suction pads. Therefore, the operation of this suction mechanism is simple and reliable.

In some robots, like DEXTER, the passive suction pad has a strap which can break the vacuum by a servo motor or solenoid valve. Sometimes, these pads need pipes, T-joints and manifolds to connect the solenoid valves. These mechanisms are complex. Hubbot directly implements a single solenoid valve with a suction pad through a specially designed adapter which makes its adhesion mechanism both simple and easy to assemble. This assembly makes Hubbot simple, reliable and inexpensive.

6.1.4 Performance Regarding Spanning Obstacles

In previous published literature, robots that use wheels or rotating-discs cannot overcome barriers while those robots that use tracks or biomimetic stickers can only span low obstacles. Compared to these robots, translation locomotion robots can step over higher obstacles. However, they all use pneumatic cylinders for linear motion of legs, which can limit their capacities of spanning obstacles as higher performance pneumatic cylinders are required. A heavier pump may be required thus reducing the robots' payload capacity or an increase of suction forces may be required. Therefore, all these methods of locomotion do not have enough flexibility to meet the requirements.

However, it was found that ELAs have the following advantages. They are very light and do not need a pump. Their weights only increase a small amount when a longer stroke is required. The Hubbot, with 4 ELAs can span obstacles up to 50 mm in height, which meets the requirements for operating on most building.

6.2 Merits of Hubbot

Based on the success criteria of window glass cleaning robots, Hubbot presents a number of advantages listed below, with evaluations and comparisons to the other listed window cleaning robots in Table 5.2.

1) A simpler mechanical structure and assembly. Hubbot applies the simplest locomotion mechanism to achieve the four motions: linear motion, rotational motion, leg extension/retraction motion and interference avoidance motion. And it directly implements a single solenoid valve with a suction pad on each foot without pipes, T-joints and manifolds to connect them together.
2) A lighter weight. The three motion mechanisms are actuated by two light servo motors and four light ELAs. It not only decreases the number of motors but also increases the capacity of payload.
3) Reliable suction forces. A smaller suction pad, having a diameter of 50mm, provides an adhesion force of up to 147.19N. This adhesion force can support more than 4 times the weight of Hubbot and each module has 4 suction pads.
4) Better obstacles spanning ability. Hubbot can operate on high buildings, having obstacles of up to 50mm high.
5) Fewer or no marks left. Each module moves on the window glass, with its suction pads detached from the window glass, whether sliding or rotating.
6) ELAs instead of pneumatic actuators and passive suction pads as an alternative to active suction pads prevent Hubbot from creating noise. Also, the chosen micro servo motors have the advantages of accurate positioning, high torque and light weight.
7) Lower manufacture cost. It is only about NZD 2379.64.

However, the Hubbot also has the following limitations:

1) Moves relatively slowly. Hubbot moves linearly only at the speed of 22mm/s. However, since robots can work 24/7 (except for maintenance), slow speed may not a problem. When this robot is prototyped and tested, we may be able to increase its speed.
2) Discontinuous slide-stick-slide movements. The two modules can only move or rotate, retracting their suction pads from the window glass after the other suction pads adhere to the window glass.

6.3 Recommendations for Future Work

There are some issues for future improvement as follows:

1) Span wider obstacles faster. The limited displacement and lower speed of the linear motions could be improved.
2) Improving control precision. Better bearings and rack and pinion gears, might improve the design of Hubbot. Some non-standard parts such as the hub and the slider could be optimally designed and manufactured. Also, the mating of each touching surface could be improved.
3) Discontinuous slide-stick-slide movements. This problem cannot be avoided but the interval between movements could be shortened.
4) Prototype manufacture. A physical prototype of this robot is planned for future manufacture to suit the market. However, all non-standard elements would be 3D printed. Then all standard and non-standard elements will be assembled to produce a physical prototype to test and improve its functions.
5) Development specifications of the electrics and control systems for the robot.
6) Simulations of working process of Hubbot.
7) Cleaning system is yet to be designed.

1. *images of window glass climbing robots*. [cited 28/1/2019]; Available from: https://www.google.com/search?biw=1920&bih=889&tbm=isch&sa=1&ei=ENZOXNiiMNq8rQG-v43ABg&q=window+glass+climbing+robots+&oq=window+glass+climbing+robots+&gs_l=img.3...87513.95210..96182...0.0..0.280.2909.0j1j12.....1....1..gws-wiz-img.8ulSwnvdVVw.
2. *images of wall climbing robots on concrete*. [cited 28/1/2019]; Available from: https://www.google.com/search?biw=1920&bih=889&tbm=isch&sa=1&ei=vtROXKnkHILe9QOhmbhQ&q=wall+climbing+robots+on+concrete&oq=wall+climbing+robots+on+concrete&gs_l=img.12...52043.56079..58084...0.0..0.260.2182.0j9j3.....1....1..gws-wiz-img.....0i30j0i5i30.ILsd8G6o8nk.
3. Wagner, M., et al. *A novel wall climbing robot based on Bernoulli effect*. in *Mechtronic and Embedded Systems and Applications, 2008. MESA 2008. IEEE/ASME International Conference on*. 2008. IEEE.
4. Silva, M.F. and J.A.T. Machado. *New Technologies for Climbing Robots Adhesion to Surfaces*. in *NTST 2008 – International Workshop on New Trends on Science and Technology*. 2008.
5. Davies, T.H., et al., *Robotic climbing platform*. 2017, Google Patents.
6. Miyake, T., H. Ishihara, and M. Yoshimura. *Basic studies on wet adhesion system for wall climbing robots*. in *Intelligent Robots and Systems, 2007. IROS 2007. IEEE/RSJ International Conference on*. 2007. IEEE.
7. Nansai, S. and R.E. Mohan, *A survey of wall climbing robots: Recent advances and challenges.* Robotics, 2016. **5**(3): p. 14.
8. Chang, Y., *Development of a wall climbing inspection robot with high mobility on complex shaped walls.* 2015.
9. Chu, B., et al., *A survey of climbing robots: Locomotion and adhesion.* International journal of precision engineering and manufacturing, 2010. **11**(4): p. 633-647.
10. San-Millan, A. *Design of a teleoperated wall climbing robot for oil tank inspection*. in *Control and Automation (MED), 2015 23th Mediterranean Conference on*. 2015. IEEE.
11. *windoro window cleaning robot review*. [cited 28/01/2019]; Available from: https://www.youtube.com/watch?v=w38XcECO5fc.
12. Kim, J., et al. *Wheel & Track hybrid robot platform for optimal navigation in an urban environment*. in *SICE Annual Conference 2010, Proceedings of*. 2010. IEEE.
13. Tâche, F., et al. *Adapted magnetic wheel unit for compact robots inspecting complex shaped pipe structures*. in *Advanced intelligent mechatronics, 2007 IEEE/ASME international conference on*. 2007. IEEE Press.
14. Fu, Y., et al. *Development of a wall climbing robot with wheel-leg hybrid locomotion mechanism*. in *Robotics and Biomimetics, 2007. ROBIO 2007. IEEE International Conference on*. 2007. IEEE.
15. Wu, S., et al. *A magnetic wall climbing robot with non-contactable and adjustable adhesion mechanism*. in *Real-time Computing and Robotics (RCAR), 2017 IEEE International Conference on*. 2017. IEEE.
16. Adkins, R. *The Best Magnetic Window Cleaners : 2018 Reviews & Guide*. [cited 29/01/2019]Robert AdkinsRobert AdkinsRobert Adkins]; Available from: https://gadgetsliving.com/magnetic-window-cleaners/.
17. Jin, M., *Eight-legged Bionic Crab-liked Robot Path Planning and Gait Simulation Analysis*. 2013, Huadong Shanghai, China.
18. Hirose, S. and K. Arikawa, *Coupled and decoupled actuation of robotic mechanisms.* Advanced Robotics, 2001. **15**(2): p. 125-138.
19. Unver, O. and M. Sitti. *A miniature ceiling walking robot with flat tacky elastomeric footpads*. in *Robotics and Automation, 2009. ICRA'09. IEEE International Conference on*. 2009. IEEE.

20. Li, Y., D. Sameoto, and C. Menon. *Properties validation of an anisotropic dry adhesion designed for legged climbing robots*. in *Robotics and Biomimetics (ROBIO), 2009 IEEE International Conference on*. 2009. IEEE.
21. Wei, T.E., R.D. Quinn, and R.E. Ritzmann. *Robot designed for walking and climbing based on abstracted cockroach locomotion mechanisms*. in *Advanced Intelligent Mechatronics. Proceedings, 2005 IEEE/ASME International Conference on*. 2005. IEEE.
22. X.L.Yu, *Development of Spider Biomimetic Robot and Research on Its Gait Issue*. 2013, Harbin Engineering University.
23. Liu, C.-H., et al. *The development of a multi-legged robot using eight-bar linkages as leg mechanisms with switchable modes for walking and stair climbing*. in *Control, Automation and Robotics (ICCAR), 2017 3rd International Conference on*. 2017. IEEE.
24. Wang, L., et al. *The research on bionic crab-liked robot prototype*. in *Proceedings of the IEEE International Conference on Mechatronics and Automation*. 2005. Piscataway, NJ, USA: IEEE.
25. Ciszewski, M., et al., *Virtual prototyping, design and analysis of an in-pipe inspection mobile robot.* Journal of Theoretical and Applied Mechanics, 2014. **52**(2): p. 417-429.
26. Zhu, J., D. Sun, and S.-K. Tso, *Development of a tracked climbing robot.* Journal of Intelligent and robotic Systems, 2002. **35**(4): p. 427-443.
27. Zhao, X., et al., *Structure Design and Application of Combination Track Intelligent Inspection Robot Used in Substation Indoor.* Procedia Computer Science, 2017. **107**: p. 190-195.
28. Liu, Y. and T. Seo. *Linkage-Type Walking Mechanism for Unstructured Vertical Wall*. in *2018 15th International Conference on Ubiquitous Robots (UR)*. 2018. IEEE.
29. Zhang, H., et al., *Sky cleaner 3: A real pneumatic climbing robot for glass-wall cleaning.* IEEE Robotics & Automation Magazine, 2006. **13**(1): p. 32-41.
30. Y.P. Liu, S.Y.Z., K.B.Lin, *design of control system for high-rise buildings glass-wall cleaning robot.* machinery and electronic, 2015: p. 4.
31. Liu, Y., et al. *A leg-wheel wall-climbing robot utilizing bio-inspired spine feet*. in *Robotics and Biomimetics (ROBIO), 2013 IEEE International Conference on*. 2013. IEEE.
32. S.B.Chen, M.H.W., , Y.Z,Zhao, Z,Fu, X.F.Gao, *the climbing robotic wheels system of the combined wheels and legs to step over the obstacles and the non-touched magnetic adhesion*. 2011: China.
33. M.H.Wu, Y.Z.Z., S.B.Chen, Z.Fu,X.F.Gao, *Wheeled climbing robot of spanning obstacles*. 2011: China.
34. Unver, O. and M. Sitti, *Flat dry elastomer adhesives as attachment materials for climbing robots.* IEEE transactions on robotics, 2010. **26**(1): p. 131-141.
35. Menon, C., M. Murphy, and M. Sitti. *Gecko inspired surface climbing robots*. in *Robotics and Biomimetics, 2004. ROBIO 2004. IEEE International Conference on*. 2004. IEEE.
36. Jagtap, A., *Skyscraper's Glass Cleaning Automated Robot.*
37. Miyake, T., H. Ishihara, and M. Yoshimura. *Application of Wet Vacuum-based Adhesion System for Wall Climging Mechanism*. in *2007 International Symposium on Micro-NanoMechatronics and Human Science*. 2007. IEEE.
38. Bouchard, S. *Robot Vacuum Cup Grippers: Top 5 Problems*. 2014 [cited 29/01/2019]; Available from: https://blog.robotiq.com/bid/53128/Vacuum-cups-robot-gripper-Top-5-problems.
39. Bi, Z., et al. *A miniature biped wall-climbing robot for inspection of magnetic metal surfaces*. in *Robotics and Biomimetics (ROBIO), 2012 IEEE International Conference on*. 2012. IEEE.
40. Fischer, W., F. Tâche, and R. Siegwart. *Inspection system for very thin and fragile surfaces, based on a pair of wall climbing robots with magnetic wheels*. in *2007 IEEE/RSJ International Conference on Intelligent Robots and Systems: San Diego, CA, 29 October-2 November 2007*. 2007. IEEE.
41. *Windoro window washing robot unboxing & demo by robotshop.com*. [cited 29/1/2019]; Available from: https://www.youtube.com/watch?v=04BOdvsPdSU.

42. Autumn, K., et al., *Adhesive force of a single gecko foot-hair.* Nature, 2000. **405**(6787): p. 681.
43. Qing-xuan, J., et al. *Research on theoretical models of synthetic Geckos' adhesion technology*. in *Robotics, Automation and Mechatronics, 2006 IEEE Conference on*. 2006. IEEE.
44. Kim, S., et al., *Smooth vertical surface climbing with directional adhesion.* IEEE Transactions on robotics, 2008. **24**(1): p. 65-74.
45. Wang, Z., et al. *Optimal attaching and detaching trajectory for bio-inspired climbing robot using dry adhesive*. in *Advanced Intelligent Mechatronics (AIM), 2014 IEEE/ASME International Conference on*. 2014. IEEE.
46. Kim, G., T. Ahn, and H.Y. Hwang, *Durability Improvement of Synthetic Dry Adhesives by Metal Coatings.* Advances in Materials Science and Engineering, 2017. **2017**.
47. Liu, Y., et al. *Dry adhesion optimization design for a wall-climbing robot based on experiment*. in *International Conference on Ubiquitous Robots and Ambient Intelligence*. 2015.
48. *How to choose a motor for your robot*. [cited 29/01/2019]; Available from: http://www.robotoid.com/howto/choosing-a-motor-type.html.
49. Eich, M. and T. Vögele. *Design and control of a lightweight magnetic climbing robot for vessel inspection*. in *Control & Automation (MED), 2011 19th Mediterranean Conference on*. 2011. IEEE.
50. Yunquan Li, M.Z.Q.C., Yong Hua Chen, and James Lam *Design of a One-motor Tree-climbing Robot.* International Conference on Information and Automation, 2015. **Proceeding of the 2015 IEEE**: p. 6.
51. [cited 11/03/2019]; Available from: https://commons.wikimedia.org/wiki/File:Stepper_motor..png.
52. *Servo Motor – Types and Working Principle*. [cited 11/03/2019]; Available from: https://www.edgefx.in/servo-motor-types-and-working-principle/.
53. Alciatore, D.G. and M.B. Histand, *Introduction to mechatronics and measurement systems*. 4th, international ed. 2012, Singapore: McGraw-Hill.
54. Shetty, D. and R.A. Kolk, *Mechatronics system design, SI version*. 2010: Cengage Learning.
55. Hashemnia, N. and B. Asaei. *Comparative study of using different electric motors in the electric vehicles*. in *Electrical Machines, 2008. ICEM 2008. 18th International Conference on*. 2008. IEEE.
56. *the images of brushless DC motor*. [cited 29/01/2019]; Available from: https://www.google.com/search?biw=1920&bih=889&tbm=isch&sa=1&ei=CShQXN_wPNStoAST_ZqoAQ&q=brushless+dc+motor&oq=brushless+dc+motor&gs_l=img.1.0.0j0i7i30j0i30l8.355675.364335..366902...1.0..0.342.3343.2-11j2.....0....1..gws-wiz-img.....0i7i30i19j0i19.PYIK9BDdJSo.
57. Zhao, Q., et al. *Design And Realization Of A Glass-Curtain Wall-Cleaning Robot*. in *Joint International Information Technology, Mechanical and Electronic Engineering Conference*. 2017.
58. *What are the types of motors?* [cited 29/01/2019]; Available from: https://www.quora.com/What-are-the-types-of-motors.
59. Lee, J.-W. and T.-W. Kim. *Design and experimental analysis of embedded servo motor driver for robot finger joints*. in *Ubiquitous Robots and Ambient Intelligence (URAI), 2011 8th International Conference on*. 2011. IEEE.
60. Guo, H., Z. Mao, and J. Zhang. *Humanoid robot system design based on DC reduction servo motor*. in *Artificial Intelligence, Management Science and Electronic Commerce (AIMSEC), 2011 2nd International Conference on*. 2011. IEEE.
61. Zhou, H. *DC servo motor PID control in mobile robots with embedded DSP*. in *Intelligent Computation Technology and Automation (ICICTA), 2008 International Conference on*. 2008. IEEE.

62. Van de Straete, H.J., et al., *Servo motor selection criterion for mechatronic applications.* IEEE/ASME Transactions on mechatronics, 1998. **3**(1): p. 43-50.
63. *the images of stepper motor*. [cited 2019/29/1]; Available from: https://www.google.com/search?biw=1920&bih=889&tbm=isch&sa=1&ei=cydQXM6RNNb8wAO8q5fgCQ&q=stepper+motor&oq=stepper+motor&gs_l=img.12..0l3j0i7i30l7.7586.7586..11269...0.0..0.330.330.3-1.....0....1..gws-wiz-img.D8Ci6M1EXVQ.
64. *the images of servo motor*. [cited 2019/29/1]; Available from: https://www.google.com/search?biw=1920&bih=889&tbm=isch&sa=1&ei=gCdQXLf6D4jh-Aa946XwAw&q=servo+motor&oq=servo+motor&gs_l=img.12..0l3j0i30l7.133196.134284..136769...0.0..0.346.1392.2-3j2.....0....1..gws-wiz-img.....0i7i30.u2vXLAinAvo.
65. *the images of pneumatic cylinder*. [cited 29/01/2019]; Available from: https://www.google.com/search?biw=1920&bih=938&tbm=isch&sa=1&ei=eSlQXNujNMXAoASr0YrACQ&q=pneumatic+cylinder&oq=pneumatic+cyli&gs_l=img.1.0.0j0i30l9.2788.12756..15146...0.0..0.370.3502.2-12j2.....0....1..gws-wiz-img.huGuxkL2HHI.
66. Brusell, A., G. Andrikopoulos, and G. Nikolakopoulos. *A survey on pneumatic wall-climbing robots for inspection*. in *Control and Automation (MED), 2016 24th Mediterranean Conference on*. 2016. IEEE.
67. Sun, D., J. Zhu, and S.K. Tso, *A climbing robot for cleaning glass surface with motion planning and visual sensing*, in *Climbing and Walking Robots: towards New Applications*. 2007, InTech.
68. Jose-Eduardo Gaspar-Badillo, e.a., *Four DOF pneumatic robot design and hardware.* IEEE Robotics & Automation Magazine, 2017: p. 7.
69. Yamamoto, Y., et al. *Mechanism and jumping pattern of one-legged jumping robot with pneumatic actuators*. in *Control, Automation and Systems (ICCAS), 2016 16th International Conference on*. 2016. IEEE.
70. MOTORS, I.L. *Cost optimization for linear motion* [cited 29/01/2019]; Available from: http://www.linmot.com/fileadmin//user_upload/Downloads/databooks/D-1V0_BR_Cost_optimization_.pdf.
71. *Electric linear motion Superior to pneumatic cylinders in many applications.* [cited 29/01/2019]; Available from: https://stevenengineering.com/tech_support/PDFs/LINMOT_ELECTRIC-LINEAR-MOTION-ADVANTAGES.pdf
72. *the images of electric linear actuator*. [cited 29/01/2019]; Available from: https://www.google.com/search?biw=1920&bih=938&tbm=isch&sa=1&ei=8i1QXO3IHouJoAS8mY-ABA&q=electric+linear+actuator&oq=electric+linear+actuator&gs_l=img.12..0i19j0i8i30i19l2.1219777.1219777..1221501...0.0..0.225.225.2-1.....0....2j1..gws-wiz-img.PzMqenP8rVY.
73. Boldea, I. and S.A. Nasar. *Linear electric actuators and generators*. in *Electric Machines and Drives Conference Record, 1997. IEEE International*. 1997. IEEE.
74. Ohyama, K., Y. Hyakutake, and H. Kino. *Verification of operating principle of flexible linear actuator*. in *Electrical Machines and Systems, 2009. ICEMS 2009. International Conference on*. 2009. IEEE.
75. Na, B., H. Choi, and K. Kong. *Design of a direct-driven linear actuator for development of a cheetaroid robot*. in *Robotics and Automation (ICRA), 2013 IEEE International Conference on*. 2013. IEEE.
76. Yasuaki, H. and N. Tomoharu. *A proposal of small linear actuators for small entertainment robots*. in *Computers & Informatics (ISCI), 2012 IEEE Symposium on*. 2012. IEEE.
77. Shao, H., T. Wu, and F. Song. *A new type of intelligent linear electric actuator and vibration detection*. in *Control and Decision Conference (CCDC), 2016 Chinese*. 2016. IEEE.
78. *LINAK*. [cited 29/01/2019]; Available from: https://www.linak.com/products/linear-actuators/la23/.

79. *Engineering Refresher: The Basics and Benefits of Electromechanical Actuators*. 2018 [cited 29/01/2019]; Available from: https://www.machinedesign.com/motion-control/engineering-refresher-basics-and-benefits-electromechanical-actuators.
80. *LINMOT LINEAR MOTORS*. [cited 29/01/2019]; Available from: https://johnbrooks.co.nz/linmot-linear-motors.
81. *Linear Motors*. [cited 29/01/2019]; Available from: https://linmot.com/products/linear-motors/.
82. *Linear Motion Manufacturing and Design*. [cited 29/01/2019]; Available from: http://www.linmot-usa.com/.
83. *LinMot Linear Motors Application Demonstration*. 2010 [cited 29/01/2019]; Available from: https://www.youtube.com/watch?v=w-omXb8VcfU.
84. *LinMot Linear Motors in Packaging System Applications*. 2010 [cited 29/01/2019]; Available from: https://www.youtube.com/watch?v=vW3A1H-tJV8.
85. *food products*. [cited 29/01/2019]; Available from: https://linmot.com/applications/food-products/.
86. *What Is The Difference Between DC Motor, Servo Motor And Stepper Motor?* [cited 29/01/2019]; Available from: https://www.elprocus.com/difference-dc-motor-servo-motor-stepper-motor.
87. Zhang, H., et al., *A series of pneumatic glass-wall cleaning robots for high-rise buildings.* Industrial Robot: An International Journal, 2007. **34**(2): p. 150-160.
88. Unver, O., et al. *Geckobot: a gecko inspired climbing robot using elastomer adhesives*. in *Proceedings 2006 IEEE International Conference on Robotics and Automation, 2006. ICRA 2006.* 2006. IEEE.
89. Choi, Y.-H. and K.-M. Jung. *Windoro: The world's first commercialized window cleaning robot for domestic use*. in *2011 8th International Conference on Ubiquitous Robots and Ambient Intelligence (URAI)*. 2011. IEEE.
90. Choi, Y.-H., et al. *SMART WINDORO V1. 0: Smart window cleaning robot*. in *2012 9th International Conference on Ubiquitous Robots and Ambient Intelligence (URAI)*. 2012. IEEE.
91. Brockmann, W., *Concept for energy-autarkic, autonomous climbing robots*, in *Climbing and Walking Robots*. 2006, Springer. p. 107-114.
92. Brockmann, W. and F. Mösch, *Climbing without a vacuum pump*, in *Climbing and Walking Robots*. 2005, Springer. p. 935-942.
93. Kim, Y.S., et al., *Conceptual design and feasibility analyses of a robotic system for automated exterior wall painting.* International Journal of Advanced Robotic Systems, 2007. **4**(4): p. 417-430.
94. San-Millan, A. *Design of a teleoperated wall climbing robot for oil tank inspection*. in *2015 23rd Mediterranean Conference on Control and Automation (MED)*. 2015. IEEE.
95. Bódai, G., *Material and frictional behavior of rubber sliding on glass surface.* 2012.
96. Bhattacharyya, H., *A Note on Some Results of Friction Between Non-metals.* Defence Science Journal, 1955. **5**(3): p. 355-358.
97. *Wood's power-grip*.
98. Karbassi, J. *Vacuum Systems For Successful Robot Implementation*. 2013 [cited 25/4/2019]; Available from: https://www.roboticstomorrow.com/article/2013/10/vacuum-systems-for-successful-robot-implementation/206.
99. SKF Ball Bearing Co. (N.Z.) Ltd, S.F., *SKF bearings in machine tools*. 1969, Wellington: SKF Ball Bearing Co. (N.Z.) Ltd1969.
100. (Firm), S., *SKF general catalogue* 1994: SKF.
101. NSK. *Technical information*. [cited 18/5/2019]; Available from: file://file/UsersZ$/zyu27/Home/Downloads/NSK_CAT_E1103a_PartA.pdf.
102. Parmley, R.O., *Mechanical components*. 2000 New York ; London : McGraw-Hill, .

103. Huili Yu, X.F.e.a., *Concise Mechanical Design Manual in Mechanical Engineer in Mechanical Engineer Version*. 2017: China Machine Press.
104. Wolovich, W.A., *Robotics: basic analysis and design*. 1987, New York: Holt, Rinehart and Winston.